

Systematic review of metal-based alloys with autogenous antibacterial capability

Y. Alshammari, N. Elkork, L. Moussa, F. Esmail, M. Saeed, M. Alsarraf, A. Alfarhan, M. A. Alrashidi & L. Bolzoni

To cite this article: Y. Alshammari, N. Elkork, L. Moussa, F. Esmail, M. Saeed, M. Alsarraf, A. Alfarhan, M. A. Alrashidi & L. Bolzoni (07 Apr 2025): Systematic review of metal-based alloys with autogenous antibacterial capability, Critical Reviews in Solid State and Materials Sciences, DOI: [10.1080/10408436.2025.2483676](https://doi.org/10.1080/10408436.2025.2483676)

To link to this article: <https://doi.org/10.1080/10408436.2025.2483676>



© 2025 The Author(s). Published with license by Taylor & Francis Group, LLC



Published online: 07 Apr 2025.



Submit your article to this journal [↗](#)



View related articles [↗](#)



View Crossmark data [↗](#)

Systematic review of metal-based alloys with autogenous antibacterial capability

Y. Alshammari^{a,b,c}, N. Elkork^b, L. Moussa^b, F. Esmail^b, M. Saeed^a, M. Alsarraf^{cd}, A. Alfarhan^e, M. A. Alrashidi^f, and L. Bolzoni^c

^aEnergy and Building Research Centre, Kuwait Institute for Scientific Research, Safat, Kuwait; ^bCollege of Engineering, The International University of Science and Technology in Kuwait, Ardiya, Kuwait; ^cSchool of Engineering, The University of Waikato, Hamilton, New Zealand; ^dIndustrial Institute, Public Authority for Applied Education and Training, Shuwaikh, Kuwait; ^ePetroleum Research Center (PRC), Kuwait Institute for Scientific Research (KISR), Safat, Kuwait; ^fCollege of Technology Studies, Public Authority for Applied Education and Training, Shuwaikh, Kuwait

ABSTRACT

Pathogenic bacterial infection, especially in surgical and nosocomial settings, is an outstanding and long-lasting challenge due to the ability of microorganisms to evolve and develop mechanisms to become drug-resistant (i.e., superbugs). Considerable efforts have been made in recent years to develop metal-based alloys with autogenous antibacterial capability and to comprehend their mechanism of action, which are systematically reviewed in this work. To comprehensively understand current developments, antibacterial mechanisms (e.g., cell wall/membrane disruption), resistance mechanisms (e.g., permeability barrier), and the primary standardized techniques used to assess the antibacterial response (e.g., plate-count method) are initially introduced. Subsequently, metallic elements with intrinsic antibacterial response are presented alongside a brief discussion of the effects that manufacturing methods have on the ability to achieve metal-based alloys with autogenous antibacterial properties. The several antibacterial metal-based alloys currently being developed, which include Co-, Fe-, Mg-, Ti-, and Zn-based alloys, and some few other metal-based alloy systems, were analyzed in detail, and an effort to comparatively evaluate the antibacterial and mechanical response of the different alloys developed so far was made. Generally, the incorporation of Cu or Ag, which are well-known antibacterial metallic elements, shows remarkable effectiveness against both Gram-positive and Gram-negative bacteria. Additionally, some few other elements like Ca, Ce, and rare earths have been investigated, and some of them show antibacterial capability. The work is complemented with some challenges to be addressed and opportunities to be taken.

KEYWORDS

Antibacterial alloys; controlled ion release; antibacterial property; antibacterial resistance; metallic biomaterials

Table of contents

1. Introduction	2
2. Metal-based alloys antibacterial mechanisms	4
2.1. Metal ions release	5
2.1.1. Cell wall/membrane disruption	5
2.1.2. Protein dysfunction and inhibition of essential enzymes	5
2.1.3. Oxidative stress induction	6
2.2. Bacteria resistance mechanisms	6
2.2.1. Permeability barrier	7
2.2.2. Enzyme-mediated resistance	7
3. Antibacterial properties evaluation	7
3.1. Disk diffusion assay	8
3.2. Plate-count method	8
3.3. Live/dead staining	8

CONTACT Y. Alshammari  yshammari@kISR.edu.kw

© 2025 The Author(s). Published with license by Taylor & Francis Group, LLC

This is an Open Access article distributed under the terms of the Creative Commons Attribution License (<http://creativecommons.org/licenses/by/4.0/>), which permits unrestricted use, distribution, and reproduction in any medium, provided the original work is properly cited. The terms on which this article has been published allow the posting of the Accepted Manuscript in a repository by the author(s) or with their consent.

3.4. Factors affecting the evaluation of antibacterial performance	8
4. Alloys with antibacterial capability	9
4.1. Antibacterial metallic elements	10
4.2. Role of manufacturing methods	10
4.3. Antibacterial metal-based alloys	12
4.3.1. Co-based alloys	12
4.3.2. Fe-based alloys	15
4.3.3. Mg-based alloys	20
4.3.4. Ti-based alloys	25
4.3.5. Zn-based alloys	31
4.3.6. Other metal-based alloys	35
4.4. Potential applications	36
5. Concluding remarks	37
6. Challenges and opportunities	38
Disclosure statement	38
Data availability statement	38
References	38

Terminology and acronyms

<i>Acinetobacter baumannii</i>	<i>Aggregatibacter</i>	<i>S. gordonii</i>	<i>Streptococcus mutans</i>
<i>A. baumannii</i>	<i>actinomycetemcomitans</i>	<i>S. mutans</i>	Template replication technique
<i>A. actinomycetemcomitans</i>	Antibacterial activity	TRT	Transmission electron microscopy
<i>R</i>	<i>Bacillus subtilis</i>	TEM	Trypticase soy broth
<i>B. subtilis</i>	<i>Candida albicans</i>	TSB	Ultimate compressive strength
<i>C. albicans</i>	Colony forming unit	UCS	Ultimate tensile strength
CFU	Compressive yield stress	UTS	X-ray diffraction
CYS	Confocal laser scanning microscope	XRD	Yield stress
CLSM	DAPI staining method	YS	
4',6-diamidino-2-phenylindole staining	Deoxyribonucleic acid		
DNA	<i>Escherichia coli</i>		
<i>E. Coli</i>	Inhibition zone diameter		
IZD	Laser powder bed fusion		
LPBF	Mechanical alloying		
MA	Metal additive manufacturing		
MAM	Methicillin-resistant		
MRSA	<i>Staphylococcus aureus</i>		
MRSE	Methicillin-resistant		
NAD	<i>Staphylococcus epidermidis</i>		
<i>P. gingivalis</i>	Nicotinamide adenine dinucleotide		
PM	<i>Porphyromonas gingivalis</i>		
<i>P. Aeruginosa</i>	Powder metallurgy		
<i>P. putida</i>	<i>Pseudomonas aeruginosa</i>		
ROS	<i>Pseudomonas putida</i>		
SLM	Reactive oxygen species		
SEM	Selective laser melting		
SPS	Scanning electron microscopy		
SS	Spark plasma sintering		
<i>S. Aureus</i>	Stainless steel		
<i>S. epidermidis</i>	<i>Staphylococcus aureus</i>		
	<i>Staphylococcus epidermidis</i>		
	<i>Streptococcus gordonii</i>		

1. Introduction

As their names indicate, antibacterial materials are materials able to kill bacteria and prevent their spreading. A wide range of both natural and synthetic materials, such as ceramic biomaterials,^[1–3] polymeric biomaterials,^[4,5] and metallic biomaterials^[6–9] possess antimicrobial properties and thus provide the ability to slow or stop the growth of bacteria in different scenarios. In particular, these materials actively prevent the colonization of bacteria, which offers an essential protection line against disease spread and possible infections.^[10,11] This is not the case for non-antimicrobial materials. The development of antibacterial materials is significant as they offer fundamental support to maintain hygiene in a substantial range of environmental and biomedical applications by preventing the transmission of bacterial infections. These applications include, but are not limited to, hospitals, food safety, public transportation health, and body implants.^[12,13] Moreover, antibacterial materials have been extensively used in products such as textiles, personal care

products, and home appliances, considerably reducing bacterial loads.^[14,15]

Bacterial infections and their consequences have a significant impact on public health. These infections can be due to many reasons, among which are changes in lifestyles, changes in population health status, and increased global connectivity.^[16] These have led to a dramatic increase in bacterial infections. These bacterial infections also affect individuals with body implants, as bacterial adhesion is the first and most crucial step in the inflammation of implants. This complex process is influenced by environmental factors, bacterial properties, material surface properties, and the presence of serum or tissue proteins.^[17] It is known that bacterial infections have been accelerating worldwide due to the rise of antibiotic-resistant microbial strains (i.e., superbugs). Such bacteria can resist drugs, which have been purposely developed to demolish the bacteria using different mechanisms. According to the centers of disease control and prevention, globally, all significant bacterial strains are developing resistance to their specific antibiotic treatment of choice.^[18] A major unresolved challenge of medical implants like orthopedic prostheses (market value of \$46.5 billion^[19]), dental implants (global market value of \$4.6 billion^[20]), and cardiac devices (global market value of \$34 billion^[21]) is the high risk of bacterial infection.^[22] The surface of the implants may act as a breeding ground for the bacteria, leading to biofilm formation (i.e., a community of bacteria encountered within the protective matrix) as schematically shown in Figure 1. The biofilm acts as a shield against the host's immune system and the antibiotics, making it difficult to treat and eventually leading to chronic infections.^[23,24] Inhibiting the formation of this biofilm on the implant's surface is the best possible way to treat biofilm-based infections.^[25]

As bacterial infections also concern healthcare-associated infections, implant-related infections lead to considerable economic and health problems, including extended hospital stays and raised cost of treatment, and could also induce patient illness and mortality.^[29] For biomedical implants, this issue has been lingering around since decades ago, as according to a study conducted in the early 2000s, implant devices caused 45% of all nosocomial infections (i.e., hospital-acquired infections). These infections are highly resistant to antibiotics and frequently persisted until the removal of the implant.^[30] Furthermore, immunosuppressive therapy used on patients with permanent implants influences bone healing around the implants and leads to increased infection occurrences.^[31–33] In response to

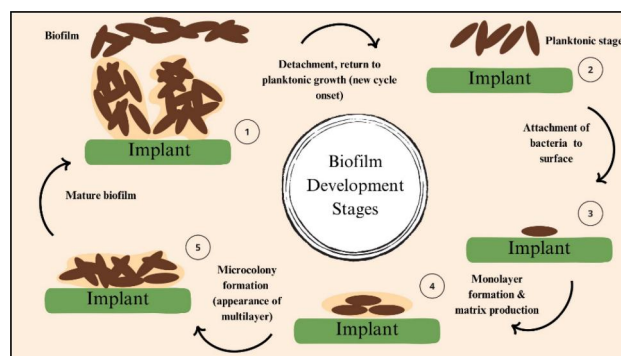


Figure 1. Development stages of bacterial biofilm formation on an implant (adapted from ^[26–28]).

that, metal-based alloys that exhibit antibacterial properties have thus been investigated. Specifically, certain metals such as Cu, Ag, and Zn and some alloys (i.e., certain types of stainless steels – SS) have inherent antibacterial characteristics. These materials have been extensively studied for their ability to inhibit the growth and survival of bacteria on their surfaces, often referred to as “contact killing.”^[34] However, these metal-based alloys have different antibacterial properties depending on the type of bacteria they target, their surface properties, and their composition. With reference to the latter, it is worth mentioning that one of the main objectives and challenges is to fine-tune the chemical composition to be able to design antibacterial materials that kill pathogenic agents without interfering and harming mammalian cells. For instance, Cu is a well-known antibacterial agent but, in too high a concentration, leads to cuproptosis (i.e., cell death triggered by accumulation of Cu in the mitochondria). Consequently, continuous efforts are devoted to exploring and optimizing these materials for various applications, including medical devices, surface coatings, and everyday items, to inhibit the spread of harmful bacteria.

It is thus clear that understanding and analyzing the most recent metal-based alloys characterized by antibacterial capability and elucidating their operating mechanisms is crucial to help finding solutions to prevent bacterial infections. Therefore, the aim of this work is to provide a systematic and comprehensive background and critical analysis of the available literature about bulk metals and their alloys that possess antibacterial properties. After the introduction, the review starts with the analysis of their mechanisms of antibacterial action, for setting the foundations. This is followed by the in-depth analysis of the different metal-based alloys available, and ends with potential applications in various fields, such as medical devices, water purification, and consumer products. To

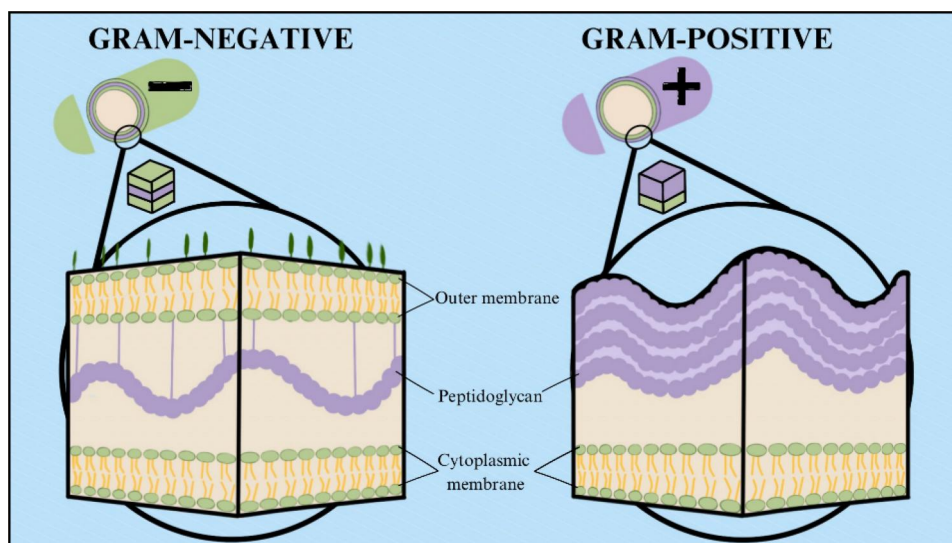


Figure 2. Sketch illustrating the differences between Gram-positive and Gram-negative bacterial cell walls (adapted from^[35,36]). *Note.* Sketches are not to scale.

complement the findings, this review also highlights knowledge gaps, opportunities, and future directions in researching and developing metal-based antibacterial materials.

2. Metal-based alloys antibacterial mechanisms

Some metals and their alloys possess notable antibacterial properties that can offer a defense line against bacterial growth and propagation by several different mechanisms. They can be summarized as killing the bacteria by direct/indirect contact with specific released ions or generation of reactive oxygen species (ROS). Both ions and ROS can disturb the functionality of bacteria and damage cellular components, for instance, by inhibiting protein and enzyme functions and by changing the bacteria's deoxyribonucleic acid (DNA). Regardless of the specific mechanism, antibacterial materials inhibit bacterial growth, eventually leading to bacterial cell mortality. Therefore, to properly understand the antibacterial mechanisms of metals, it is fundamental to have a basic knowledge of the bacterial cell structure, with particular respect to the cell wall. Through their cell wall structure, bacteria can protect themselves from the harsh surrounding environment while still allowing the passage of nutrients and cellular waste products. For that, the multi-layered bacterial cell wall is a mesh-like structure mainly composed of proteins, lipids, and carbohydrates. Based on the structure of the bacteria cell cover, bacteria are classified into two groups: Gram-positive and Gram-negative (Figure 2).

Gram-positive bacteria, an example of which are *Staphylococcus aureus* (*S. Aureus*), *Streptococcus*

mutans (*S. mutans*), and *Bacillus subtilis* (*B. subtilis*), are distinguished by a main outer structure that consists of a thick peptidoglycan cell wall (about 50–80% of its mass) and an underlying cytoplasmic phospholipid bilayer membrane. Conversely, Gram-negative bacteria, such as *Escherichia coli* (*E. coli*), are characterized by a less pronounced (10–20% of the cell wall mass) peptidoglycan wall and have both an outer and a cytoplasmic membrane. The outer membrane has a lipid bilayer containing phospholipids and lipopolysaccharide with transmembrane proteins embedded in it. Non-covalent bonds stabilize the lipopolysaccharide present, these bonds involve Mg and Ca ions. The membrane and the peptidoglycan layer are connected by replacing lipoproteins with a phospholipid layer. The robust structure of the bacterial cell wall is due to the presence of the peptidoglycan wall, which means that the wall's basic structure is constant for different bacterium types. The wall is mainly composed of different polysaccharides/carbohydrates. The cross-link between these polysaccharides and their frequency plays a vital role in the strength of the macromolecular structure formed. Finally, the cell membrane (or the cytoplasmic membrane), primarily a 4 nanometre-thick phospholipid bilayer with embedded proteins, plays a crucial role in maintaining the cell stability and its metabolic functions.^[37–39] The cell wall composition and thickness also influence the bacterial sensitivity.^[30] In particular, literature shows that Gram-negative bacteria are considered to be less sensitive to metal ions due to the low permeability of their outer membrane.^[40,41] Conversely, some strains of Gram-positive bacteria show less susceptibility to well-established

antibacterial metallic elements (e.g., Cu and Ag nanoparticles^[42]).

2.1. Metal ions release

Metallic materials generally release metal ions, and this has been established as an essential antibacterial mechanism for specific elements such as Ag, Cu, and Zn, which are characterized by intrinsic antibacterial activity.^[43] Generally, the released ions target the surroundings of planktonic bacteria.^[44] Such release of atoms carrying an electric charge depends on changes in temperature, pH, and the existence of other chemicals, which might hinder or accelerate the ion-releasing process.^[45] Once released in the surrounding environment, the metal ions act through different mechanisms (e.g., disruption, induction), which in turn determines the overall antibacterial efficacy. The latter is, nevertheless, also dependent on the type of ions, their concentration, the bacterial species, and the conditions of the environment.

2.1.1. Cell wall/membrane disruption

Metal ions can bind to the components of bacterial cell walls, causing structural changes that increase permeability. The disrupted membrane can no longer effectively contain the cell's contents, leading to leakage and, ultimately, cell death. More in detail, the embedded membrane proteins often exhibit anionic net charge, facilitating the binding of positively charged ions at a circumneutral pH and impairing membrane function. Additionally, the different types and numbers of proteins present cause a difference in the membrane's susceptibility to ions. The difference in membrane susceptibility is thought to impact the antibacterial effect of the metals significantly and, therefore, explains the contrasting results obtained by studies applying the same metal against different bacterial species.^[40,41,46–48] As for the lipids, the major component of the membrane bilayer, they are immediately affected by the binding of metal ions. When these ions bind to the membrane, the dipole potential of the membrane is reduced, and the lipids head groups hydration ability is altered.^[49] This results in the disruption of the overall charge of the membrane (Figure 3), accounted for by the increase in permeability and in ROS formation, and the eventual death of the cell.^[48,50–52] Summarizing, the imbalance of ions and the instability established at the membrane level cause impaired cell respiration, disrupt cellular energy transduction, and ultimately lead to the death of the bacteria.^[53]

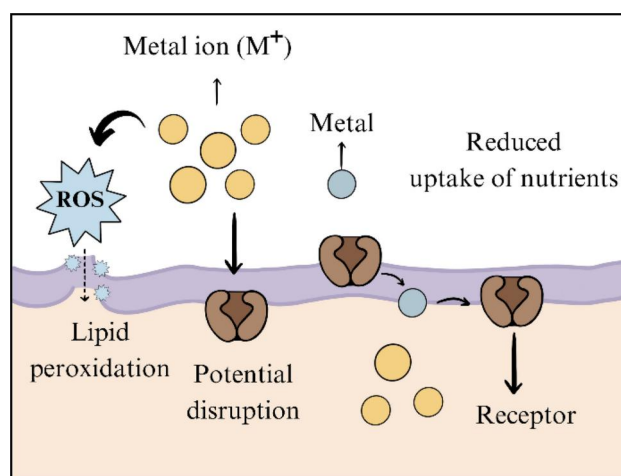


Figure 3. Sketch of the effect of metal ions disrupting the membrane permeability (adapted from^[54]).

2.1.2. Protein dysfunction and inhibition of essential enzymes

Within the bacterial cell, metal ions can bind to critical proteins and enzymes, rendering them nonfunctional. The inhibition of these essential biomolecules disrupts vital biochemical reactions, interfering with the life-sustaining processes of the bacteria. Literature shows that proteins are an obvious target for metal toxicity due to the presence of several amino acid-mediated binding sites. Once the metal ions bind to a protein, they start catalyzing the oxidation of the susceptible amino acids, thus impairing the protein's function, reducing its stability, and leading to its degradation.^[55,56] It has been shown that killing bacteria by inhibiting their growth can happen through the "Trojan horse" mechanism. This mechanism occurs as the bacterial cell takes up a metal ion different from the one in need due to the similarity in chemical properties. Once the cell takes the wrong metal ion, the metallic pathway is disrupted as the cell cannot reduce the ion, and thus, the cell's metabolism is altered.^[57] Site-specific enzyme inhibition is also a mechanism activated by metal ions to kill or inhibit the growth of bacteria (Figure 4a). For instance, the displacement of the catalytic Zn^{2+} , by Pb^{2+} on the active site of the δ -aminolaevulinic acid dehydratase enzyme leads to strong enzyme inhibition^[58] and to antimicrobial activity.^[59] Another process that causes inhibition of enzymatic activity is substituting metals at a non-catalytic metal-binding site (Figure 4b). This is exemplified by Ni^{2+} substituting Zn^{2+} at a non-catalytic Zn binding site in an important enzyme, leading to the inhibition of this enzyme as proven in *E. coli*.^[60]

2.1.3. Oxidative stress induction

Specific metal ions can catalyze the formation of ROS, which cause oxidative damage to various cellular components, including proteins, DNA, and lipids, leading to cellular dysfunction and death. ROS generally define a wide range of oxidant molecules with different properties and broad biological functions ranging from contributing to cell signaling to causing cell damage.^[61] ROS are an intermediate oxidation state species formed due to the incomplete reduction of oxygen molecules. It includes compounds with reactive oxygen without unpaired electrons, such as hydrogen peroxide (H_2O_2), as illustrated in Figure 5a.^[62] In the homeostasis stage, during which a cell maintains a stable internal environment, ROS levels are controlled in such a way that the intracellular antioxidant defense system cleanses all the excess ROS.^[63] When a bacterial cell comes in contact with metal ions, the formation of ROS is enhanced. When the ROS levels exceed the antioxidant's ability to cleanse, ROS cause severe damage to the bacterial cell's components like

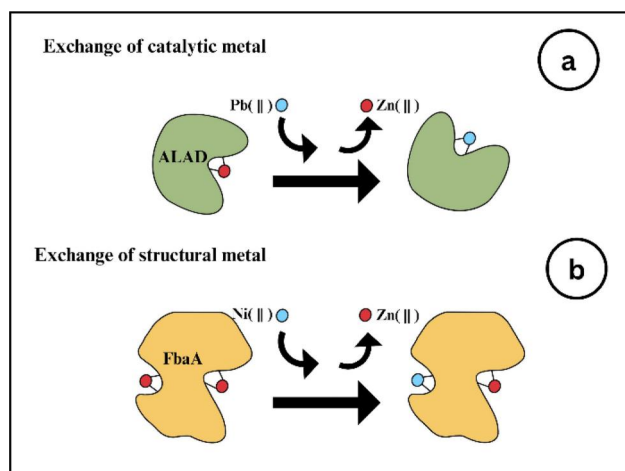


Figure 4. Sketch of the inhibition of enzymes by the site-specific enzyme inhibition mechanism (adapted from^[54]): (a) exchange of a catalytic metal Zn^{2+} ion by a Pb^{2+} ion, and (b) exchange of a structural Zn^{2+} with a Ni^{2+} ion.

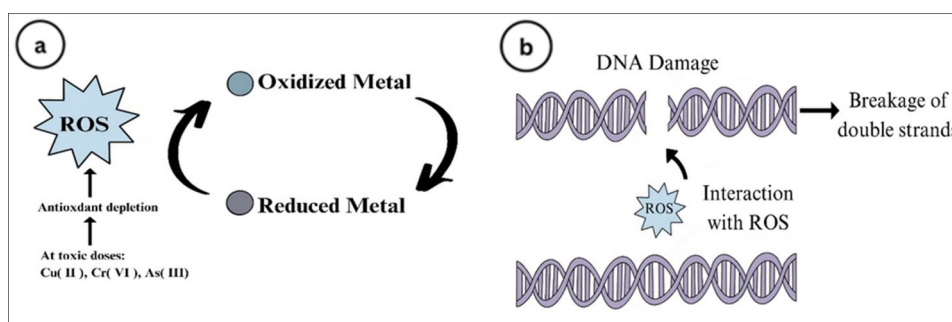


Figure 5. Sketch of reactive oxygen species (ROS) formation and interaction (adapted from^[54]): (a) ROS formation due to toxic doses of metal ions, and (b) breakage of double-stranded DNA due to its interaction with ROS.

DNA (as shown in Figure 5b), lipids, and proteins, thus accumulating oxidative stresses and causing the bacterial cell death.^[64,65]

Many studies have shown that the ions essential for cells, like Fe^{2+} and Cu^{2+} , alongside non-essential ions like Cr^{4+} and As^{3+} , increase the production of ROS in the cell's intracellular environment.^[55,56] The output of these ROS in the intracellular environment has three different mechanisms depending on the specific metal ion. Redox-active metals including Fe, Cu, Cr, and Ni^[62] play a role in Fenton chemistry, the process that converts ROS into toxic hydroxyl free radicals. Some metals interrupt the cellular donor ligand that coordinates Fe in the cell. For instance, metals like Ag, Al, and Cu are able to directly target proteins containing [4Fe-4S] clusters and interrupt the protein's electron transfer function. The above results in the uncontrolled release of Fe into the cytoplasm, further promoting ROS formation.^[66] The presence of specific metal ions can also cause oxidative stress on the bacteria by decreasing the antioxidants present in the cell, reducing the cell defense system, and increasing metal-mediated ROS vulnerability.^[62]

2.2. Bacteria resistance mechanisms

Bacteria have developed various resistance mechanisms against the aforementioned antibacterial mechanisms.^[67] Generally, bacteria are considered to have three main defense strategies to help them survive and provide their cells with the required resistance against metal ions or any other antibacterial agents. The three lines of defense that bacteria have against antibacterial agents (Figure 6) are biofilm formation to prevent antimicrobial agents from penetrating too deeply; reducing absorbance or increasing excretion of antimicrobial agents (comprising the cell wall, cell membrane, and encased efflux pumps); and changing target sites, controlling gene expression, and producing specific enzymes.^[68]

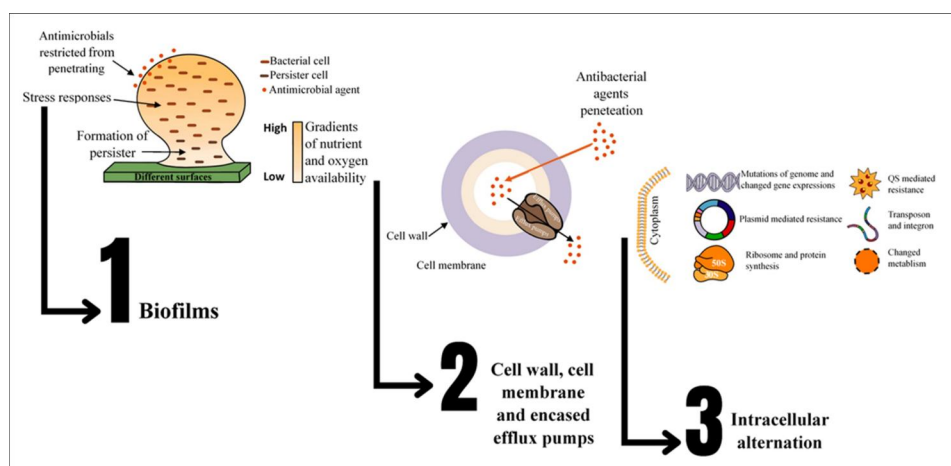


Figure 6. Sketch summarizing the three main resistance mechanisms (i.e., defence lines) of a bacteria (adopted from^[68]).

2.2.1. Permeability barrier

The first step in the action of any bactericide is binding to the bacterial cell surface. From there, it must pass through the Gram-positive or Gram-negative cell wall or outer membrane to get to the cytoplasm or cytoplasmic membrane, which is where it acts. Therefore, limiting the diffusion through the biofilms and cell wall/membrane (i.e., permeability barrier) is one of the available resistance mechanisms. Gram-positive bacteria have no particular permeases or receptor molecules to help or prevent bactericide penetration. Thus, Gram-positive bacteria have a low intrinsic resistance to bactericides. Nonetheless, the Gram-negative cell envelope has developed to control material entry and exit with an astounding level of specificity. Peptidoglycan is the only component of the cell envelope that is not involved in the barrier mechanisms because it is permeable due to its sponginess.^[67] In the case of metal ions, they can diffuse and kill the bacterial cells. However, bacteria can modify their cell wall, membrane, or envelope as a resistance mechanism.^[69] Specifically, a reported bacterial resistance mechanism involves the mutational modification or reduction in expression levels of proteins. An example is porins, which are involved in the uptake of Ag ions and nanoparticles smaller than 10 nm.^[70] Similarly, the alteration of the porin membrane channel by *E. coli* strain B against Cu^{2+} has also been reported.^[71] Additionally, bacteria have the natural ability to create an extracellular polysaccharide coating, once again termed biofilm, that can absorb metal ions and prevent them from interacting with vital cellular components, preventing bacterial cell disruption.^[69,72] In general, bacteria exhibit enhanced resistance by altering the physical barrier in the bacteria membrane, limiting the penetration of metal ions and other forms of bactericides, and hindering their diffusion into deeper layers of the cell.^[73]

2.2.2. Enzyme-mediated resistance

In this mechanism, the enzymes can change bactericides into nontoxic compounds. Typically, the phenomenon is examined and evaluated from the perspective of biodegradation, where the bacteria transform harmful agents in such a way that they become safe for bacterial cells and, therefore, eventually ineffective.^[74] Formaldehyde and heavy metal resistance are two examples of enzyme-mediated resistance mechanisms. For instance, in the detoxification of formaldehyde, which is available and forms naturally, the bacteria develop an antibacterial resistance mechanism by oxidizing to formate and CO_2 .^[75] Research on formaldehyde detoxication conducted on *Pseudomonas aeruginosa* (*P. Aeruginosa*) and *Pseudomonas putida* (*P. putida*) showed that formaldehyde is reduced by a dehydrogenase that is dependent on nicotinamide adenine dinucleotide (NAD) and glutathione, resulting in formaldehyde NAD+oxidoreductase.^[76] In the case of resistance to heavy metals, elements and compounds like Ag, Cd, Co, Cu, Ni, Pb, Sb, Zn, arsenate, chromates, and tellurite have been reported to be heavy metal resistant. These elements are incorporated in heavy metal-resistant genes, which are either chromosomal or carried on plasmids, and detoxication is typically achieved by the enzymatic reduction of the cation to the metal. Arsenate, arsenite, and antimony, for example, induce resistance to each other in *E. coli*.^[76]

3. Antibacterial properties evaluation

Several methods and techniques have been developed to study the antibacterial properties of different substances. These methods include but are not limited to disk diffusion assay, plate-count method, etc., and are based on quantifying the colony-forming unit (CFU), which is an

estimation of the number of microbial cells (e.g., bacteria) present in a sample that can successfully multiply. In order to study the antibacterial properties of metal-based alloys, different approaches have been used. The main ones are discussed hereafter, and they mainly entail observing the bacteria adhesion, the biofilm formation, or the bacterium death.

3.1. Disk diffusion assay

The disk diffusion method is performed by placing the metal-based alloy on a two-layered agar plate (Figure 7). The lower agar layer is composed of a culture medium free of bacteria, and the upper layer of the agar is inoculated by spreading the bacteria to be tested. The prepared plate is generally incubated for 24 h at $35 \pm 2^\circ\text{C}$. After the incubation period, the plate is analyzed to assess the antibacterial properties of the metal-based alloy used by calculating the width of the inhibition zone diameter (IZD) created around the metal sample, which depends on the diameters of the bacteria-free zone and that of the sample itself. After measuring IZD, tweezers are used to remove the sample from the plate to analyze its surface under a microscope. Normally, an IZD of 1 mm or more indicates that the sample tested has good antibacterial properties.

3.2. Plate-count method

The plate-count method is another option available to assess the antibacterial activity (Figure 8), and it is conventionally used for non-porous surfaces. The sample to be tested is placed on a Petri dish with the bacterial suspension poured on it, along with a negative and a positive control sample. Triplicate measurements are commonly carried out. Each prepared

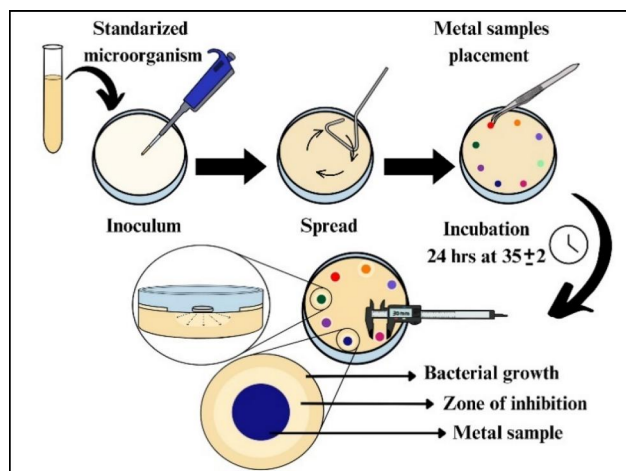


Figure 7. Sketch of the disk diffusion assay (adapted from^[77]).

sample is then covered using a sterile polyethylene film with its dimensions cut precisely to ensure that the bacterial suspension is evenly spread and yet it does not leak beyond the edges of the film. Subsequently, the plate is incubated at $35 \pm 1^\circ\text{C}$ for a period of 24 h, maintaining the humidity level $\geq 90\%$.

After the incubation period, the sample and the polyethylene films are washed by adding sterilized saline water to the Petri dish. This step is crucial to ensure that the sample and the film no longer carry any bacteria. A small amount (generally 0.1 mL) of the used washing solution is then inoculated into a nutrient agar and incubated at $35 \pm 1^\circ\text{C}$ for 24 h, once again maintaining a minimum humidity level of 90%. The number of bacteria colonies on the plate after incubation is quantified for both samples and control. The average number of bacterial colonies present in the control (N_{control}) and in the sample (N_{sample}) are then used to calculate the antibacterial activity (R) using Equation (1).

$$R = \frac{N(\text{control}) - N(\text{sample})}{N(\text{control})} \times 100 \quad (1)$$

3.3. Live/dead staining

The third available option to assess the antibacterial activity is the Live/Dead staining method (Figure 9). This technique relies on staining the bacteria with special dyes that differentiate the live bacteria from the dead ones. Initially, the bacterial suspension of interest is dripped on the surface of the antibacterial sample, or the sample itself is submerged in the bacterial suspension. After incubating for 24 h, the surface of the sample is gently washed three times using a phosphate buffer saline solution to ensure the removal of any traces of the culture medium. Subsequently, two different fluorescent dyes are added to the bacteria on the sample in the dark at room temperature, and the sample is observed with a confocal laser scanning microscope (CLSM). The dominance of red reflects a high number of dead bacteria, indicating high antibacterial activity. On the other hand, the dominance of green reflects a high number of live bacteria, associated with low antibacterial activity.

3.4. Factors affecting the evaluation of antibacterial performance

It is important to stress that, throughout the evaluation, testing conditions must be standardized to evaluate the antibacterial properties of metal-based alloys. Many factors, such as temperature, humidity,

water availability, and gaseous concentration, contribute to the growth of bacterial cultures on surfaces. The variation of any of these factors while performing the tests might affect the results, leading to false positive or false negative readings. For instance, while spreading the bacterium inoculum on the metal surface, *in vitro* tests usually keep the surface wet for 24 h. This is not necessarily maintained in real-case scenarios, as most microbial contaminants dry, thus limiting the time available for the bacteria to interact with the surface. Furthermore, evaluating the antibacterial properties of non-porous surfaces such as bulk metals is not always ideal, as identifying the best control surface is challenging.^[79] Moreover, the standard adapted to evaluate the antibacterial activity also plays a role in determining if the metal is marked as a good or bad antibacterial agent. For instance, the United States standards mark an agent as a good sanitizer if it kills more than 99.9% of pathogens for 1 h intervals. On the other hand, the Japanese and European standards provide a framework for standardized

quantification of antibacterial activity instead of giving a threshold like the US standard.^[80]

Another crucial aspect is the roughness of the tested metallic surface, as it was shown that a higher antibacterial activity is expected in rougher surfaces.^[81] This is due to the fact that bacterial cells can be trapped in the concavities formed by the surface roughness, inhibiting their ability to form a biofilm. Additionally, a rough surface has a greater contact surface area with respect to a polished surface, which is beneficial in antibacterial capability terms. Finally, the increase in the contact surface area is accompanied by an increased moisture content in the surface, enhancing the ability of the hydrophilic bacterial cells to adhere to the surface. Therefore, these effects can lead to an overestimation of the antibacterial effect of metal-based alloys.^[80]

4. Alloys with antibacterial capability

The use of metal-based alloys (e.g., Ag, Fe, Mg, Ti, Zn, and Zr) with antibacterial activity has attracted

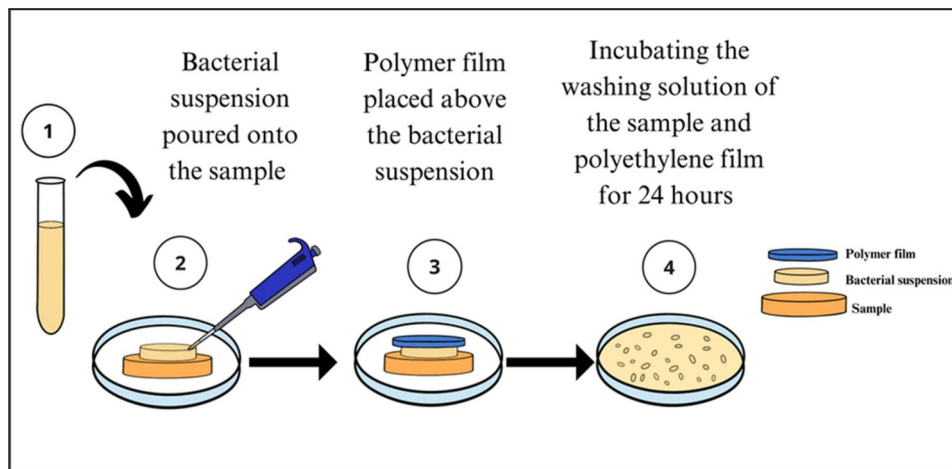


Figure 8. Sketch of plat count method (adapted from^[78]).

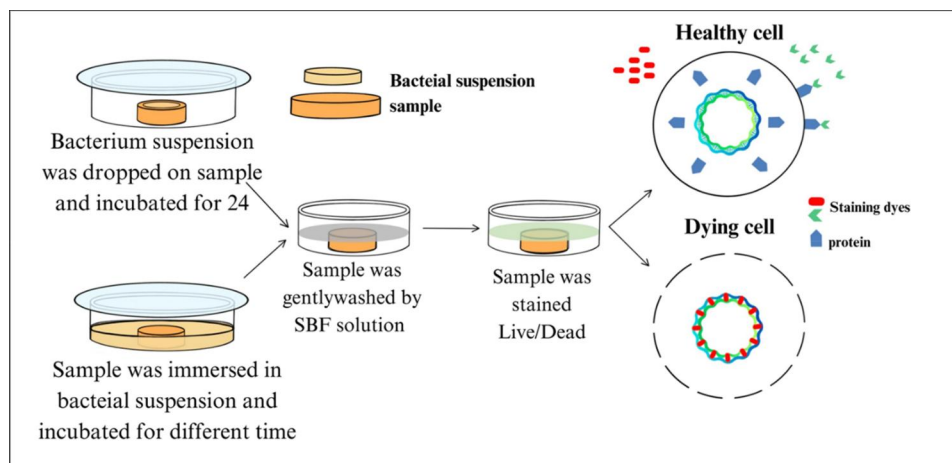


Figure 9. Sketch of the live/dead staining method (adapted from^[54]).

scientists in many fields, such as but not limited to water treatment, food processing, healthcare setting, marine applications, body implants, and biomedical devices.^[82,83] This is due to the fact that these metal-based alloys are characterized by proper combinations of physical properties and mechanical behavior along with good antibacterial activity, which is proven to be effective in inhibiting microbial growth. As an overview, Ag and Cu are well-known for their intrinsic antibacterial activity and capability and are, therefore, highly utilized as alloying elements and in surface coatings.^[84] Co-based alloys are excellent alloys due to their high melting point, which allows them to work in high-temperature and high-pressure environments.^[85,86] Fe- and Zn-based alloys have developed potential for agricultural uses as well as for water purification.^[87,88] Mg-based alloys are well known for their bioactivity, biodegradability, and biocompatibility.^[89,90] Finally, Ti- and Zr-based alloys are used for body implants and medical devices^[91,92] due to their corrosion resistance, biocompatibility, and mechanical properties.^[93,94] From that, the aim of this systematic review is to comprehensively analyze and discuss recent works and progress about metal-based alloys with antibacterial capability based on the previously mentioned elements. Nonetheless, before delving into it, a brief analysis of the effect of the specific alloying elements and manufacturing methods is provided.

4.1. Antibacterial metallic elements

For specific engineering applications such as biomedical devices, the first choice is the metal-based (i.e., metallic matrix), which is selected due to its intrinsic properties. For instance, Ti-based alloys are generally chosen for permanent total replacement implants because Ti is biocompatible, is corrosion resistant, has a good weight-strength ratio, has excellent mechanical properties, and has a stiffness much more comparable to that of human bones with respect to other competing metals like SS. Supposing that Ti itself might have some antibacterial capability, this may not be sufficient as the antibacterial activity might not be as strong or effective as in other materials. The addition of alloying elements is then considered to enhance the antibacterial response or any other property of interest for that specific application. Therefore, it is essential to first understand and evaluate the antibacterial properties of pure metallic elements to be able to utilize them in the design of metal-based alloys with antibacterial capability.^[54,95] The most well-known metallic elements used as antibacterial agents are Cu

and Ag. It has been proven that their addition transforms an inert metal into an active antibacterial metal-based alloy, which is exemplified by Ag being globally considered one of the earliest materials used in surgical applications due to its intrinsic antibacterial activity.^[96] The addition of Ag or Cu is also considered to increase an alloy's antibacterial rate substantially.

Metallic elements like Co, Cu, Mo, Ni, Pb, Zn, and Zr have been confirmed to possess antibacterial activity against both Gram-positive and Gram-negative bacteria.^[97] In the 24 h incubation period, CFU on their surfaces decreased from 10^6 to 10^1 . Amongst them, Co, Cu, and Pb were reported to be the most effective metals that can resist bacteria and eventually kill them. Similarly, another study analyzed the antibacterial properties of a group of pure metals, which were tested to find their antibacterial activity using two methods after 24 h of incubation.^[54] The plate-count method showed that Co, Cu, Ni, Mo, Pb, Zn, and Zr have antibacterial properties against Gram-negative and Gram-positive bacteria, whereas Ti was only effective against Gram-negative bacteria. The shaking flask method – a method where cells are exposed to low oxygen concentration – demonstrated that only Co and Zn have excellent antibacterial properties against Gram-negative bacteria and only Pb has good antibacterial properties against Gram-positive bacteria. Kawakami et al.^[98] also investigated various metallic elements' antibacterial ability against Gram-positive and Gram-negative bacteria using the plate-count method. It was found that Ag, Al, Co, Cu, Mo, Ni, Pd, W, and Zn showed antimicrobial activity against both bacteria. Additionally, Pt has antibacterial ability against Gram-negative, whereas V and Zr against Gram-positive. All these studies confirmed that Ag and Cu are characterized by superior antibacterial effectiveness in comparison to all the other metallic elements tested.^[99]

To summarize, reported metals that exhibit some antibacterial activity against Gram-positive bacteria include Ag, Co, Cu, Ni, Mo, Pb, Pd, V, W, Zn, and Zr and metals that show good antibacterial activity against Gram-negative bacteria are Ag, Co, Cu, Ni, Mo, Pb, Pd, Pt, Ti, W, Zn, and Zr.

4.2. Role of manufacturing methods

One of the significant areas of research in antibacterial metal-based alloys is the impact of manufacturing processes on the antibacterial response. This is because metallic elements with intrinsic antibacterial

capability are, most of the time, used as alloying elements in base metals to establish or enhance the antibacterial response. The actual manufacturing process used to obtain the antibacterial element(s)-containing metal-based alloys has a direct impact on final antibacterial activity. Therefore, the manufacturing method can, and it is most of the time used to, alter the base metal composition,^[100,101] internal structure,^[102,103] and surface properties,^[104,105] all of which affect the material's capacity to inhibit bacteria growth.^[54]

One of the most common manufacturing processes used to obtain antibacterial metal-based alloys is casting, due to its simplicity.^[106-109] Nonetheless, casting generally does not lead to the required internal structure and thus, heat treatments such as solution plus aging are commonly used to modify the internal structure.^[110-112] Several investigations showed that the temperature and duration of the aging heat treatment influence the antibacterial properties as they should be highly effective in inducing the precipitation of nano-scale intermetallic particles (e.g., Cu-rich phase) within the metal-based matrix for achieving high antibacterial activity. For example, in Wang et al.'s study^[113] the Cu-bearing martensitic SS only had an antibacterial rate of 69.2% against *S. aureus* after aging at 500 °C for 4 h. However, the antibacterial rate was significantly increased to as high as 94.0% after different aging treatments in the 500–800 °C temperature range for 6 h. Xie et al.^[114] showed that the Ti-xFe ($x=3, 5$ and 9) alloys possessed excellent antibacterial properties (above 90.0%) as a consequence of the heat treatment applied to them. It has also been reported that heat treatments significantly influence the antibacterial characteristics of binary Ti-Ag and Ti-Cu, where, once again, the primary effect of the heat treatment is the modification of the internal structure of the antibacterial Ti-based alloys. In particular, heat treatments for binary Ti-Ag and Ti-Cu alloys are designed to maximize the precipitation of nanoscale Ti_2Cu or Ti_2Ag intermetallic particles within the microstructure, which results in a significant improvement of the antibacterial properties.^[115,116] It is, however, worth noticing that any heat treatment applied to enhance the antibacterial response does also affect the mechanical behavior. It is commonly found that the most common heat treatments (i.e., solution plus aging) deteriorate the ductility as they generally improve both strength and hardness.^[115,116] Additionally, as any heat treatment changes the microstructure of the alloy, they have also been used with the aim of enhancing other

properties.^[117] For instance, it has been proven that heat treatments such as annealing, solid solution, and aging improve the corrosion resistance of Co-xCu alloys without sacrificing the antibacterial properties.^[118] Finally, in the case of cast antibacterial metal-based alloys, hot forming processing and/or thermo-mechanical techniques like extrusion are often used to modify the microstructure with the aim of improving the mechanical performance (e.g., strength and ductility) while maintaining antibacterial capability.^[119]

The most commonly used manufacturing technique as an alternative to casting is powder metallurgy (PM), where the alloy is designed and produced starting from loose powder particles, which are consolidated (i.e., pressed and sintered) into a solid metal-based alloy.^[120-122] It has been shown that PM is beneficial to achieve antibacterial properties in metal-based alloys, where the antibacterial response is influenced by the base metal of choice, the properties of the powder, the consolidation technique, and any additional heat/surface treatments. For example, PM has been used to create antibacterial Ti-Ag alloys whose properties are comparable and whose Ag content is lower with respect to cast Ti-Ag alloys. Furthermore, the previously described heat treatments have been shown to be suitable to induce antibacterial capability in the PM Ti-6Al-4V-Cu alloy.^[123,124] Amongst PM techniques, metal additive manufacturing (MAM) is one of the latest development, which is commonly used because the geometry and the superficial structure of a component can be precisely controlled. Through this technique the properties of the surface can then be tailored to discourage the growth and adhesion of bacteria, where surface roughness, texture, and specific patterns can be optimized to prevent bacterial colonization. The addition of antibacterial metallic elements like Ag and Cu to conventional metal-based alloys processed by MAM has been proven to produce products with intricate geometries and antibacterial properties.^[125,126] For example, selective laser melting (SLM), one of the MAM processes, has been used to fabricate a series of Ti-6Al-4V-xCu alloys where the inclusion of Cu led to the development of an antibacterial response. Specifically, research on Ti-6Al-4V-xCu produced by SLM revealed that the antibacterial activity increases with the Cu content and is able to reach a high level of antibacterial activity against *S. aureus* and *E. coli* (>90.0%); a Cu content of at least 4 wt.% is required.^[127] Similarly to SLM, the broader field of study of laser powder bed fusion (LPBF) has focused on the individual adjustment of the surface roughness,

Table 1. Summary of the Co-based alloys with antibacterial capability.

Composition (wt.%)	Bacteria	Test method	Antibacterial rate (%)	Ref.
Co-(1-4)Cu	<i>S. aureus</i>	CFU method	94.2 – 99.6	[130]
Co-Cr-Mo-(1-4)Cu	<i>S. aureus</i>	CFU method	90.0 – 99.0	[131]
Co-29Cr-6Mo-1.8Cu	<i>S. aureus</i>	–	>99.0	[132]
Co-Cr-W-(2-4)Cu	<i>E. coli</i>	Plate-count method	–	[133]
Co-Cr-W-Ni-4.39Cu	<i>E. coli</i>	SEM biofilm observation	>90.0	[134]
CoCrFeCuNi (Cu = 22)	<i>S. aureus</i>	Plate-count method	98.0	[135]
	<i>E. coli</i>			
	<i>S. aureus</i>			
Co-30Cr-5Ag (at.%)	<i>S. aureus</i>	Live/Dead staining technique	99.0	[136]
	<i>E. coli</i>	SEM observation of bacteria	90.5	
	<i>S. aureus</i>		72.6	

texture, and topography of metal-based alloys, aiming at influencing the material's bacterial adhesion and biocompatibility.^[128] For instance, Behjat et al.^[129] analyzed the *in situ* alloying of the AISI316L SS with Cu, demonstrating that practically all of the bacteria were eradicated and the material's antibacterial qualities were strengthened, achieving antibacterial rates of $93.4 \pm 1.2\%$ for *S. aureus* and $97.8 \pm 0.8\%$ for *E. coli*.

4.3. Antibacterial metal-based alloys

4.3.1. Co-based alloys

This section considers the development of antibacterial Co-based alloys and analyzes the available performance reported in literature, which is summarized in Table 1. It is worth mentioning that Co-based alloys are primarily used for structural applications such as permanent dental implants and biomedical prostheses.

Binary Co-based alloys were proposed by Zhang et al.^[130] who examined the antibacterial properties of the Co-xCu alloys with a range of Cu content from 1 wt.% to 4 wt.% produced *via* casting. The *S. aureus* bacteria were incubated for 24 h in Petri dishes, and the results of the CFU method showed that with the increment of Cu content, the antibacterial effect increased. In addition, it was observed that the Co-1Cu and Co-2Cu samples had a small number of bacterial colonies, and the Co-4Cu samples showed almost no bacterial colonies. The antibacterial rate of the Co-1Cu alloy was 94.2%, that of the alloy Co-2Cu was 98.5%, and that of the Co-4Cu alloy was 99.6%, indicating their superior antibacterial performance. The authors confirmed that releasing Cu ions is vital to killing the bacteria. Co-1Cu had a YS of 310 MPa, a UTS of 447 MPa, an elongation of 18.5%, and a microhardness of 292 HV. Co-2Cu had a YS of 432 MPa, a UTS of 499 MPa, an elongation of 11.5%, and a microhardness of 279 HV. Finally, Co-4Cu had a YS of 440 MPa, a UTS of 620 MPa, an elongation of 15.2%, and a microhardness of 274 HV.

Much more attention has been paid to quaternary Co-based alloys on the basis of the fact that they are

expected to have superior performance. For example, Duan et al.^[131] investigated the antibacterial properties of cast Co-Cr-Mo-Cu alloys, where the Cu content ranged from 1 wt.% to 4 wt.%. After incubating *S. aureus* in the agar medium for 24 h, it was observed that the Co-Cr-Mo-1Cu alloy showed a few bacterial colonies, which were significantly less in the Co-Cr-Mo-2Cu alloy, and, finally, the Co-Cr-Mo-4Cu alloy nearly showed no bacterial colonies. It was found that the Co-Cr-Mo-2Cu alloy had good antibacterial performance with a rate above 90.0%, and the Co-Cr-Mo-4Cu alloy had excellent performance with a rate above 99.0%. The authors reported that the release of Cu ions contributed to such performance. No mechanical properties were quantified. Zhang et al.^[132] examined the antibacterial behavior of the Co-29Cr-6Mo-1.8Cu (wt.%) alloy prepared *via* casting and found that very fine Cu precipitates existed in the microstructure. This led to the enhancement of the antibacterial behavior of the alloy against *S. aureus* to >99.0%. The hardness of the alloy reached 21 HRC. Lu et al.^[133] studied the antibacterial behavior of the Co-Cr-W-Cu alloy with a range of Cu content from 2 wt.% to 4 wt.% fabricated using SLM. It was observed that the Cu-free Co-Cr-W alloy showed the greatest mechanical properties, which decreased after adding Cu. On the other hand, using the plate-count method, the *E. coli* bacterial colonies decreased gradually with the increment of the Cu content. There was a limited number of colonies in the Co-Cr-W-3Cu alloy, and in the case of the Co-Cr-W-4Cu alloy, the bacterial colonies vanished, indicating superior antibacterial performance as a result of Cu ions releasing. With the increment of Cu content, the elongation decreased to 5%. YS and UTS also decreased, yet the YS was >500 MPa.

Regarding quinary Co-based alloys, Wang et al.^[134] analyzed the antibacterial behavior of the Cu-bearing Co-Cr-W-Ni alloy subjected to different solution and aging heat treatments. The antibacterial rates against *E. coli* and *S. aureus* were more than 90.0% for the alloy that had the highest Cu content (i.e., 4.39 wt.%)

for which the number of Cu ions released is high enough to improve the antibacterial performance. Scanning electron microscopy (SEM) results confirmed that no *S. aureus* biofilm formation on the surface occurred. No mechanical properties were reported. In another work about quinary Co-based alloys, Gao et al.^[135] investigated the antibacterial properties of the Co-Cr-Fe-Cu-Ni alloy fabricated using SLM and *in situ* alloying, quantifying the compressive yield stress (CYS), which was 516 MPa. Also, no fracture occurred during the compression test, indicating that the alloy is highly ductile. Using the plate-count method for the Gram-positive *S. aureus* and the Gram-negative *E. coli*, it was observed that the alloy had a small CFU, and the antibacterial rate against *E. coli* and *S. aureus* was 98.0% and 99.0%, respectively. The Live/Dead staining technique had similar results, as it showed thin biofilm on the surface of the alloy, which was prevented from growing by the release of Cu ions.

Apart from the use of Cu as an antibacterial metallic element, the addition of Ag was also considered in Co-based alloys. For instance, Jiang et al.^[136] studied the antibacterial properties of the ternary Co-30Cr-5Ag (at.%) alloy prepared using MA and sintering. After 24 h of incubation of *S. aureus* and *E. coli* in the agar media, it was observed that the alloy had a smaller number of bacterial colonies than the alloy that did not bear Ag as an alloying element. Its antibacterial rate against *E. coli* was 90.5% and 72.6% against *S. aureus*, ascribed to the release of Ag ions. The alloy had a CYS of 2090 MPa, an ultimate compressive strength (UCS) of 2300 MPa, and a hardness of 650 HV.

Figure 10 shows the comparison of the antibacterial efficacy of different Co-based alloys. Against Gram-positive bacteria, a consistently high antibacterial rate among the various Co-based alloys is found (Figure 10a), meaning that the inclusion of Cu is beneficial, with the Co-Cr-Mo-1.4Cu and Co-Cr-W-Ni-4.3Cu alloys showing a very high rate of antibacterial activity. Notably, the Co-29Cr-6Mo-0.18Cu alloy does not perform as well as others with higher Cu content, reinforcing that the Cu content is critical for maximizing the antibacterial effect. The alloys that include other elements such as W, Ni, and Fe, namely Co-Cr-W-Ni-4.3Cu and Co-Cr-Fe-Cu-Ni, also exhibit high antibacterial rates, pointing to the synergistic effects that these elements may have when combined with Cu. In the case of Gram-negative bacteria, a similar trend is found (Figure 10b), although the variation in antibacterial rates is more pronounced. The Co-Cr-W-Ni-4.3Cu alloy stands out with the highest

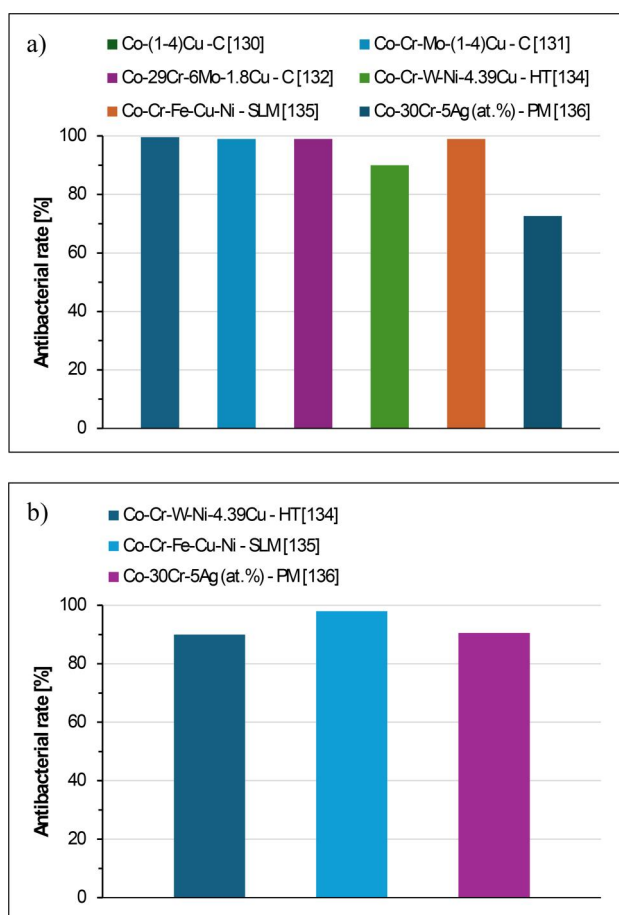


Figure 10. Comparison of the antibacterial efficacy of various Co-based alloys: (a) antibacterial rate against Gram-positive bacteria, and (b) antibacterial rate against Gram-negative bacteria. Legend. C: cast, HT: Heat treated, SLM: selective laser melted, and PM: powder metallurgy.

value. Moreover, the Ag-containing alloy (i.e., Co-30Cr-5Ag) also has a high antibacterial rate, which is comparable to that of Cu-containing Co-based alloys. The Co-Cr-Fe-Cu-Ni alloy demonstrates an excellent antibacterial rate, suggesting that combining these five elements creates an effective barrier against Gram-negative bacteria. Therefore, Co-based alloys effectively prevent bacterial growth when alloyed with Cu and other elements such as W, Ni, and Fe. The fact that Cu consistently appears to be a strong contributor to the antibacterial efficacy reinforces the notion that Cu is a versatile antimicrobial agent. Moreover, the presence of Ag in the Co-30Cr-5Ag alloy and its notable antibacterial rate against Gram-negative bacteria is in line with the well-documented antimicrobial properties of Ag. The data suggest that creating Co-based alloys with a balanced combination of these elements could provide a tailored approach to combatting specific bacterial threats. It is, however, worth noting that this comparison does not take into

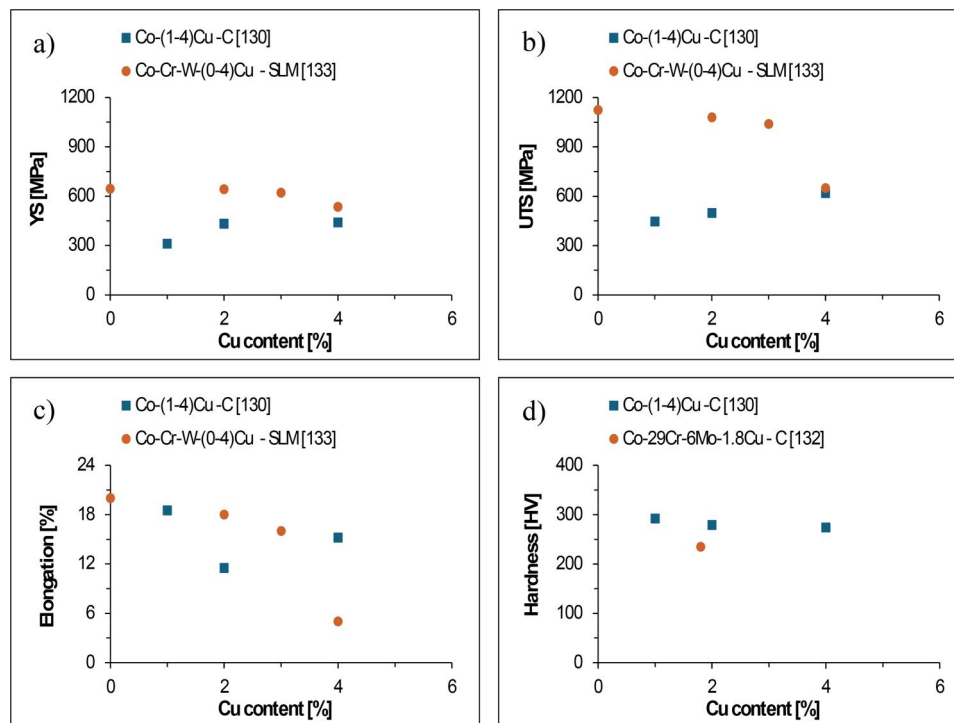


Figure 11. Mechanical properties (tensile and hardness) of antibacterial Co-based alloys as a function of the Cu content: (a) YS, (b) UTS, (c) elongation, and (d) hardness. Legend: C: cast, and SLM: selective laser melted.

Table 2. Summary of the Fe-based alloys with antibacterial capability.

Composition	Bacteria	Test method	Antibacterial rate (%)	Ref.
Fe-1.5Cu	<i>E. coli</i>	Plate-count method	96.5	[138]
Fe-(2.3–10.1)Cu			>99.9	
Fe-8Cu	<i>E. coli</i>	Plate-count method	99.9	[139]
Fe-30Mn-1C-0.8Cu	<i>S. aureus</i>	Live/Dead staining method	99.0	[140]
Cu-containing (1.5–5.5) SUS 304 SS	<i>S. aureus</i>	Plain-plate dilute method	99.9	[141]
SS316–2.5Cu (aged)	<i>E. coli</i>	Plate-count method	94.5	[142]
SS316–3.5Cu (aged)			98.9	
2205–3.02Cu duplex SS	<i>P. aeruginosa</i>	CFU method	70.3	[143]
200 SS-1.45–3.57Cu	<i>E. coli</i>	SEM observation of bacteria	56.1 – 99.9	[144]
SS316L-3.77Cu	<i>S. aureus</i>		42.8 – 99.9	
	<i>E. coli</i>	Plate-count method	94.8	[145]
	<i>S. aureus</i>	SEM observation of bacteria	95.2	
	<i>S. epidermidis</i>		94.1	
3.8Cu-austenitic SS	<i>E. coli</i>	Film attachment method	99.9	[146]
Cu-bearing (3.9) 304SS	<i>P. gingivalis</i>	standard film-covered method	95.6–100	[147]
Cu-containing (4.46) SS317L	<i>S. aureus</i>	DAPI staining method	99.0	[148]
Cu-containing (4.5) 317 L	<i>E. coli</i>	SEM biofilm observation	–	[149]
	<i>S. aureus</i>	Plate-count method		
SS-9.5Cu	<i>E. coli</i>	–	20.0	[150]
SS-18Cu			65.0	
Ag-containing (0.07) CD4MCu duplex SS	<i>E. coli</i>	Plate-count method	>99.9	[151]
Ag-containing (0.1–0.3) 304SS	<i>E. coli</i>	Gram-stain technique	70.8 – 99.9	[152]
	<i>S. aureus</i>		99.7 – 99.9	
2205–0.2Ag duplex SS	<i>E. coli</i>	–	100	[153]
	<i>S. aureus</i>		99.5	
La-containing steel (La = 0.05–0.42)	<i>E. coli</i>	Plate-count method	15.0 – 99.6	[154]
	<i>S. aureus</i>		9.0 – 99.0	

account any effect derived by the specific manufacturing process used to obtain the alloys.

A summary of the tensile properties and hardness reported in literature for the Co-based alloys analyzed is presented in Figure 11. It can be seen that two

contrasting trends are found depending on the actual base metal, as YS (Figure 11a) and UTS (Figure 11b) both increase with the amount of Cu added when pure Co is the base metal, but the same properties decrease if Co-Cr-W is used. A more consistent

behavior is found in terms of ductility as the elongation (Figure 11c) generally decreases with the amount of Cu regardless of the actual base alloy. Similarly, the hardness (Figure 11d) of the antibacterial Co-based alloys decreases with the Cu content. The mechanical behavior achieved is obviously the outcome of the combined effects of the chemical composition of the Co-based alloys and the manufacturing process used to obtain them. This reinforces the fact that the selection of the base metal and the antibacterial metallic elements chosen is crucial, as their combination can lead to unpredictable synergistic effects that might be beneficial from a biological point of view but not for the mechanical behavior, and the other way around.

4.3.2. Fe-based alloys

The antibacterial Fe-based alloys developed in literature and their performance are reported in this section and summarized in Table 2, where it can be seen that the majority of the reported studies considered the modification of existing ferrous alloys,^[137] especially SS, with different elements. This is because SS is a standard metal-based alloy utilized in biological applications due to its corrosion resistance, and it is primarily used for structural biomedical applications. However, some few studies also considered the modification of pure Fe with Cu to test the antibacterial response, where the main idea is to use pure Fe or its modifications in transient biodegradable biomedical implants.

In that respect, Guo et al.^[138] examined the antibacterial properties of the Fe-xCu alloys prepared by SLM, where x is the Cu content, which had a range of 1.5 wt.% to 10.1 wt.%. It was observed that the antibacterial rate against *E. coli* had a direct proportionality with the Cu content added, meaning that with the increment of the Cu content, the antibacterial rate improved. In addition, using the plate-count method, it was concluded that the agar plate for the alloys created by SLM, pure Fe, was obscured by *E. coli*. On the other hand, when Cu was alloyed with Fe in the SLM Fe-xCu alloys, the number of *E. coli* colonies reduced significantly with the increases of the Cu content. The inhibition of *E. coli* colonization was the result of Cu ions releasing. It was indicated that all of the Fe-xCu alloys exhibited superior antibacterial activity with the following observation: the antibacterial rate of the SLM Fe-1.5Cu alloy was 96.5%, and that of the Fe-2.3Cu, Fe-7.8Cu, and Fe-10.1Cu alloys was higher than 99.9%. The hardness of the alloy increased with the increment of the Cu content, reaching 400 HV.

The study conducted by Deng et al.^[139] examined the antibacterial properties of Fe-8Cu (wt.%) alloy produced by PM. Using the plate-count method with the *E. coli* bacteria, it was observed that the sintered pure Fe surface had many bacterial colonies. In contrast, the colonies vanished in the Fe-8Cu samples. Moreover, it was clear that the sintered Fe-8Cu samples had outstanding antibacterial capabilities since the Cu ions released from the samples had antibacterial rates that were up to 99.9% effective against *E. coli*. The two major factors causing this antibacterial efficacy were the structure and phase composition of the sintered Fe-8Cu samples. Specifically, it was reported that the presence of a porous structure may result in the bacterial cell membranes being perforated, deformed, or damaged, killing the microorganisms. When the Cu-rich phase on the surface of sintered Fe-Cu samples came into contact with the solution, redox reactions happened. The two elements, Cl^- and Fe^{3+} ions, which might encourage the release of Cu ions, were the primary causes of these redox reactions. The released Cu ions encountered the bacteria on the surface of the sintered Fe-Cu samples. Cu ions stripped bacteria of their electrons and decreased cell membrane permeability, leading to bacterial cytoplasm loss. The hardness of the microwave-sintered pure Fe was recorded as 101 HV and it increased to 127 HV with the addition of Cu.

Apart from the antibacterial properties of binary Fe-based alloys, a specific quaternary Fe-based alloys, was also considered in the study carried out by Ma et al.^[140] who investigated the antibacterial activity of the Fe-30Mn-1C-0.8Cu (wt.%) alloy produced by ingot melting and hot forging. The antibacterial rate of the Fe-30Mn-1C-0.8Cu alloy was up to 99.0%, indicating excellent antibacterial efficacy against *S. aureus*. In addition, Live/Dead staining revealed that the Fe-Mn-C-Cu alloy could destroy the bacterial cell wall. SEM observation showed that the pure Fe surface had spherical *S. aureus* and formed biofilm. On the other hand, the Fe-Mn-C-Cu has a minimal amount of widely scattered bacteria, and it was not prone to creating a biofilm. The primary explanation was that the Cu^{2+} ions released from the Fe-Mn-C-Cu alloy surface could effectively kill the bacteria through degradation. The bacteria adhesion and proliferation on the surface of the alloy were obstructed by the constant release of Cu^{2+} ions, preventing the bacterial biofilm development. YS of the alloy was 536 MPa, UTS was 1078 MPa, and the elongation was 35%.

As previously indicated, the majority of the work done on antibacterial Fe-based alloys was on SS, and

different grades were analyzed, which are reviewed afterwards on the basis of the increase of the antibacterial metallic element used. Hong et al.^[141] examined the antibacterial properties of the Cu-containing SUS 304 austenitic SS with a range of Cu content from 1.5 wt.% to 5.5 wt.% prepared by the casting method followed by an aging treatment. *S. aureus* was the microorganism used to test antibacterial activity. Using the plain-plate dilute method, results showed that as the Cu content and aging treatment time increased, the antibacterial performance was enhanced. Cu ions are formed from the precipitated ϵ -Cu phase on the surface of SS, which then comes into contact with the bacteria. These Cu ions killed the bacteria by rupturing their cell walls and membranes, where they are able to capture their electrons, causing the bacteria's cytoplasm to leak out and their cell nucleus to get oxidized. As the Cu content was over 3.5 wt.% the antibacterial rate was recorded to be 99.9%, indicating excellent antibacterial performance. The hardness and UTS decreased with adding Cu content below 2.5 wt.%, yet they increased when more than 2.5 wt.% of Cu was added. UTS was 580 MPa, and hardness was 240 HV. A similar amount of Cu (i.e., 2.5–3.5 wt.%) was used by Xi et al.^[142] to examine the antibacterial properties of 316-Cu austenitic steel exposed to different solutions and aging treatments. Using the plate-count method, it was observed that many *E. coli* colonies almost covered the Petri dishes of the solution-treated steel specimens. However, the aging-treated specimens had a drastically lower number of colonies. Thus, the antibacterial performance was greatly affected by the Cu content and the aging treatment, as well as the Cu ion release, which had a significant role in killing the bacteria. The aging-treated specimens exhibited an antibacterial rate of up to 98.2%, indicating excellent antibacterial performance. The alloy sample with the highest Cu content and undergoing aging treatments had the best YS (257 MPa) and UTS (543 MPa) results with an elongation of 60%. Similarly, Lou et al.^[143] scrutinized the antibacterial properties of Cu-bearing 2205 duplex SS with a Cu content of 3.02 wt.%, comparable to previous studies, subjected to different heat treatments. It was observed that as the incubation period of *P. aeruginosa* increased, the antibacterial performance of the 2205-Cu duplex SS improved till the rate reached 70.3%. This indicates that it has a bacterial inhibition capability, which was observed using the CFU and Live/Dead staining method. The 2205-Cu duplex SS effectively prevented biofilm development and growth, reduced biofilm thickness, and eliminated sessile *P.*

aeruginosa. No mechanical properties were mentioned. Lastly, Nan et al.^[144] studied the antibacterial behavior of type 200 austenitic SS after adding Cu with a range of 1.45–3.57 wt.%, produced using different heat treatments followed by aging treatments. It was observed that the antibacterial performance increased with the increment of Cu content as the samples had a range of antibacterial rates against planktonic bacteria of *E. coli* from 56.1% to 99.9% and the rate against planktonic bacteria of *S. aureus* from 42.8% to 99.9%. The steel had a higher antibacterial effect on *E. coli* than *S. aureus*, most likely due to the thicker cell wall, which better resisted the attack from Cu ions. No mechanical properties were mentioned.

Cu contents around 3.5–4.0 wt.% were also used for different types of SS. Specifically, Zhuang et al.^[145] studied the antibacterial activity of Cu-bearing 316L SS produced by hot forging followed by an annealing treatment. The plate-count method was used to count the bacterial adhesion on the disk sample. It was observed that the antibacterial rate for *S. aureus* was 95.2%, *E. coli* was 94.8%, and *Staphylococcus epidermidis* (*S. epidermidis*) was 94.1%. In addition, it was shown that 316L-Cu SS had the ability to inhibit biofilm formation for the three bacteria. SEM results detected several spherical bacteria that appeared as confluent colonies on 316L SS in comparison with 316L-Cu SS samples, which had a relatively small number of bacteria. The Cu^{2+} ion releasing increased over time. It was indicated that by applying electrostatic force, the Cu^{2+} ion can bind to the negatively charged bacterial cell wall and membrane, causing the lipopolysaccharide patches to dissolve and the signal transducing system to be destroyed. Additionally, Cu^{2+} ions have the ability to intercalate into double-stranded DNA, which causes its unwinding and breakage. Finally, ROS are produced as a result of Fenton-like processes catalyzed by the Cu^{2+} ion, which may result in protein and lipid peroxidation. Thus, Cu^{2+} ion releasing had a major role in exhibiting antibacterial performance of the 316L-Cu SS. No mechanical properties were mentioned. Nan et al.^[146] inspected the antibacterial behavior of the Cu-bearing austenitic SS against the Gram-negative bacteria *E. coli*. Using the film attachment method, it was found that the antibacterial rate rose as time increased, reaching a 99.0% antibacterial rate. This was due to the amount of Cu ions released from the surface of the steel. Due to an increase in Cu ions leaking over time, the interaction between the ions and bacteria was facilitated, and as a result, the antibacterial rate was significantly increased. No

mechanical properties were mentioned. Finally, Zhang et al.^[147] studied the antibacterial properties of SS with a chemical composition of C 0.016 wt.%, Cr 18.52 wt.%, Ni 8.36 wt.%, Mn 0.43 wt.%, Si 0.61 wt.%, Cu 3.90 wt.%, subjected to different heat treatments. It was observed that as the culture time increased, the number of *Porphyromonas gingivalis* (*P. gingivalis*) bacteria on the control steel rose, contrary to the antibacterial SS that had a smaller number of bacteria on its surface as assessed using the standard film-covered method. As the culture time increased, the sterilization rate of the antibacterial SS gradually reached 95.6% and up to 100% with longer culture time, indicating its superior antibacterial performance against *P. gingivalis*. The authors stated that the Cu ions releasing was the reason behind the antibacterial performance. In this instance, the Cu ions have an antibacterial effect that was summarized in the subsequent two phases. In a humid environment, the Cu ions that were eluted from the substance first stuck to the surface of the bacterial cells. Subsequently, they damaged the cell membranes and solidified the structure of the proteins in the bacterial cells. No mechanical properties were reported.

Studies on SS with Cu content of approximately 4.5 wt.% were performed by Sun et al.^[148] and Chai et al.^[149] In particular, Sun et al.^[148] investigated the antibacterial behavior of heat-treated 317L-Cu SS with a Cu content of 4.46 wt.%. The DAPI staining method was used to test the biofilm mitigation ability. It was observed that over time, the inhibition ability of the 317L-Cu SS surface increased, and the *S. aureus* bacterial colonies significantly decreased. For the previous reason, it can be said that the Cu^{2+} ion release improved the antibacterial performance of 317L-Cu SS, which resulted in the inhibition of biofilm formation, exhibiting an antibacterial rate of 99.0%. The hardness of 317L-Cu was 167 HV. Chai et al.^[149] also investigated the antibacterial properties of alloying Cu to 317L SS with a Cu content of 4.5 wt.%. CLSM and SEM results showed that compared with the non-Cu-containing 317L, the Cu-containing 317L had the capability of colony growth and bacterial adhesion inhibition of *S. aureus* and *E. coli*. In addition, such ability increased until the bacterial colonies reached zero. It was observed that with the time of Cu exposure, the Cu^{2+} concentration rose, which had a significant role in antibacterial activity. No mechanical properties were mentioned. Higher Cu content was used by Guan et al.^[150] who studied the antibacterial properties of Cu-bearing SS fabricated using simulated strip casting with Cu

contents up to 18 wt.%. It was observed that the SS with the highest Cu content (18 wt.%) exhibited the most antibacterial activity against *E. coli*, with an antibacterial rate of 65.0%. This indicated that there is a chance it might contribute to preventing bacterial contamination as a consequence of the toxicity of released Cu ions from the metal surface. No mechanical properties were mentioned.

Apart from Cu, the use of Ag as the antibacterial metallic element was also analyzed. Xiang et al.^[151] inspected the antibacterial behavior of an Ag-containing CD4MCu duplex SS with an Ag content of 0.07 wt.% fabricated using casting. Ag ions releasing appeared to rise over time and with the increasing of the temperature. Compared to the 316L sample, where many bacterial colonies were found through the plate-count method, the Ag-containing CD4MCu duplex SS samples exhibited excellent antibacterial performance as they had a few numbers of the Gram-negative *E. coli* bacteria. In addition, the antibacterial rate of the Ag-containing CD4MCu duplex SS samples was more than 99.9%, contrary to the non-containing Ag samples, which had an antibacterial rate of 16.7%. As a result of the reaction between the Ag ions and the bacteria adsorbed on the surface, the metabolism of the bacteria was slowed, preventing the bacteria from growing and reproducing. The UTS of the alloy was 725 MPa, elongation was 22%, and Rockwell hardness was 25.8 HRC. Liao et al.^[152] investigated the antibacterial properties of 304SS alloyed with Ag prepared by casting using an Ag content ranging from 0.1 wt.% to 0.3 wt.%. After the *E. coli* specimens were incubated for different durations, it was observed that the alloys that had an Ag content of 0.1 and 0.2 wt.% did not display a good antibacterial performance, so a Gram-stain technique was performed after the incubation of *E. coli*. The results confirmed that the alloy exhibited better antibacterial properties with increased Ag content. Thus, the 304SS that had an Ag content of 0.3 wt.% had superior antibacterial activity with a rate of almost 100%. No mechanical properties were mentioned. Finally, Yang et al.^[153] studied the antibacterial properties after adding Ag to the 2205 duplex SS with an Ag content of 0.2 wt.% manufactured via casting. It was observed that the 2205-base duplex SS displayed no antibacterial activity. On the other hand, the 2205-0.2Ag duplex SS exhibited an antibacterial rate of 100% against *E. coli* and more than 99.5% against *S. aureus*, showing its efficacy against both bacteria. It was reported that Ag^+ , which strongly adheres to electron donor groups in biological molecules consisting of sulfur, oxygen, or

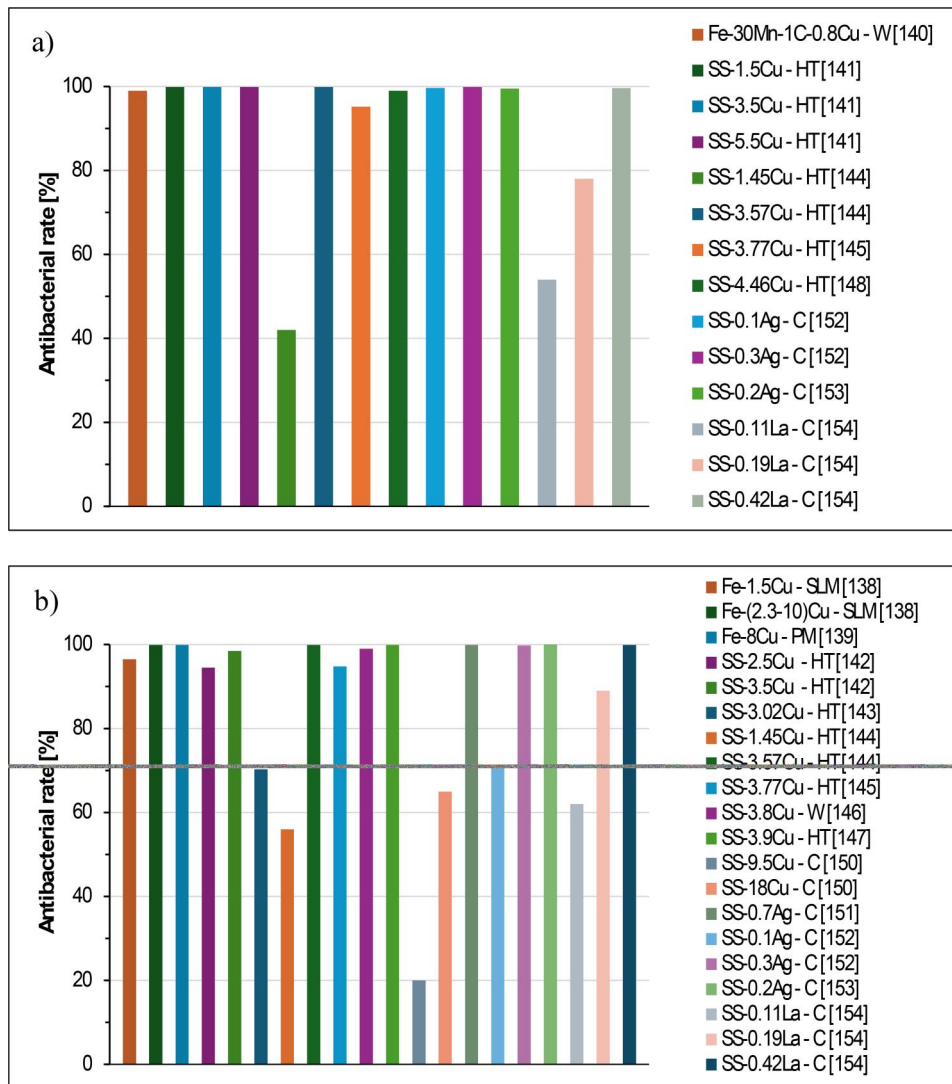


Figure 12. Comparison of the antibacterial efficacy of various Fe-based alloys: (a) antibacterial rate against Gram-positive bacteria, and (b) antibacterial rate against Gram-negative bacteria. Legend: W: wrought; HT: Heat treated; C: cast; SLM: selective laser melted; PM: powder metallurgy.

nitrogen, is vital for Ag⁺'s antibacterial effect. Ag⁺ can interact with the amino groups or amino acids in membranes or enzymes inside bacterial cells, thus killing the bacteria eventually. No mechanical properties were mentioned.

In terms of analyzing the effect of other antibacterial metallic elements, Yuan et al.^[154] studied the antibacterial behavior of cast 316 L SS after adding La, which had a range of 0.05 wt.%–0.42 wt.%. The plate-count method results confirmed that the antibacterial performance improved with the increment of La content. When the La content was 0.05 wt.%, there was no antibacterial activity; however, as the content reached 0.42 wt.%, the average sterilization rate against *E. coli* and *S. aureus* was almost 99.0%. It was reported that the La-modified 316 L SS releases La ions into the solution when it comes into contact with

the suspension of bacteria. By interacting with DNA, enzymes, proteins, or other biological components, the La ions can impair the bacteria's normal physiological metabolism, leading to the death of bacteria. No mechanical properties were mentioned.

Based on the data analyzed, the type and quantity of antibacterial metallic element utilized influence the effectiveness of Fe-based alloys in combating both Gram-positive and Gram-negative bacteria. As shown in Figure 12, the greatest antibacterial rate against Gram-positive bacteria is achieved by 304SS (with Ag values of 0.1 wt.% and 0.2 wt.%) at 100%, while the lowest is observed in 316 L-Cu SS at 94.6%. Similarly, the highest antibacterial rate against Gram-negative bacteria is achieved by 304SS (with Ag values of 0.1 wt.% and 0.2 wt.%) and 304 Cu-bearing SS at 100%, while the lowest is by Cu-bearing SS (with Cu

values ranging from 0.27 to 18 wt.%) at 65.0%. Generally, the antibacterial rate of Fe-based alloys against Gram-positive bacteria is comparable to that against Gram-negative bacteria, except for 2205-3.02Cu duplex SS, which has a lower rate of 70.3% against Gram-negative bacteria and a higher rate of 99.9% against Gram-positive. On the one side, from Figure 12a), which displays the antibacterial rates of different Fe-based alloys against Gram-positive bacteria, it can be seen that these alloys exhibit significant antibacterial activity, with most of them being highly effective. Alloys containing Cu are remarkably efficient, which aligns with the trends observed in Co-based alloys. This seems to indicate that Cu is a highly effective antimicrobial agent, regardless of the base metal added to it. The graph shows a relatively consistent level of high antibacterial rates across various compositions, suggesting that the Fe-Cu combination is a reliable option for combating Gram-positive bacteria. On the other side, Figure 12b) shows that a

comparable trend of significant effectiveness in antibacterial rates against Gram-negative bacteria is found. Nevertheless, there seems to be a more substantial inconsistency in the efficacy of various alloys compared to the results against Gram-positive bacteria. While certain Fe-based alloys exhibit a remarkably high antibacterial rate, others, particularly those with less Cu content, show reduced effectiveness. This variability suggests that Gram-negative bacteria possess greater resistance to specific alloy compositions and to the Cu concentration.

Other elements, such as Ag and La, are also valuable to achieve antibacterial action against Gram-negative bacteria. Based on the evidence presented in Figure 12, it appears that the presence of certain elements, such as Mn and Al, can impact antibacterial rates to some degree but not as significantly as Cu. This is evident in alloys like 316 L and 304 SS, which do not contain Cu and exhibit lower antibacterial activity with respect to their Cu-containing alloy counterparts. These findings are

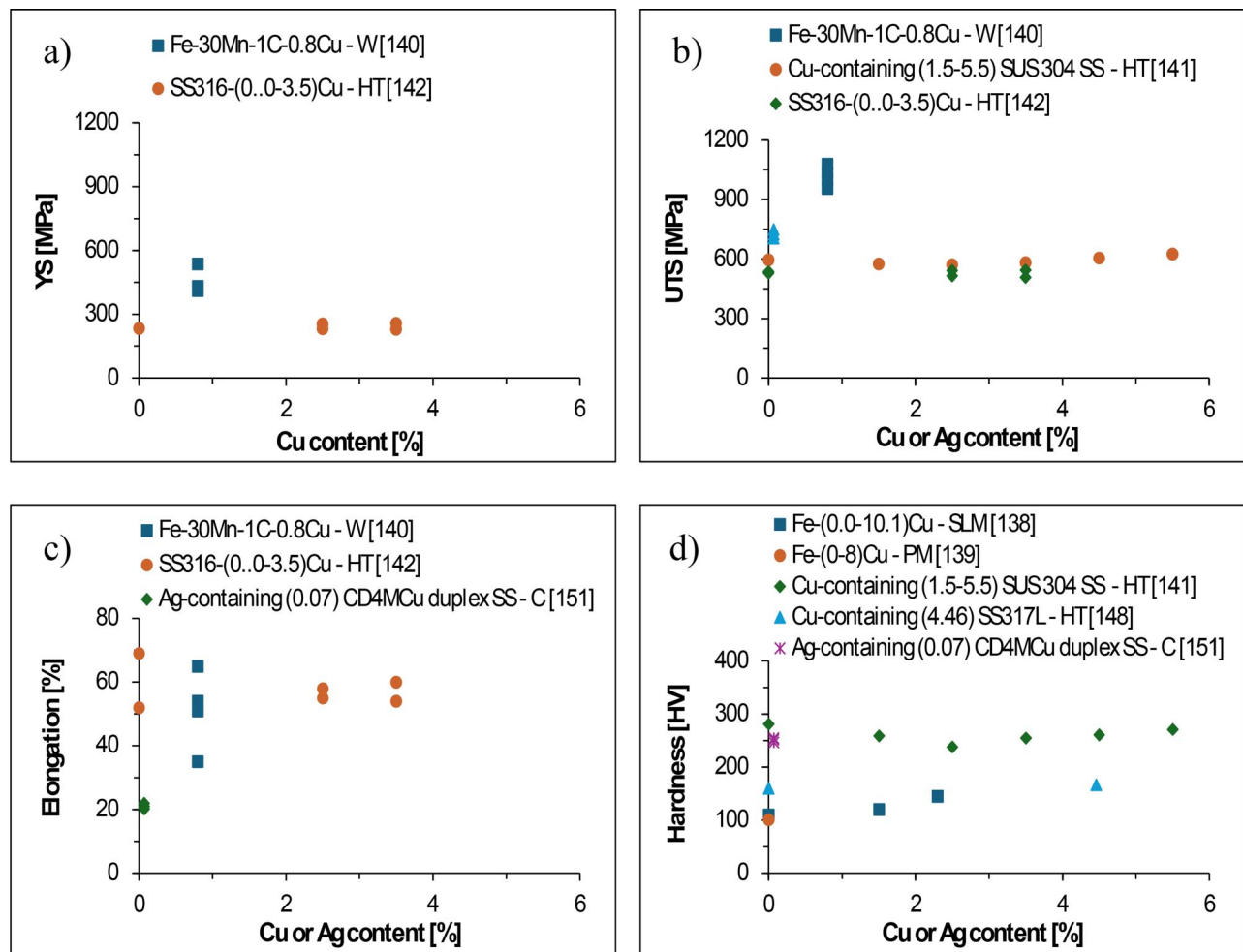


Figure 13. Mechanical properties (tensile and hardness) of antibacterial Fe-based alloys as a function of the Cu/Ag content): (a) YS, (b) UTS, (c) elongation, and (d) hardness. Legend: W: wrought; HT: Heat treated; C: cast; SLM: selective laser melted; PM: powder metallurgy.

crucial in the development of Fe-based materials for clinical use. Furthermore, the ability of these materials to inhibit the growth of a wide range of bacteria makes them ideal for public health applications. Figure 12 demonstrates that the elemental composition of Fe-based alloys is a critical factor in determining their antibacterial effectiveness, with Cu being a standout element for enhancing this property. The different responses of Gram-positive and Gram-negative bacteria to these alloys indicate the need for customized approaches in designing alloys for antimicrobial applications.

Although the mechanical behavior of antibacterial Fe-based alloys is paramount for most types of applications, literature shows that the majority of the studies performed to assess the antibacterial response did not quantify the mechanical properties, as can be seen from the amount of data available in Figure 13. Generally, it found that both YS (Figure 13a) and UTS (Figure 13b) are affected by the intrinsic composition of the Fe-based alloy as well as the heat treatment applied to enhance the antibacterial response. This is clearly distinguishable for the Fe-30Mn-1C-0.8Cu alloy and the Ag-containing SS where data are grouped together. A much higher impact from the antibacterial metallic element used (e.g., Cu) is found for the ductility (Figure 13c), which either decreases, increases, or is spread around a wide range of values depending on the applied heat treatment. In terms of hardness (Figure 13d), which, due to

its simplicity, is the property most often quantified, the addition of antibacterial metallic elements to Fe-base alloys generally results in the increment of the hardness, where the actual improvement is still dependent on the chemistry of the alloy and the manufacturing process used to obtain them.

4.3.3. Mg-based alloys

Mg-based alloys have been primarily developed for biodegradable biomedical applications like bone grafting rather than for structural products such as permanent implants due to the intrinsic low mechanical behavior of Mg and its alloys. Such biodegradable alloys commonly bear an antibacterial metallic element in their compositions, and they are summarized in Table 3.

The mere modification of pure Mg through the addition of an antibacterial metallic element has been investigated, where either Cu or Ag was used and tested against different bacterial strains. In the case of Cu, Li et al.^[155] studied the antibacterial properties of the Mg-Cu alloy with Cu contents of 0.05, 0.1, and 0.25 wt.% prepared *via* casting. It was observed that with the increment of Cu content, the Mg²⁺ and Cu²⁺ ion release increased gradually, with Mg-0.25Cu having the greatest ion release. Bacterial adhesion of the *E. coli*, *S. epidermidis*, and methicillin-resistant *Staphylococcus aureus* (MRSA) bacteria was tested. It appeared that the Mg-0Cu was well coated with

Table 3. Summary of the Mg-based alloys with antibacterial capability.

Composition (wt.%)	Bacteria	Test method	Antibacterial rate (%)	Ref.
Mg-(0.05–0.25)Cu	<i>E. coli</i> <i>S. epidermidis</i> MRSA	Spread plate analysis CLSM	–	[155]
Mg-(0.1–0.3)Cu	<i>C. albicans</i>	CFU method	99.9	[156]
Mg-(0.1–0.4)Cu	<i>P. gingivalis</i>	Live/Dead staining method	–	[157]
Mg-(0.03–0.57)Cu	<i>A. actinomycetemcomitans</i>	SEM + TEM analysis	–	[158]
Mg-Zn-Y-Nd-(0.2–0.8)Ag	<i>S. aureus</i>	CFU method	–	[159]
Mg-(2–6)Ag	<i>E. coli</i> <i>S. aureus</i>	Plate-count method	–	[160]
Mg-(2–6)Ag	<i>S. aureus</i> <i>S. epidermidis</i>	Live/Dead cell assay	92.0	[160]
Mg-Nd-Zn-Zr (0.2)	<i>E. coli</i> <i>S. aureus</i> <i>S. epidermidis</i>	Spread plate method SEM CLSM	74.8 – 94.8 74.2 – 88.4 69.5 – 89.5	[161]
Mg-3.24Nd-0.21Zn-0.44Zr	<i>E. coli</i> MRSA	Live/Dead staining method	92.1 90	[162]
Mg-1Zn-0.5Sn	<i>E. coli</i>	Biofilm test	99.9	[163]
Mg-9Al-1Zn	<i>S. aureus</i> <i>A. baumannii</i>	Live/Dead staining method CFU method	– 1.39 ± 0.12	[164]
Mg-2Zn-0.5Ca	MRSA	SEM observation of bacteria	–	[165]
Mg-1Ca-0.5Sr-(2–6)Zn	<i>S. aureus</i>	SEM observation of bacteria	–	[166]
Mg-6Zn-0.3Mn-(0.2–0.5)Ca	<i>S. aureus</i>	Direct bactericidal assay	>96.6	[167]
Mg-0.1Ga-0.1Sr	<i>E. coli</i>	Spread plate method	86.4	[168]
Mg-0.1Ga-0.1Sr	<i>S. aureus</i> <i>S. epidermidis</i>	Spread plate method	95.0 94.2 94.5	[168]
Mg-0.2Zr-0.1Sr-0Ce	<i>E. coli</i>	Plate-count method	69.1 – 71.5	[169]
Mg-0.2Zr-0.1Sr-0.5Ce			76.7	
Mg-2Sc-2Sr	<i>E. coli</i> <i>S. aureus</i>	Live/Dead staining images Spread plate approach	–	[170]

biofilm, contrary to the Mg-0.25Cu alloy, which had a small amount of bacterial colonization. For *E. coli*, *S. epidermidis*, and MRSA bacteria, decreasing CFU ranges of 11.5→7.9, 18.7→5.2, and 30.3→8.2, respectively, were reported as a function of the increment of the Cu content. No specific mechanical properties were discussed, although they were mentioned. Chen et al.^[156] studied the antibacterial properties of binary Mg-Cu alloys with a Cu content of 0.1 to 0.3 wt.% produced *via* casting. After incubation for 24 h, the agar plates of *Candida albicans* (*C. albicans*) colonies on the Mg-Cu alloys decreased significantly with the increment of Cu content. It was observed that the Mg-0.2Cu and Mg-0.3Cu alloys exhibited an antibacterial efficacy of 99.9%, indicating superior antibacterial properties. Two aspects were reported to be responsible for the antibacterial properties of the Mg-Cu alloys, namely the highly alkaline environment and the release of Cu ions. No mechanical properties were mentioned. Zhao et al.^[157] scrutinized the antibacterial properties of cast Mg-xCu alloys, where x ranged from 0.1 to 0.4 wt.%. It was observed that with the increment of Cu content, the pH levels and Mg²⁺ and Cu²⁺ ion releasing increased. In addition, *P. gingivalis* and *Aggregatibacter actinomycetemcomitans* (*A. actinomycetemcomitans*) concentration and colony numbers were consistently lower in the Mg-Cu alloys than in pure Mg and over time. This indicated that the release of Cu²⁺ boosted the antibacterial performance of Mg. SEM and transmission electron microscopy (TEM) results confirmed that both bacteria failed to form a continuous biofilm, leading to the cell membrane's instant damage and leakage of all intracellular structures. No mechanical properties were mentioned. Finally, Liu et al.^[158] investigated the antibacterial properties of Mg-Cu with a range of Cu content from 0.05 wt.% to 0.5 wt.% produced by means of casting. It was observed that the number of *S. aureus* colonies decreased with the immersion time. As time and Cu content increased, the alloys exhibited higher antibacterial activity, and the number of bacterial colonies was approximately zero. More Cu ion releasing was confirmed to boost the antibacterial ability of the Mg-Cu alloys, showing that Cu, in addition to the high pH, played a part in the process. UTS of the Mg-0.57Cu alloy was 104 MPa, and its hardness was 38 HV.

Although considered, much less work has been done analyzing the effect of the addition of Ag. For instance, Feng et al.^[159] investigated the antibacterial behavior of the cast Mg-Zn-Y-Nd-xAg alloy, where x had a range of 0.2 wt.% to 0.8 wt.%. *E. coli* and *S.*

aureus bacterial concentrations decreased as the Ag content was increased. Additionally, it was indicated that due to the abundance of OH⁻ produced during the corrosion of the Mg alloys upon the co-culture experiment, the pH of the agar environment increased, making it unfavorable for the growth and proliferation of the bacteria. It was reported that the alloy with an Ag content of 0.2 wt.% had a hardness of 50.3 HV, for 0.4 wt.% it was 50.0 HV, for 0.6 wt.% it was 55.6 HV, and for 0.8 wt.% it was 51.2 HV. The effect of a greater amount of Ag was analyzed by Tie et al.^[160] when quantifying the antibacterial properties of the binary Mg-Ag alloys with a range of Ag content from 2 to 6 wt.% subjected to heat treatments. Mg-Ag alloys exhibited a 50.0–75.0% bacterial adhesion decrease and a 74.0–79.0% decrease in bacterial viability, observed by the Live/Dead cell assay against *S. aureus* and *S. epidermidis*. The increment of the Ag content resulted in improved antibacterial performance. Thus, it was observed that the Mg-6Ag exhibited the best antibacterial performance, exceeding 92.0%. Ag ions release and high pH values contributed to the antibacterial activity. UTS of the Mg-6Ag alloy was 216 ± 11 MPa, and the Vickers hardness increased from 32.9 for the Mg-2Ag alloy to 35.9 for the Mg-6Ag alloy.

The addition of Zn as an antibacterial metallic element has also been investigated in the case of Mg-based alloys where Zn was intentionally added or it was already part of the chemical composition of standard Mg alloys (e.g., Mg-9Al-1Zn). The addition of a very small amount of Zn (i.e., 0.2 wt.%) was studied by Qin et al.^[161] for assessing the antibacterial properties of the Mg-Nd-Zn-Zr alloy prepared *via* casting. Using the spread plate method, it was observed that the antibacterial rate of the alloy against *E. coli* had a range of 74.8–94.8% over time, 69.5–89.5% against *S. epidermidis*, and 74.2–88.4% against *S. aureus*, indicating its ability to inhibit bacterial growth. In addition, the CLSM and SEM results detected that as time increased, the intensity of green fluorescence decreased, and there was a decrease in the bacterial colonies and biofilm formation. The enhanced antibacterial activity was attributed to the presence of Zn and Zr on the surface, the Zn ion release, and the increased alkalinity caused by the degradation of the alloy. No mechanical properties were mentioned. A comparable amount of Zn was also analyzed by Xie et al.^[162] in their study about the antibacterial properties of the porous 3D-printed Mg-3.24Nd-0.21Zn-0.44Zr (wt.%) alloy fabricated *via* SLM. The Live/Dead staining results after 24 h of

incubation showed a decline in biofilm formation. The antibacterial rate against *E. coli* and *S. aureus* was 92.1% and 90.0%, respectively. Mg^{2+} at high concentrations could restrict *MRSA* bacterial adherence. Furthermore, high Mg^{2+} concentrations destroyed *MRSA* colonies, which was reported as the bacterial inhibition mechanism of this alloy. In terms of mechanical properties, CYS and UTS were 54 MPa and 97 MPa, respectively. A higher amount of Zn of 1 wt.% was used by Zhao et al.^[163] in the cast Mg-1Zn-0.5Sn alloy. It was observed that the alloy showed a noteworthy decline in *E. coli* and *S. aureus* populations using the biofilm test and Live/Dead staining method, which showed an antibacterial rate of 99.9%. In addition, the Mg-1Zn-0.5Sn exhibited a slow pH increase, which allowed for the early adhesion of cells while maintaining an alkaline environment; however, it displayed good antibacterial behavior. Furthermore, it was reported that Sn was a key reason for such antibacterial activity, as it inhibits bacterial proliferation. The alteration of the alkaline microenvironment and the release of Zn^{2+} significantly enhanced bacterial intracellular ROS. No mechanical properties were mentioned. Last, Brooks et al.^[164] studied the antibacterial properties of the extruded Mg-9Al-1Zn (wt.%). SEM images showed that the alloy had limited bacterial adhesion, and after incubation, there was no clear evidence of biofilm formation. The author believed that the alkaline pH change caused by the corrosion of Mg and its alloys was responsible for the materials' antibacterial properties. The irregular membrane of *Acinetobacter baumannii* (*A. baumannii*) bacteria appeared after observing the CFU count (i.e., 1.39 ± 0.12), due to the disruption of the integrity of the cell membrane. No mechanical properties were mentioned.

The antibacterial properties of Mg alloys bearing concurrently Zn with Ca were also quantified in literature. Zhang et al.^[165] examined the Mg-2Zn-0.5Ca (wt.%) alloy prepared by casting and extrusion. As indicated by SEM images, CFU of the *MRSA* bacteria appeared to be significantly less in the Mg-2Zn-0.5Ca alloy compared to pure Mg, indicating excellent antibacterial performance against *MRSA* growth and adhesion. UCS of the alloy was 321 ± 14 MPa. He et al.^[166] examined the antibacterial effect of alloying Zn to a ternary Mg-Ca-Sr alloy. The nominal composition of the cast alloys was 1 wt.% Ca, 0.5 wt.% Sr, and 2–6 wt.% Zn. After 24 h of incubation of *S. aureus* bacteria, it was observed that the Mg alloys had a smaller number of alive bacteria contrary to the Ti-6Al-4V control sample. Moreover, the antibacterial

rate of the Zn-containing alloys was nearly 90.0%. The number of bacteria on the specimens was evaluated to examine the direct bactericidal assay. The antibacterial rate of the Mg-1Ca-0.5Sr-4Zn and Mg-1Ca-0.5Sr-6Zn alloys was above 96.6%. In addition, the Mg-1Ca-0.5Sr-2Zn alloy displayed a significantly lower antibacterial rate of 76.9%, especially in comparison to the Mg-1Ca-0.5Sr, which displayed an antibacterial rate of 90.0% without Zn. The microscopic fluorescent image results showed that the number of live bacteria stained in green declined as the incubation period increased. Furthermore, the presence of gas evolution on the surface of the alloys was synchronized with the incubation period, as gas bubbles could obstruct the adhesion of bacteria on the surface of the alloy. The pH value rose due to the OH^- release that resulted from the alloy degradation influencing the adhesion and growth of bacteria. Another critical factor in combating bacteria was the corrosion products on the alloy surface, which appeared from the degradation process. No mechanical properties were mentioned. Liu et al.^[167] studied the antibacterial properties of Mg-6Zn-0.3Mn-xCa, where x is 0.2 wt.% and 0.5 wt.% of Ca content, fabricated by semi-continuous casting followed by hot-extrusion. The spread plate method using *S. aureus* showed that with the increment of Ca content, the antibacterial activity improved until it reached a rate of 86.4% for the alloy that had a Ca content of 0.5 wt.%. The authors indicated that the Zn ions releasing prevented bacterial growth and adhesion as it produces ROS, and Ca also had an antibacterial role. UTS of the Mg-6Zn-0.3Mn-0.2Ca alloy was 313 MPa, and that of the Mg-6Zn-0.3Mn-0.5Ca alloy was 334 MPa, while the elongation decreased from 22.2% for the Mg-6Zn-0.3Mn-0.2Ca alloy to 20.3% for the Mg-6Zn-0.3Mn-0.5Ca alloy.

Lastly, a series of Mg alloys whose antibacterial response was quantified was developed on the addition of different chemicals, where all the alloys have in common to bear Sr in their composition. For instance, Gao et al.^[168] examined the antibacterial ability of the cast Mg-0.1Ga-0.1Sr, and using the spread plate method, it was observed that the alloy inhibition ability against Gram-positive *S. epidermidis* and *S. aureus*, as well as Gram-negative *E. coli*, rose over time. After the solution heat treatment, the antibacterial rate against the three bacteria reached 94.5%, 94.2%, and 95%, respectively, which was justified to be the consequence of the release of the Ga^{3+} , Mg^{2+} , and Sr^{2+} ions and the high pH levels reached. In particular, it was reported that the rapid release of Ga^{3+} and Sr^{2+} helps to create fibrous tissues

and suppress bacterial existence. No mechanical properties were mentioned. Sahoo et al.^[169] studied the antibacterial behavior of the Mg-0.2Zr-0.1Sr-xCe alloy (called MZS), where x ranges from 0 wt.% (i.e., MZS alloy) to 0.5 wt.% (i.e., MZS-Ce alloy). The alloys were produced *via* a bottom-pouring stir casting process plus forging. The microorganism used to test the antibacterial properties in this study was *E. coli*, and the plate-count method was utilized. The MZS alloys displayed antibacterial efficacy with a rate of 69.1–71.5%, whereas the MZS-Ce alloy exhibited a rate of 76.73%. After 24 h of incubation in an agar plate, the recultivated colony was utilized to prove such efficacy. It was observed that the bacterial colonies for those alloys almost vanished. The authors stated that Mg²⁺ ion releasing contributed to reaching greater bacterial inhibition due to the osmotic pressure on the cell wall that the Mg²⁺ ions produce. Additionally, Zr prevents bacterial colonization when present. It has been noted that the negatively charged bacterial cell wall and the positively charged (Mg²⁺ and Zr²⁺) ions interact efficiently. The integrity of the membrane was disrupted, and proteins and intracellular components leaked out because of Ce⁴⁺ ions in the fluid. It was reported that CeO₂ binds to the bacterial membrane through electrostatic attraction, converting Ce⁴⁺ to Ce³⁺. This causes ROS, disrupting vital functions like DNA replication and cell division, leading to bacterial breakdown. YS of the MZS-Ce alloy was 174 ± 11 MPa, and UTS was 224 ± 14. Finally, Aboutalebaniaraki et al.^[170] studied the antibacterial behavior of the cast Mg-2Sc-2Sr alloy subjected to heat treatment. Using Live/Dead staining images of *S. aureus* colonies on disk surfaces, it was observed that the Mg-2Sc-2Sr (wt.%) alloy exhibited a considerably high red fluorescent intensity of dead cells, less bacterial adherence, and less biofilm formation. In addition, the spread plate approach was used to test the antibacterial effects against *E. coli*. Its bacterial number was considerably lower than that of the Mg matrix used as control. The use of Sr greatly affected the antibacterial behavior because of its high pH levels, which enhanced bacteria inhibition. UCS was reported to be 276 ± 7 MPa.

According to the data in Figure 14a, the interaction of Mg-based alloys with Gram-positive bacteria shows that many compositions exhibit good antibacterial rates, with some achieving high efficacy. Notably, the inclusion of Cu in Mg-based alloys appears to significantly enhance their antibacterial properties, achieving better performance than when adding Ag. The Mg-Zn-Ca series shows a range of antibacterial rates, with some compositions performing exceptionally well while others show moderate effectiveness. Additionally, the

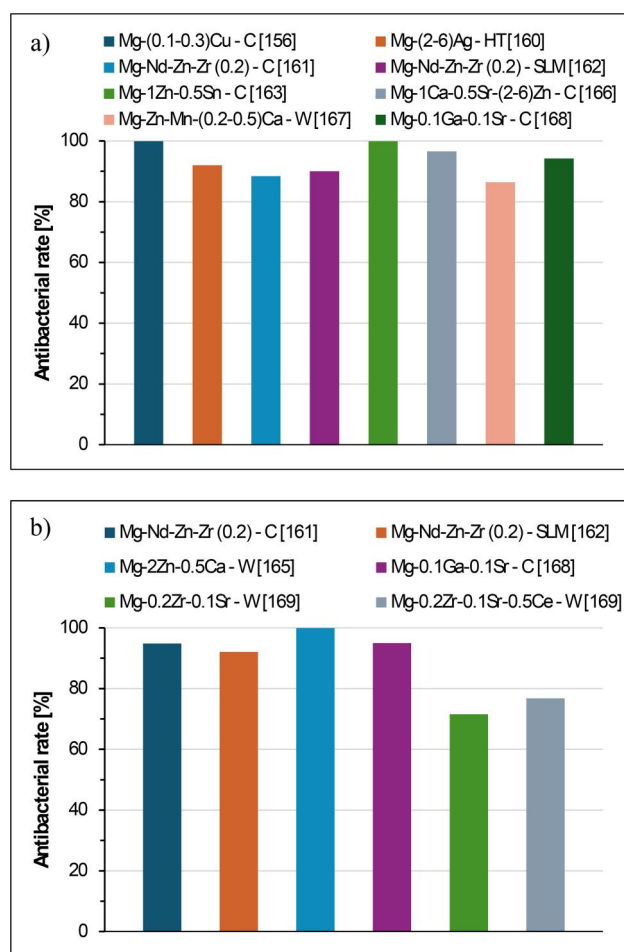


Figure 14. Comparison of the antibacterial efficacy of various Mg-based alloys: (a) antibacterial rate against Gram-positive bacteria, and (b) antibacterial rate against Gram-negative bacteria. Legend: C: cast; HT: Heat treated; SLM: selective laser melted; W: wrought.

combination of elements like Ga and Sr to Mg suggests that alloying Mg with these elements could be exploited to create materials that protect against Gram-positive bacteria. Figure 14b, focusing on Gram-negative bacteria, indicates a broader range of antibacterial rates, signifying variability in efficacy among different Mg-based alloy compositions. Interestingly, the addition of rare earth elements permits reaching high antibacterial rates, indicating that they could significantly contribute to the antimicrobial activity of Mg-based alloys. The Mg-Ga-1Sr alloy exhibits an exceptionally high antibacterial rate, suggesting that Ga and Sr synergistically enhance the antibacterial performance.

As in the case of Fe-based antibacterial alloys, the mechanical properties of Mg-based antibacterial alloys (Figure 15) have been far less investigated with respect to their antibacterial response. Only two out of all the studies reported YS (Figure 15a), which generally increases with the amount of antibacterial metallic element used. The same trend is found for UTS

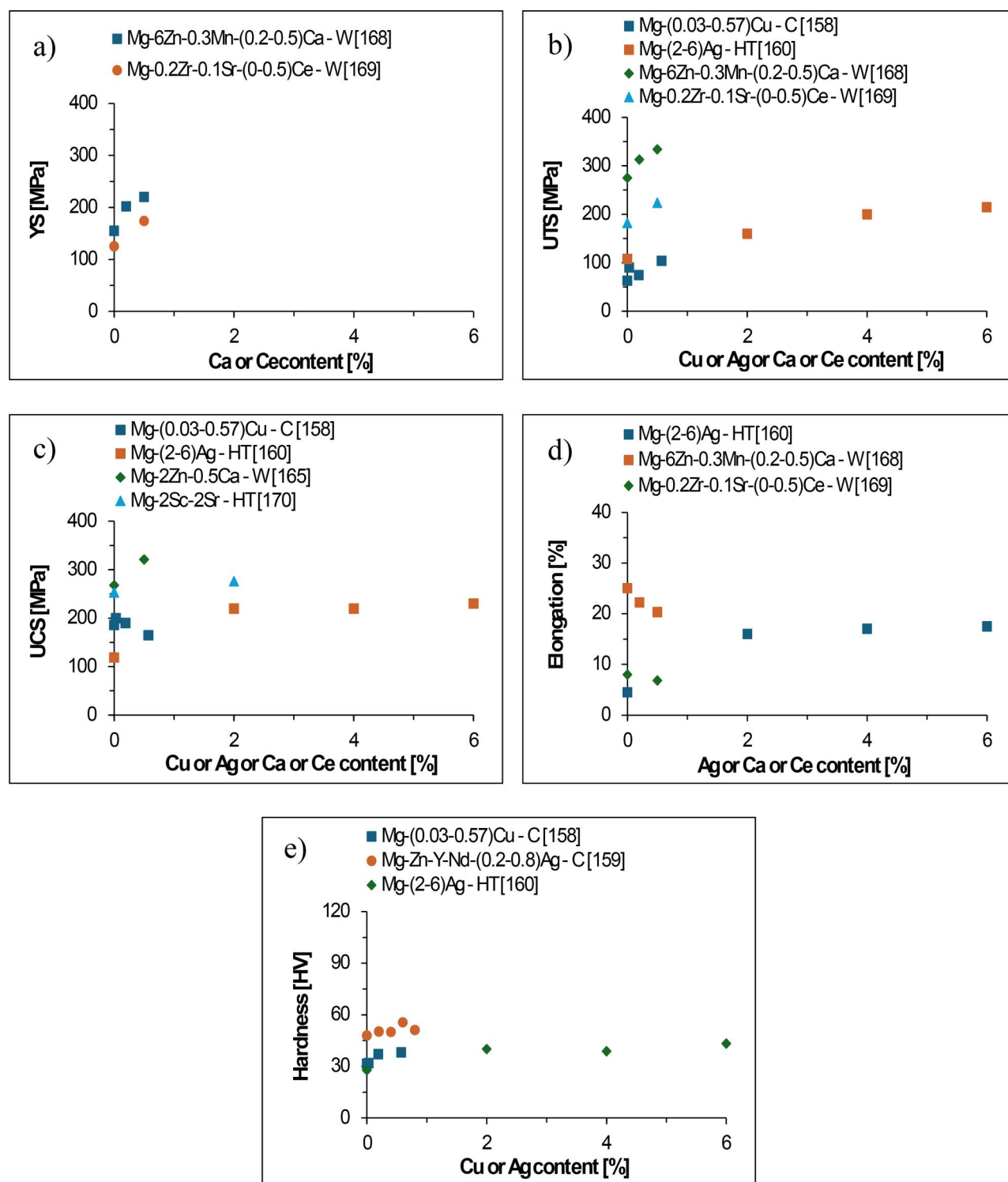


Figure 15. Mechanical properties (tensile, compression, and hardness) of antibacterial Mg-based alloys as a function of the Cu/Ag/Ca/Ce/Sr content): (a) YS, (b) UTS, (c) UCS, (d) tensile elongation, and (e) hardness. Legend: W: wrought; C: cast; HT: Heat treated.

(Figure 15b) and UCS (Figure 15c), although a much clearer influence from the specific material used is visible with Mg-based alloys such as Mg-6Zn-0.3Mn-(0.2–0.5)Ca and Mg-2Sc-2Sr being much stronger than binary Mg-alloys developed purely on the addition of the antibacterial metallic element (i.e., Cu or

Ag). In terms of elongation (Figure 15d), it is found that the addition of Ag to Mg actually increases the ductility, while the incorporation of Ca or Ce to Mg-based alloys decreases the ability to plastically deform. In general, it is also found that the hardness of the Mg-based alloys (Figure 15e) is not significantly

Table 4. Summary of the Ti-based alloys with antibacterial capability.

Composition (wt.%)	Bacteria	Test method	Antibacterial rate (%)	Ref.
Ti-3Cu	<i>S. aureus</i>	<i>In vitro</i> plate antibacterial experiment	>96.7	[174]
Ti-3Cu	<i>P. gingivalis</i>	IZD method	62.8 ± 0.02	[175]
Ti-5Cu	<i>S. mutans</i>	Plate-count method	78.2 ± 0.2	
		ROS staining method		
Ti-3Cu	<i>S. aureus</i>	Plate-count method	>90.0	[176]
Ti-5Cu	<i>E. coli</i>	Plate-count method	70.7 – 99.9	[177]
Ti-2Cu	<i>E. coli</i>	Plate-count method	99.0	[178]
Ti-7Cu	<i>S. aureus</i>			
Ti-10Cu				
Ti-3Cu	<i>S. aureus</i>	Live/Dead staining	92.5	[179]
Ti-5Cu			99.4	
Ti-7Cu			99.5	
Ti-2Cu	<i>E. coli</i>	Plate-count method	57.0 – 79.0	[180]
Ti-5Cu	<i>S. aureus</i>		99.0 – 99.2	
Ti-10Cu			>99.9	
Ti-25Cu				
Ti-10Cu	<i>E. coli</i>	Plate-count method	99.4–100	[181]
	<i>S. aureus</i>			
Ti-(0.2-4.8)Mn-(0.2-4.8)Cu	<i>E. coli</i>	Plate-count method	>90.0	[182]
Ti-2Mn-1Cu	<i>E. coli</i>	<i>In vitro</i> antibacterial test	>90.0	[183]
Ti-3.5Mn-1.7Cu				
Ti-5Mn-2.5Cu				
Ti-5Cu-5Mn	<i>E. coli</i>	<i>In vitro</i> antibacterial test	96.5 – 97.6	[184]
Ti-(0.5-5)Cu-(0.25-2.5)Mn	<i>E. coli</i>	<i>In vitro</i> antibacterial capability assessment	89.0 – 90.0	[185]
Ti-10Mo-(1-5)Cu	<i>E. coli</i>	Plate-count method	15.0 – 60.0	[186]
Ti-10Mo-3Cu	<i>S. aureus</i>			
Ti-30Nb-3Ag	<i>S. aureus</i>	Agar diffusion method	85.7	[187]
	<i>E. coli</i>		88.8	
Ti-10Au	<i>S. aureus</i>	Live/Dead staining observation	21.5 – 89.6	[188]
		SEM morphology of bacteria		
		ROS staining		
Ti-6Al-4V-5Cu	<i>S. aureus</i>	Live/Dead staining observation	–	[124]
		SEM observation of bacteria		
Ti-6Al-4V-(1-5)Cu	<i>E. coli</i>	Plate-count method	–	[189]
	<i>S. aureus</i>			
Ti-6Al-4V-4Cu	<i>E. coli</i>	Plate-count method	93.5 – 97.4	[127]
Ti-6Al-4V-6Cu	<i>S. aureus</i>		99.0	
Ti-6Al-4V-6Cu	<i>P. gingivalis</i>	Plate-count method	98.0	[190]
Ti-13Nb-13Zr-3Cu	<i>S. aureus</i>	Plate-count method	>90.0	[191]
Ti-13Nb-13Zr-7Cu		Live/Dead staining		
		SEM morphology of bacteria		
Ti-13Nb-13Zr-(4-13)Cu	<i>E. coli</i>	Plate-count method	67.8 – 99.4	[192]
	<i>S. aureus</i>			
Ti-13Nb-13Zr-13Ag	<i>S. aureus</i>	Plate-count method	87.0 – 95.0	[193]
		Live/Dead staining		

affected by the introduction of an antibacterial metallic element into their chemical composition.

4.3.4. Ti-based alloys

Ti-based alloys, with their combination of excellent mechanical properties, including low density and high strength, corrosion resistance, and biocompatibility, have been established as one of the leading classes of materials for various engineering applications.^[92,171,172]

Due to their high usage in body implants, scientists have paid attention to developing Ti-based alloys with antibacterial properties.^[173] The antibacterial Ti-based alloys developed in literature and their antibacterial performance are reported in this section and summarized in Table 4, where it can be seen that such development is divided between two distinct investigation lines. On the one side, new Ti-based alloys primarily created on the basis of the addition of an antibacterial metallic

element (i.e., Cu, Ag, and Au) have been significantly studied with the idea of achieving an overall better mechanical behavior coupled with the antibacterial response. On the other side, the composition of standard Ti-based alloys, namely Ti-6Al-4V and Ti-13Nb-13Zr (wt.%), have been modified by means of the addition of an antibacterial metallic element (i.e., Cu or Ag) with the main purpose of functionalizing these alloys with antibacterial capability.

With respect to new antibacterial Ti-based alloys developed on the addition of different Cu contents to pure Ti, Yang et al.^[174] examined the antibacterial properties of the binary Ti-3Cu (wt.%) alloy obtained *via* cold rolling and annealing. An *in vitro* plate antibacterial experiment was used to help count the bacterial colonies, and the bacteria used was the Gram-positive bacteria *S. aureus*. It was shown that the Ti-3Cu alloy exhibited superior antibacterial properties

with an antibacterial rate of more than 99.0%. In addition, when exposed to diverse conditions, the binary alloy maintained excellent antibacterial properties with a rate greater than 96.7%, displaying a strong antibacterial effect. It was observed that because of cold rolling, YS was 618 ± 15 MPa, and UTS was 928 ± 26 MPa. The microhardness increased from 198 HV to 308 HV after cold rolling. On the other hand, microhardness slightly decreased as the annealing temperature increased. Yang et al.^[175] studied the antibacterial properties of the PM Ti-(3-5)Cu (wt.%) alloys in which the SEM results showed the presence of the eutectoid Ti_2Cu phase. In addition, the X-ray diffraction (XRD) results confirmed that the Ti_2Cu phase presence increased in the Ti-5Cu alloy due to the increment of the Cu content. Similarly, Cu^{2+} ion releasing was higher in the Ti-5Cu alloy with respect to the Ti-3Cu alloy. With increasing Cu concentration, the diameter of the IZD rose, demonstrating the potential of Cu-containing alloys to impede bacterial growth. Moreover, the plate-count method showed that the bacteria colonies of both *P. gingivalis* and *S. mutans* were significantly lower than those present in commercial pure Ti (CP-Ti) and kept reducing as the incubation period increased. The antibacterial rates of the Ti-3Cu and Ti-5Cu alloys were 62.7% and 78.2%, respectively. Additionally, the ROS staining method indicated the ability of the Ti-Cu alloys to generate ROS in the bacterial culture, contrary to the CP-Ti. It was reported that the Ti_2Cu phase is responsible for the release of Cu^{2+} ions, which is key for the antibacterial activity of these alloys. In terms of mechanical properties, YS of the Ti-5Cu alloy was 551 ± 17 MPa, UTS was 722 ± 13 MPa, and the elongation was $18 \pm 1\%$. Bao et al.^[176] studied the antibacterial properties of the Ti-3Cu (wt.%) alloy manufactured by means of ingot metallurgy followed by forging. Using the plate-count method against *S. aureus*, it was confirmed that the CP-Ti had a large number of bacterial colonies; however, the Ti-3Cu alloy exhibited strong antibacterial ability as it had a smaller number of colonies. Specifically, the antibacterial rate of the specimens tested was more than 90.0%. XRD results detected the appearance of the intermetallic compound Ti_2Cu , and it was found that the treatment done on the alloy increased the effective contact between the Ti_2Cu phase and the bacteria. This then resulted in an excellent antibacterial ability, which plays a vital role in preventing the bacterial biofilm formation and suppression of bacterial adhesion. After different heat treatments, YS and UTS increased and, consequently, the elongation decreased from 10% to 6%. Wu et al.^[177] studied the

antibacterial properties of the binary Ti-5Cu (wt.%) alloy subjected to aging heat treatments. SEM detected the appearance of the intermetallic compound Ti_2Cu phase in the specimens exposed to the aging treatment. In addition, it was observed that as the aging treatment increased, the number of Ti_2Cu precipitates increased, resulting in the increment of the Cu^{2+} ions releasing rate. The plate-count method using the microorganism *E. coli* indicated that the CP-Ti had many bacterial colonies, suggesting no antibacterial activity. On the other hand, the Ti-5Cu had a lower number of bacterial colonies that were exposed to multiple heat treatments, meaning that it displayed an antibacterial effect. Moreover, the specimens that were subjected to several heat treatments had a range of antibacterial rates of 49.3% to 93.1%. It was found that the antibacterial properties were enhanced with the increment of the aging treatment duration. In particular, the specimens that were exposed to an increased aging treatment duration had a range of 70.7% to 99.9%. No mechanical properties were reported in this study. Yi et al.^[178] investigated the antibacterial behavior of the binary Ti-(2-10)Cu (wt.%) alloy produced via argon-arc melting followed by heat treatment. The plate-count method against *E. coli* and *S. aureus* showed that Ti-2Cu had large bacterial growth, contrary to the Ti-7Cu and Ti-10Cu samples that displayed superior antibacterial efficacy with a rate of over 99.0% and had fewer bacterial colonies. Therefore, it was clearly shown that the antibacterial properties were enhanced by a progressively higher amount of Cu as more bacterial growth was inhibited. Moreover, it was observed that Cu ions were released from the precipitated Ti_2Cu phase as the *E. coli* and *S. aureus* bacteria were cultured in the Ti-Cu for 24 h. As the Cu content increased, the Cu ions releasing increased, and it was indicated that the released ions would attach to the bacterial cell membrane and disrupt it. As a result, the Cu ions were able to alter the bacterial proteins, which, in turn, led to the death of the bacteria. The Ti-7Cu alloy had a UCS of 2169 MPa and a hardness of 292 HV, while the Ti-10Cu alloy had a UCS of 1828 MPa and a hardness of 343 HV. Zhang et al.^[179] explored the effect of Cu into Ti in the range of 3 wt.% to 7 wt.% to create Ti-xCu alloys. *S. aureus* was the bacteria used to evaluate the antibacterial properties, and Live/Dead staining was used to identify the activity of it. It was concluded that the antibacterial rate of Ti-3Cu, Ti-5Cu, and Ti-7Cu was 92.5%, 99.4%, and 99.5%, respectively, which shows a strong bactericidal effect. Cu^{2+} ion releasing from the intermetallic compound Ti_2Cu was a great factor for bacterial inhibition. No mechanical properties

of the obtained materials were reported. Liu et al.^[180] studied the antibacterial behavior of the sintered binary Ti-Cu alloys, which were fabricated *via* the PM route. The Cu content added ranged from 2 wt.% to 25 wt.%. The Gram-negative *E. coli* and the Gram-positive *S. aureus* bacteria were used. Applying the plate-count method for both *E. coli* and *S. aureus*, a large number of bacteria were found in the Ti-2Cu sample, while the Ti-5Cu, Ti-10Cu, and Ti-25Cu samples exhibited great antibacterial activity as the bacteria colonies in them were very low. The antibacterial rate of the Ti-2Cu against *E. coli* and *S. aureus* is 57.0% and 79.0%, respectively. Meanwhile, Ti-5Cu had a rate of 99.2% for *E. coli* and 99.0% for *S. aureus*. As for Ti-10Cu and Ti-25Cu, the antibacterial rate was more significant than 99.99%, which indicates superior antibacterial activity. Moreover, the authors stated that the Ti-Cu alloys must have a Cu content of at least 5 wt.% to obtain antibacterial activity. Thus, this reinforces the fact that the Cu content substantially affects the antibacterial properties and, in turn, the Cu ion-releasing behavior. No mechanical properties of the obtained materials were reported. Finally, Zhang et al.^[181] investigated the antibacterial properties of the PM Ti-10Cu (wt.%) alloy. The plate-count method showed that the Ti-10Cu sample had no bacterial colony when tested against *E. coli* and *S. aureus*, meaning that it exhibited strong antibacterial activity. It was observed that the antibacterial rate of Ti-10Cu alloy against *E. coli* was 99.9% and 100% against *S. aureus*. XRD and SEM detected the formation of the Ti₂Cu phase and Cu-rich phase in the sintered alloy. The Cu ion release was indicated to be the reason for the antibacterial properties, as only the bacteria in contact with the alloy were killed. The alloy had a UCS of 1707 MPa and a microhardness of 369 ± 12 HV.

Considering the development of new Ti-based alloys where the simultaneous addition of an antibacterial metallic element and other alloying elements, this was investigated by Alqattan et al.^[182] who quantified the antibacterial activity against *E. coli* of ternary Ti-xMn-yCu alloys. The alloys were produced through cold uniaxial pressing plus a vacuum sintering route. The range of Mn and Cu content added was from 0.2 wt.% to 4.8 wt.%. The photographs of the 24 h incubated plates showed that the alloys with the most alloying elements exhibited high antibacterial activity as the colonies were relatively low, while the CP-Ti sample showed no antibacterial inhibition as if all the colonies remained alive. Specifically, the plate-count method showed that the antibacterial efficiency was above 90.0%. XRD proved that when the Cu content

reached 2 wt.%, the intermetallic phase Ti₂Cu precipitated, leading to the release of Cu²⁺ ions. YS and UTS of the Mn-dominant alloys were 509 MPa to 729 MPa and 599 MPa to 817 MPa, respectively, while the elongation decreased (20% → 5%) with the increment of the alloying elements, and the hardness changed from 56 HRA to 63 HRA. The Cu-dominant alloys had YS of 449 MPa to 567 MPa and UTS of 554 MPa to 692 MPa; the elongation was 16 ± 2%, and hardness values were 53 HRA to 60 HRA. In another study, Alqattan et al.^[183] examined PM Ti-Mn-Cu alloys and their antibacterial properties against *E. coli* in alloys with a constant Mn to Cu ratio of 1:2. The Mn content ranged from 0.5 wt.% to 5 wt.%, and the Cu content ranged from 0.25 wt.% to 2.5 wt.%. It was confirmed that the amount of *E. coli* colonies decreased as the content of the alloying elements increased through the *in vitro* antibacterial efficacy of the sintered Ti-Mn-Cu alloys. The antibacterial rate of the Ti-3.5Mn-1.75Cu and Ti-5Mn-2.5Cu alloys was above 90.0%. The tensile properties increased and the elongation decreased with increasing content. Likewise, Bolzoni et al.^[184] tested the antibacterial properties of ternary Ti-xCu-yMn alloys manufactured *via* the press and sinter PM route. The Cu and Mn content added ranged from 0.5 wt.% to 5 wt.% with a Cu to Mn ratio of 1:1. The XRDs identified the appearance of the Ti₂Cu phase in the Ti-2Cu-2Mn and Ti-3.5Cu-3.5Mn alloys. The *in vitro* antibacterial activity showed that the antibacterial rate of the β eutectoid-bearing functionalized Ti alloys was between 96.5% and 97.6%, which proves that they have bactericidal capability. The incremental rate of antibacterial activity was due to the formation of the intermetallic compound Ti₂Cu and the increase in alloying elements and the expected higher release of Cu²⁺ ions. With the increment of the alloying elements, the strength/hardness increased. As a result, the elongation and the ability to endure damage before fracturing decreased as the formation of the Ti₂Cu phase made the alloys more brittle. YS was in the range of 492–862 MPa, UTS was in the range of 553–931 MPa, the elongation of Ti-5Cu-5Mn alloy was 2.9%, and the hardness was up to 299 HV. Alqattan et al.^[185] also examined the antibacterial properties of PM Ti-(0.5-5)Cu-(0.25-2.5)Mn alloys. The results of the *E. coli* analysis showed that the antibacterial properties were increased with the increment of Cu concentration, which was evidenced by the *in vitro* antibacterial capability assessment. The antibacterial capability rate in materials with an alloying content less than or equal to 3 wt.% was reported to be nearly 90.0%. It was

stated that the appearance of the intermetallic compound Ti_2Cu occurred when the Cu content reached 2 wt.%, justifying the enhancement of the antibacterial properties. Finally, Xu et al.^[186] studied the antibacterial properties of the Ti-10Mo-xCu alloy fabricated via PM, where x ranged from 1 wt.% to 5 wt.%. The results of the plate-count method against *S. aureus* and *E. coli* showed that the bacterial colonies declined with the increment of Cu content. The antibacterial rate against *E. coli* ranged from 15.0% to 50.0% and 20.0% to 60.0% for *S. aureus*. Moreover, it was observed that the formation of the Ti_2Cu phase and the releasing of Cu ions played a significant role in improving the antibacterial properties of the alloy. The Ti-10Mo-3Cu alloy had the highest UTS of 1098 MPa, while the different alloy samples had a range of UTS from 916 MPa to 1162 MPa and elongation from 14% to 2%.

From the discussion so far, Cu was used as the antibacterial metallic element mostly used in Ti-based antibacterial alloys; however, Ag and Au were also studied. In that respect, Hussein et al.^[187] investigated the antibacterial capabilities of the Ti-30Nb-3Ag with an Ag content of 3 at.%, fabricated using mechanical alloying (MA) followed by powder consolidation and sintering. The agar diffusion method against *S. aureus* and *E. coli* was 85.7% and 88.8%, respectively, meaning a strong inhibiting impact. XRD detected the precipitation of Ag, which has antibacterial abilities through the release of Ag ions by means of the Ti_2Ag phase. The microhardness of the alloy was detected to be 491 HV. Fu et al.^[188] studied the effect of adding Au as an alloying element to CP-Ti and assessed the antibacterial behavior. The binary Ti-Au samples were produced via spark plasma sintering (SPS). The XRD patterns detected the appearance of the Ti_3Au phase due to the heating and annealing process done on the samples. Therefore, the heat-treated samples showed a high antibacterial rate against *S. aureus* bacteria due to the formation of the Ti_3Au phase. By disrupting the ROS homeostasis of the bacteria, Ti_3Au led to oxidative damage in the bacterial cells and inhibited the formation of a biofilm. The antibacterial activity of the samples ranged from 21.5% to 89.6%, which was calculated based on the number of bacterial colonies. In addition, the sintered sample exhibited antibacterial inhibition, and the bacteria showed no biofilm formation, as detected by the SEM morphology of *S. aureus*. Using the Live/Dead staining, it was observed that the samples had a significantly higher rate of dead bacteria, which appeared as red fluorescence compared to the other samples. Moreover, the number of dead

bacteria increased as the incubation time increased. Similarly, through ROS staining in the cells, it was found that the longer the incubation time, the more ROS signal was detected in the samples, an indication of the good antibacterial behavior. The report did not provide any information about the mechanical properties.

As previously mentioned, research has also been dedicated to modifying the composition of standard Ti-based alloys to functionalize them with antibacterial capability. For instance, Peng et al.^[124] examined the antibacterial properties of the Ti-6Al-4V-5Cu (wt.%) alloy subjected to different annealing treatments with several maximum temperatures. The CLSM results of *S. aureus* biofilm formation showed that the Ti-6Al-4V alloy had a vast number of live bacterial colonies as they appeared as green fluorescence, while a couple of specimens of the Ti6Al4V-5Cu showed a large number of dead bacteria presented as red color, indicating that the alloys have the ability to inhibit the formation of a biofilm. In addition, SEM results detected a large number of *S. aureus* on the surface of Ti-6Al-4V alloy, contrary to the Ti-6Al-4V-5Cu specimens that had scattered and much less bacteria. This indicated that the bacteria adhesion and formation of biofilm were inhibited due to the addition of Cu. XRD and SEM results detected the appearance of the Ti_2Cu . The strength of the annealed samples was relatively high, contrary to the elongation. YS had a range of 825–980 MPa, UTS was 900–1050 MPa, and the elongation was 6%. Ren et al.^[189] investigated the antibacterial properties of the Ti-6Al-4V-xCu alloys, where x had a range of 1 wt.% to 5 wt.%. The alloys were fabricated by casting followed by heat treatment. The plate-count method indicated that the number of *E. coli* and *S. aureus* colonies in the Ti-6Al-4V-xCu alloys was significantly lower than that of a Ti-6Al-4V alloy, meaning that the Ti-6Al-4V-xCu alloys exhibited antibacterial properties. In addition, it was also observed that the antibacterial effect was enhanced through the increment of the Cu content, where the bacterial colonies were almost zero in the Ti-6Al-4V-5Cu alloy. The tensile strength decreased from 1016 MPa to 387 MPa, and elongation was also reduced with the increment of Cu content. Guo et al.^[127] studied the antibacterial properties of Ti-6Al-4V-xCu alloys, where x had a range of 2 wt.% to 6 wt.%, fabricated by means of SLM. The plate-count method against the Gram-positive *S. aureus* and the Gram-negative *E. coli* showed that the Ti-6Al-4V had a large number of bacterial colonies, meaning that it exhibited no antibacterial activity. On

the other hand, the Ti-6Al-4V-4Cu had a significantly smaller number of colonies, and the Ti-6Al-4V-6Cu showed almost no bacterial colonies, displaying an antibacterial effect against both bacteria. The alloy with a 4 wt.% of Cu had an antibacterial rate of 97.4% against *E. coli* and 93.5% against *S. aureus*, whereas the alloy with 6 wt.% Cu had a rate of more than 99.0%. There was no report on the mechanical properties. Finally, Xu et al.^[190] investigated the antibacterial properties of the 3D-printed porous Ti-6Al-4V-6Cu fabricated using SLM followed by acid etching treatment. The plate-count method showed that the antibacterial capabilities against *P. gingivalis* are 98.0%, indicating good antibacterial behavior.

Apart from Ti-6Al-4V, the other standard Ti-based alloy that has been modified with either Cu or Ag as an antibacterial metallic element is the Ti-13Nb-13Zr alloy. Specifically, Mao et al.^[191] examined the antibacterial properties of the Ti-13Nb-13Zr-xCu alloys, where x is 3 wt.% and 7 wt.%, subjected to different heat treatments. It was observed that the increase in Cu content and Ti₂Cu precipitation enhanced the antibacterial ability of the Ti-13Nb-13Zr-xCu alloys. The antibacterial rate of Ti-13Nb-13Zr-3Cu was over 90.0% against *S. aureus*. After extending the aging duration from 1 to 2 h, it was observed that Ti-13Nb-13Zr-3Cu and Ti-13Nb-13Zr-7Cu alloys exhibited excellent antibacterial properties as the number of bacteria in the agar plate decreased significantly. Adding Cu and extending the aging treatment time increased the hardness of the alloy, which changed depending on the actual composition and heat treatment. Yuan et al.^[192] also investigated the antibacterial ability of Ti-13Nb-13Zr-xCu alloys prepared by the arc melting method, where x had a range from 0 wt.% to 13 wt.%, and the bacteria used were *E. coli* and *S. aureus*. The plate-count method proved that the sample with no Cu content had large bacteria colonies, meaning there was no antibacterial activity. However, with the addition of Cu content and as it increased, there was a clear reduction in the number of *E. coli* and *S. aureus* colonies in the Ti-13Nb-13Zr-xCu alloys. The antibacterial rate was 67.8% for 4 wt.% and 90.4% for 7 wt.%, 99.1% for 10 wt.%, and 99.4% for 13 wt.%. Cu ions releasing was the major responsible for the antibacterial properties, as it is able to disrupt the integrity of the bacterial cell membrane and generate ROS, which then results in the death of the bacteria. CYS of the alloy with different Cu contents ranged from 380 MPa to 950 MPa. Regarding the addition of Ag, Cai et al.^[193] studied the antibacterial effect of the Ti-13Nb-13Zr-3Ag (wt.%) alloy prepared

by alloy melting and heat treatment. XRD, SEM, and TEM results confirmed that the aging treatment contributed to the increase of the precipitation of the Ti₂Ag phase. The precipitation of the Ti₂Ag particles and the Ag ions releasing enhanced the antibacterial effect of the Ti-13Nb-13Zr-13Ag alloy. Moreover, the plate-count method indicated that the Ti-13Nb-13Zr-13Ag alloy displayed antibacterial efficacy, and the samples subjected to the longest aging treatment showed greater antibacterial efficacy. The antibacterial rate of the alloy subjected to the shortest aging treatment was 87.0%, and that of the alloy subjected to the longest aging treatment was >95.0%. The addition of Ag raised the microhardness from 288 HV to 366 HV.

From the analysis of the performance of various Ti-based alloys against Gram-positive bacteria (Figure 16a), it is clear that the Cu-bearing alloys exhibit a highly positive response with very high effectiveness. As it could be expected, the antibacterial rate normally monotonically increases with the Cu content. However, the Ti-7Cu alloy is less effective than Ti-3Cu to Ti-10Cu alloys, indicating that the manufacturing process and the consequent phases present in the microstructure of the antibacterial Ti-based alloys also play a critical role as they control the availability and rate of Cu ion releasing, especially through the presence of the intermetallic Ti₂Cu phase. The addition of Ag or Au to Ti also brings about antibacterial capability, although the antibacterial rate is not as high as that of many of the Cu-bearing Ti-based alloys. However, both Ag and Cu are able to functionalize the standard Ti-13Nb-13Zr alloy. When assessing the response to Gram-negative bacteria (Figure 16b), there is a consistent level of high effectiveness across all Ti-based alloy variants, with some few exceptions where the antibacterial rate is lower than 90.0%. Moreover, the data presented in Figure 16 clarify that Ti-based alloys with Cu additions have significantly enhanced antibacterial rates against both strains of bacteria. The Ti-25Cu alloy tops the chart with a 99.9% rate against Gram-negative bacteria, while the Ti-10Cu alloy presents a 99.7% rate against Gram-positive bacteria. Other elements like Al, Ag, Au, Mn, Mo, Nb, V, and Zr, which are intentionally added for an antibacterial response or are part of the chemical composition of Ti-based alloys, also influence the antibacterial activity to varying degrees; however, the pronounced effect of Cu is unmistakable. Notably, antibacterial rates against Gram-negative bacteria generally surpass those against Gram-positive strains, except for the Ti-10Mo-1-5Cu and Ti-10Mo-3Cu alloys, which display a reverse trend. These collective findings emphasize the importance of alloy composition in determining the

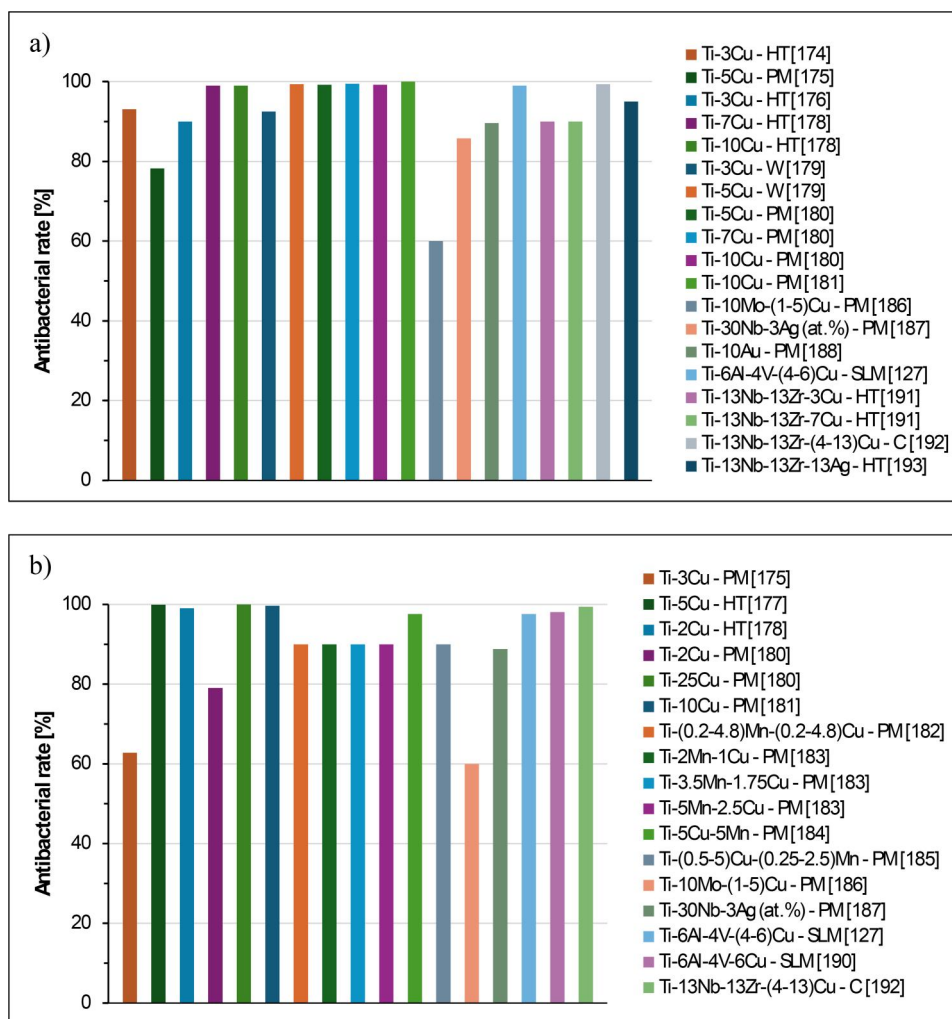


Figure 16. Comparison of the antibacterial efficacy of various Ti-based alloys: (a) antibacterial rate against Gram-positive bacteria, and (b) antibacterial rate against Gram-negative bacteria. *Legend:* HT: Heat treated; PM: powder metallurgy; W: wrought; SLM: selective laser melted; C: cast.

antibacterial potency. These alloys, particularly those enriched with Cu, could play a critical role in inhibiting bacterial growth in medical and other crucial settings, significantly improving infection prevention strategies. Furthermore, the consistent effectiveness of these materials against a range of bacteria supports their potential to create inherently antimicrobial surfaces, a development with significant implications for enhancing public health defenses and innovative new antimicrobial solutions.

As Ti-based alloys are the ultimate choice for permanent structural prostheses used in total joint replacement,^[194] quantification of their mechanical properties is much more critical than in the case of Fe- and Mg-based biodegradable alloys. Consequently, the number of investigations reporting the mechanical performance of antibacterial Ti-based alloys is remarkably higher; as can be seen in Figure 17. Generally, irrespectively of the actual composition of the Ti-

based alloy considered and of the manufacturing process employed to process them, it is found that the resistance to plastic deformation, including YS (Figure 17a), UTS (Figure 17b), and hardness (Figure 17d), increases with the amount of antibacterial metallic element added to functionalize the alloy. Therefore, the addition of such elements is not only helpful to induce an autogenous antibacterial response but also to enhance the overall mechanical performance of Ti-based alloys. As strength and toughness are mutually exclusive properties, a higher addition of antibacterial metallic element to boost the antibacterial response normally leads to the embrittlement of the Ti-based alloys. This can be seen from the decrement of the elongation (Figure 17c) with the increment of the Cu or Ag content. Nonetheless, it can be seen that a wide range of strength/elongation pairs is available due to the Ti-based alloys developed so far for biomedical

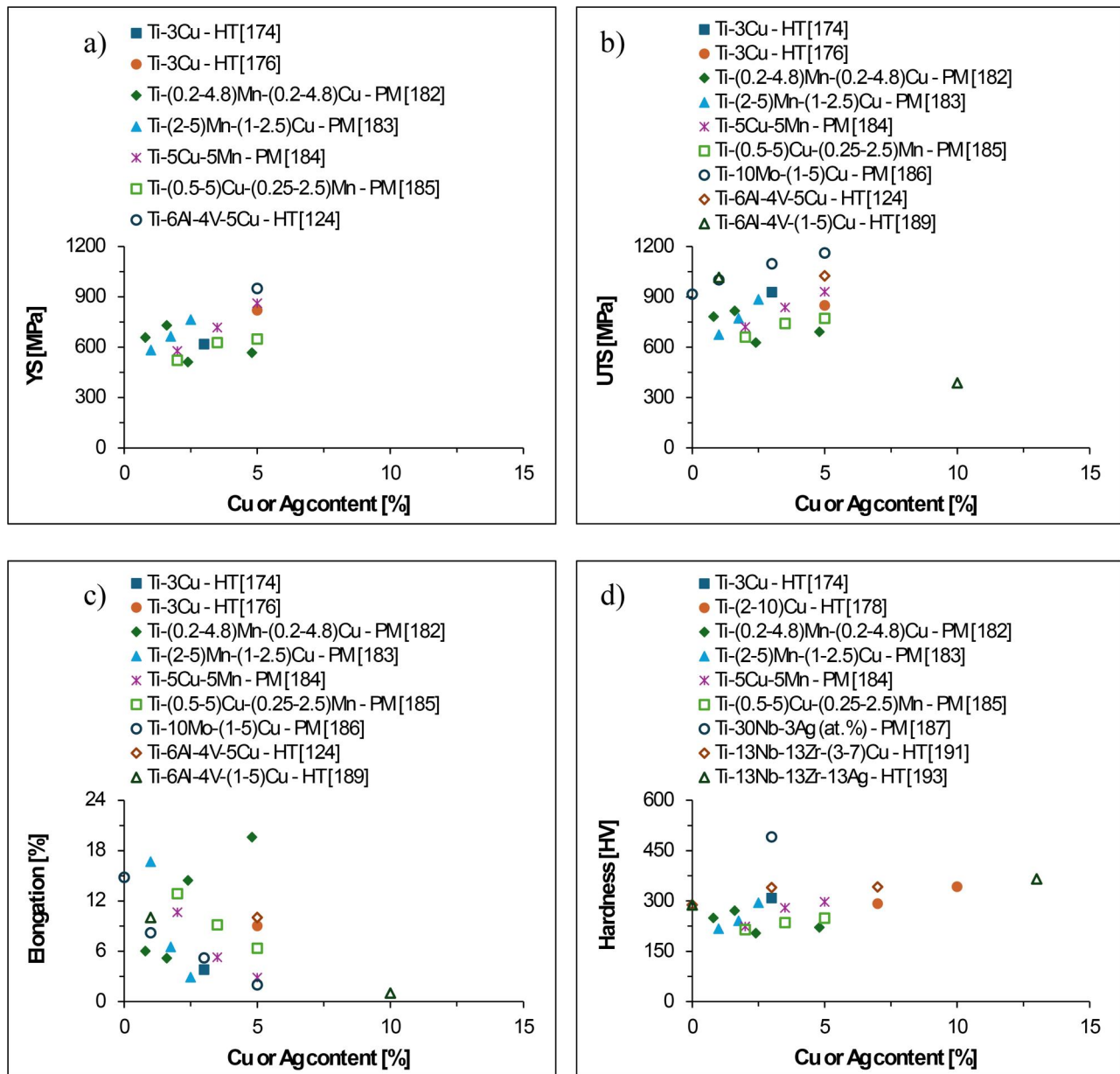


Figure 17. Mechanical properties (tensile and hardness) of antibacterial Ti-based alloys as a function of the Cu/Ag content: (a) YS, (b) UTS, (c) elongation, and (d) hardness. Legend: HT: Heat treated; PM: powder metallurgy.

applications, meaning that they should be able to be used to manufacture a great variety of medical devices.

4.3.5. Zn-based alloys

This section considers the development of antibacterial Zn-based alloys and analyzes the available performance reported in literature. Zn alloys are considered potential biodegradable metals because of their advantageous corrosion properties and excellent biocompatibility. Zn demonstrates a corrosion rate that falls between Mg and Fe, forms a tight corrosion product, and does not produce any gas during degradation.^[195] Because of these characteristics, various studies have

focused on the antibacterial properties of different Zn-based alloys. In particular, scientific efforts were focused on both binary and ternary antibacterial Zn-based alloys, as summarized in Table 5.

In the case of binary Zn-based alloys, two main strategies have been used, which include either the addition of an antibacterial metallic element (e.g., Cu or Ag) to enhance the antibacterial response or the addition of an alloying element to increase the overall performance, especially in terms of ductility. With reference to the first strategy, Qu et al.^[196] examined the antibacterial properties of the Zn-Cu alloys with a Cu content range of 0.5 wt.% to 2 wt.% prepared *via* casting. *S. epidermidis*, methicillin-resistant *Staphylococcus*

Table 5. Summary of the Zn-based alloys with antibacterial capability.

Composition (wt.%)	Bacteria	Test method	Antibacterial rate (%)/IZD (mm)	Ref.
Zn-(0.5-2)Cu	<i>S. epidermidis</i> MRSE <i>S. aureus</i> MRSA	Plating gradient dilution method	–	[196]
Zn-1Cu	<i>E. coli</i>	IZD method	71.8	[197]
Zn-2Cu			75.3	
Zn-3Cu			80.1	
Zn-4Cu			82.5	
Zn-(1-4)Cu	Mixed oral bacteria	Live/Dead staining method	–	[198]
Zn-1Ag	<i>S. epidermidis</i>	Live dead bacteria staining	–	[199]
Zn-2Ag	MRSE MRSA	SEM + TEM		
Zn-2Ce	<i>E. coli</i>	IZD method	81.3	[200]
Zn-0.8Mn	<i>E. coli</i>	Spread plate method	–	[201]
Zn-1Dy	<i>S. aureus</i>	IZD method	5.32 ± 0.22 – 7.42 ± 0.26	[202]
Zn-3Dy		CFU method		
Zn-5Dy				
Zn-0.5Cu-(0.1-0.4)Fe	<i>S. gordonii</i>	Live/Dead staining method	–	[203]
Zn-1Cu-0.1Ti	<i>S. aureus</i>	IZD method	6.99 ± 0.33	[204]
Zn-3Al-(0.5-1.5)Cu	<i>S. aureus</i>	Agar plate diffusion test CFU method	4.90 ± 0.40	[205]
Zn-0.05 Mg-0.5Ag	<i>E. coli</i>	Live/Dead staining method	98.2 – 98.6	[206]
Zn-0.05 Mg-1Ag	<i>S. aureus</i>		99.4 – 99.3	
Zn-1Ag-0.05Zr	<i>E. coli</i>	IZD method	2.90 ± 0.70	[207]
	<i>S. aureus</i>		3.90 ± 0.40	
Zn-0.04 Mg-2Ag	<i>E. coli</i> <i>S. aureus</i> <i>S. epidermidis</i>	Plate count method	–	[208]
Zn-0.8 Mg-0.2Sr	<i>S. gordonii</i>	Live/Dead staining method	–	[209]

epidermidis (MRSE), *S. aureus*, and MRSA were the microorganisms tested by the plate gradient dilution method. The Zn-Cu alloys had a significantly higher bacteriostatic efficacy than the pure Ti and Zn samples used as control. Furthermore, the Zn-2Cu alloy had no bacterial colonies. In addition, MRSE and MRSA were bacteria tested for adhesion on the surface. It was observed that the surface of the Zn-1Cu and Zn-2Cu alloys was covered in a tiny number of bacteria, contrary to the pure Ti control sample, indicating good antibacterial performance. In terms of mechanical properties, the Zn-2Cu alloy had a YS of 226 MPa and a UTS of 270 MPa, an elongation of 41%, and a hardness of 75 HV. Shuai et al.^[197] also examined the antibacterial properties of Zn-xCu alloys, where x ranged from 1 wt.% to 4 wt.%, fabricated by LPBF. The inhibition ring tests showed that all the samples had an antibacterial effect evidenced by clear inhibition zones. IZD for the Zn-3Cu and Zn-4Cu samples were the largest, meaning they exhibited strong antibacterial performance against *E. coli*. It was observed that the antibacterial rate increased with the increment of Cu content. It was 71.8% for Zn-1Cu, 75.3% for Zn-2Cu, 80.1% for Zn-3Cu, and 82.5% for Zn-4Cu. The Cu²⁺ ion released enhanced the antibacterial effect of the Zn-xCu alloys. Furthermore, the authors stated that Cu²⁺ enhances the creation of intracellular ROS, resulting in lipid peroxidation and the inactivation of membrane proteins/enzymes. Thus,

leakage of cytoplasm is expected to occur, killing the bacteria. CYS, UTS, elongation, and hardness values were reported for the Zn-(1-4Cu) alloys. Finally, Li et al.^[198] studied the antibacterial properties of the as-rolled Zn-xCu alloys, where x had a range of 1 wt.% to 4 wt.%. As observed by means of Live/Dead staining, the surface of the Zn-4Cu alloy appeared to have substantially smaller biofilm formation. It also inhibited the adhesion of mixed oral bacteria. The reason behind this antibacterial performance is believed to be due to the Zn²⁺ and Cu²⁺ ion release in addition to the rise in pH levels. The as-cast Zn-4Cu alloy had a YS of 73 MPa, a UTS of 105 MPa, and an elongation of 3.4%.

Other antibacterial metallic elements, precisely Ag and Ce, were also used to produce binary Zn-based alloys. For instance, Qu et al.^[199] examined the antibacterial properties of adding Ag to pure Zn, where the Ag content added had a range of 1 wt.% to 2 wt.%. The alloys were produced *via* casting. Live/Dead staining showed a large amount of green fluorescence (live bacteria) in the control CP-Ti sample. In contrast, pure Zn showed less green fluorescence intensity, indicating less bacterial growth and more antibacterial ability. In addition, testing of the Zn-1Ag and Zn-2Ag alloys found they had even better antibacterial performance as the green fluorescence decreased significantly. SEM and TEM results showed that the bacteria were disrupted, and the integrity of the bacteria for

the Zn-1Ag and Zn-2Ag alloys was destroyed. By interfering with the synthesis of bacterial cell walls, preventing the growth of bacterial autolysis biofilms, successfully suppressing bacterial virulence, and enhancing bacterial drug resistance, the Zn-2Ag alloy operated as a bactericidal agent. It was observed using the morphology of bacteria adhering to the material surface against two drug-resistant bacteria, precisely ATCC-43300 and MRSE-287, that the control Ti sample had significant bacterial adhesion whereas Zn had reduced growth. Significantly lower bacterial adhesion on the Zn-1Ag and Zn-2Ag alloys was then found, indicating superior antibacterial capability. The AgZn₃ phase appeared in the Zn-2Ag alloy, so it was proposed to be the phase capable of releasing Ag ions. The addition of Ag resulted in the increase of the tensile strength while maintaining a high elongation (~35–40%), but it decreased CYS. YS ranged from 125 MPa to 180 MPa, while UTS ranged from 170 MPa to 240 MPa. The addition of Ce was considered by Yang et al.^[200] to examine the antibacterial properties of the Zn-Ce alloys, with Ce contents from 1 wt.% to 3 wt.%, fabricated *via* LPBF. IZD showed that the Zn-2Ce had a larger IZD than pure Zn, indicating that it had enhanced antibacterial performance against *E. coli*. The Zn-2Ce alloy had an antibacterial rate of 81.4%, while pure Zn had a rate of 34.3%. This was justified as, through electrostatic interaction, the released Ce ions were adsorbed on the surface of the cell membrane, which affected cellular transport *via* ionic pumps and increased ion permeability. The Ce ions experienced redox processes that reduced their charge from Ce⁴⁺ to Ce³⁺ causing ROS on the lipids and proteins of the plasma membrane of the bacteria. Consequently, bacteria developed an excessive amount of ROS, resulting in bacterial death. YS of the Zn-2Ce alloy was 181 MPa, UTS was 247 MPa, and the elongation was 7.5%.

Other metallic elements, namely Mn and Dy, have also been considered for developing antibacterial Zn-based alloys. On the one side, Sun et al.^[201] examined the antibacterial behavior of the Zn-0.8Mn (wt.%) alloy subjected to a solution heat treatment. Using the spread plate method, they observed that *E. coli* CFU of all the samples analyzed was less than that of a Ti-6Al-4V sample used as a reference. The good antibacterial performance of the alloy was attributed to the heat treatment performed, where the increase of the heat treatment duration eventually led to reaching a hardness value of 70 HV. On the other side, Tong et al.^[202] studied the antibacterial properties of the binary Zn-xDy alloys ($x = 1-5$ wt.%) fabricated by casting plus hot-rolling. IZD, CFU, and SEM results

showed that the antibacterial performance improved with the increment of the Dy content. The range of IZD was from 5.32 ± 0.22 mm to 7.42 ± 0.26 mm. In addition, when compared to pure Ti, the growth and adhesion of the *S. aureus* bacteria declined, and the pH levels rose drastically. As an antibacterial mechanism used by the alloy, rare earth ions, acting as a catalytic activation center, activated oxygen molecules absorbed on sample surfaces in the culture medium, generating free hydroxyl radicals and ROS. Rare earth ions regulated the bacterial redox levels, damaging bacterial proliferation and death or at least suppressing bacterial growth. YS of the hot-rolled alloys ranged from 175 MPa to 207 MPa, UTS from 210 MPa to 287 MPa, elongation from 58.2% to 43.8%, and hardness from 70 HV to 97 HV.

In terms of ternary Zn-based alloys, both the incorporation of Cu and Ag as antibacterial metallic elements was analyzed. Specifically, Zhang et al.^[203] investigated the antibacterial properties of the hot-extruded Zn-0.5Cu-xFe alloy, where x ranged from 0.1 wt.% to 0.4 wt.%. Using the Live/Dead staining method, it was observed that the alloy exhibited. The ability to inhibit the bacterial adhesion and biofilm formation of both the Gram-positive *Streptococcus gordonii* (*S. gordonii*) and multi-species oral bacteria, as a few vital bacterial layers were found on its surface. The Zn-2Cu alloy had a higher inhibition ability than the other samples, indicating strong antibacterial properties, most likely due to increased released Zn ions and an alkaline shift in pH values. The Zn-0.5Cu-0.4Fe alloy had a YS of 182 MPa, a UTS of 240 MPa, and an elongation of 20%. Lin et al.^[204] investigated the antibacterial properties of the Zn-1Cu-0.1Ti alloy prepared through hot-rolling without and with subsequent cold-rolling. The IZD method against *S. aureus* results indicated that the Zn-1Cu-0.1Ti (wt.%) alloy exhibited an excellent antibacterial effect with a higher IZD than pure Zn, which was 6.99 ± 0.33 mm. The hot-rolled plus cold-rolled alloy had the best mechanical behavior with a YS of 204 MPa, a UTS of 250 MPa, an elongation of 75%, and a hardness of 57 HV. Finally, Zhan et al.^[205] investigated the antibacterial properties of cast Zn-3Al-xCu alloys. The Cu content added had a range of 0 wt.% to 1.5 wt.%, and it was tested against the *S. aureus* bacteria. The *in vitro* degradation behavior results showed that a large number of hydroxides were found, which raised the pH values and, in turn, killed the bacteria. As the degradation rate increased, the Cu²⁺ ions releasing rate increased, resulting in a greater antibacterial effect. Thus, the amount of Cu²⁺

released significantly influenced the antibacterial properties. The agar plate diffusion test and the CFU method were used to examine the antibacterial properties of the ternary alloy Zn-3Al-xCu against *E. coli*, which had an IZD of 4.90 ± 0.40 mm. The antibacterial effect increased significantly with the increment of the Cu element. Therefore, the Zn-3Al-1.5Cu alloy had the best antibacterial effect compared to the other alloys combined, with a UTS of 209 MPa and elongation of 9%.

With respect to the addition of Ag, Xiao et al.^[206] examined the antibacterial properties of the Zn-0.05Mg-(0.5-1)Ag wt.% alloys fabricated by indirect extrusion. The *S. aureus* and *E. coli* incubated bacterial colonies were not found on the surface of the samples, showing their superior antibacterial effect. The releasing of Ag⁺ ions from the alloys interacted with the membranes of bacterial cell walls, ruptured the walls, and ultimately killed the bacterium. The Zn-0.05Mg-0.5Ag alloy exhibited an antibacterial rate of 98.7%, and the Zn-0.05Mg-0.5Ag 99.3% for *S. aureus*. Similarly, the alloys had a rate for *E. coli* of 98.3% and 99.4%, respectively. YS of the Zn-0.05Mg-0.5Ag and Zn-0.05Mg-1Ag alloys were 160 and 170 MPa, respectively. Correspondingly, the UTS was 183 and 202 MPa, and the elongation was 7.5% and 6.5%, respectively. Wątroba et al.^[207] investigated the antibacterial properties of the Zn-1Ag-0.05Zr (wt.%) alloy subjected to a solution treatment followed by extrusion. The alloy tested had antibacterial capabilities against both the Gram-negative *E. coli* with a IZD of 2.90 ± 0.07 mm and the Gram-positive *S. aureus* with IZD of 3.90 ± 0.40 mm. Ag addition enlarged the bacteria growth IZD in the Zn-1Ag-0.05Zr alloy as a result of the releasing of Ag ions, which limited the growth of the microorganisms. Additionally, it was reported that Zr exhibits antibacterial properties, reducing bacterial growth on the surfaces. The Zn-1Ag-0.05Zr alloy had a YS of 166 ± 2 MPa, a UTS of 211 ± 1 MPa, and an elongation of $35 \pm 1\%$. Finally, Wu et al.^[208] examined the antibacterial properties of the Zn-0.04Mg-2Ag (wt.%) alloy prepared using the template replication technique (TRT). Using the Trypticase Soy Broth (TSB) culture media, it was observed that the alloy did not exhibit an antibacterial effect against *E. coli*. Nevertheless, it did show an evident antibacterial effect against *S. aureus* and *S. epidermidis*. It was indicated that Zn ions can impede bacterial growth and reproduction by interfering with cell wall formation. In addition, Ag possesses significant bactericidal capabilities, which can result in the loss of bacterial proteasome function *via* bacterial protease adsorption, giving it

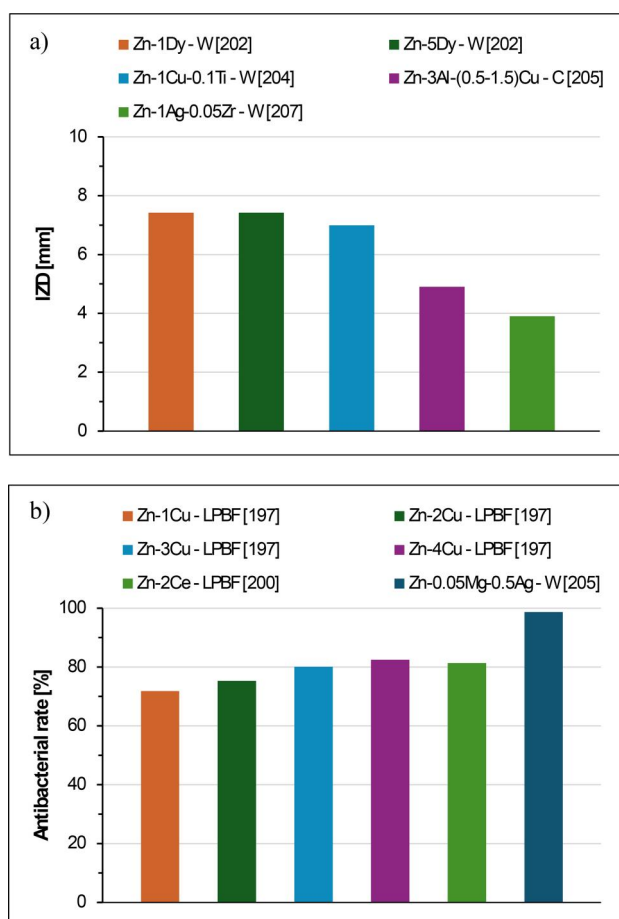


Figure 18. Comparison of the antibacterial efficacy of various Zn-based alloys: (a) inhibition zone diameter (IZD) against Gram-positive bacteria, and (b) antibacterial rate against Gram-negative bacteria. Legend: W: wrought; C: cast; LPBF: laser powder bed fusion.

antibacterial properties. The outcome of the compression test was CYS equal to approximately 8 MPa.

Apart from the addition of Cu or Ag, Sr was also investigated in the work of Čapek et al.^[209] who studied the antibacterial properties of the extruded Zn-0.8Mg-0.2Sr (wt.%) alloy fabricated using casting, homogenization, annealing, and extrusion. Using the Live/Dead staining, as the incubation period increased, the number of *S. gordonii* chains was small, and the proliferation of bacteria and biofilm formation was inhibited. The release of Zn²⁺ and OH⁻ ions and the alkaline shift in pH were pointed to as the responsible factors for the antibacterial activity of the alloy. In terms of mechanical properties, YS was 244 MPa, UTS was 324 MPa, elongation was 20%, and microhardness was 98 HV. Furthermore, in the case of Zn-based alloys, the addition of other elements (e.g., Li^[210]) and the combination of these elements (e.g., Cu-Li^[211] and Ag-Mn^[212]) have been proposed for biodegradable orthopedic applications. The comparison of the

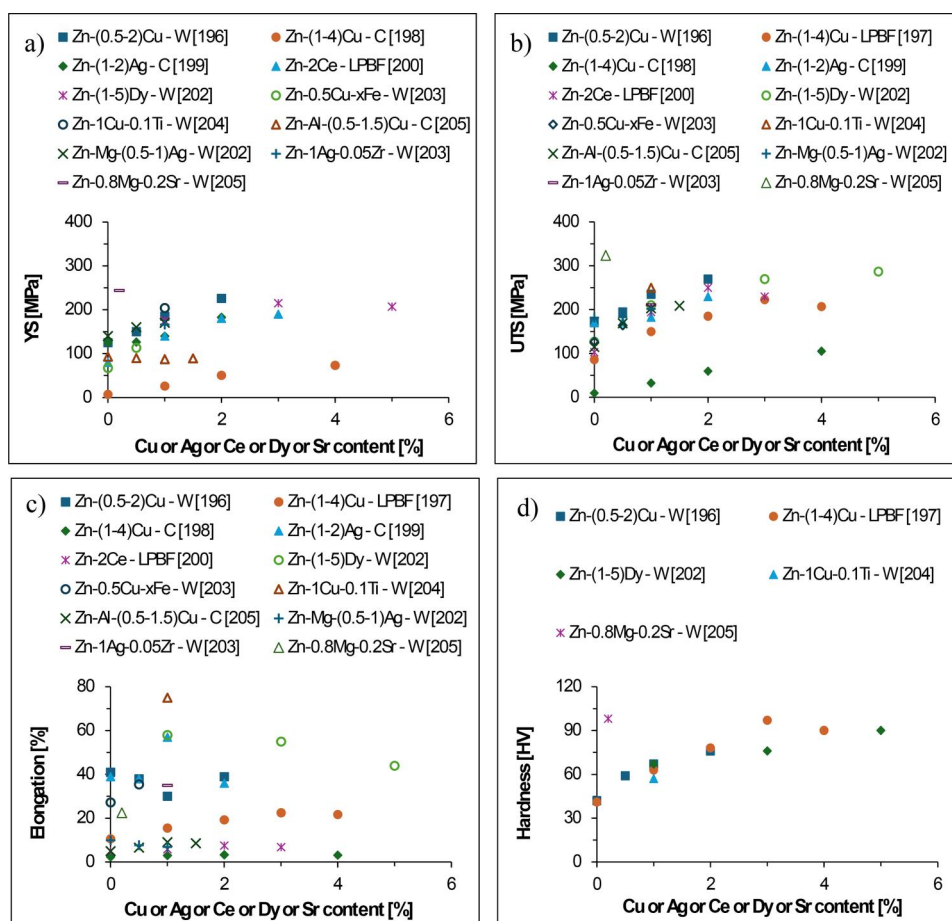


Figure 19. Mechanical properties (tensile and hardness) of antibacterial Zn-based alloys as a function of the Cu/Ag/Ce/Dy/Sr content): (a) YS, (b) UTS, (c) elongation, and (d) hardness. *Legend:* W: wrought; C: cast; LPBF: laser powder bed fusion.

antibacterial response of the Zn-based alloys currently available in literature, if pertinent data were reported, is shown in Figure 18. From IZD data against gram-positive bacteria (Figure 18a), it is found that the addition of lanthanides elements like Ce and Dy yields comparable results, whereas smaller IZD values are achieved when using well-known antibacterial metallic elements like Cu and Ag. In the case of the response against Gram-negative bacteria (Figure 18b), the progressive addition of a greater amount of Cu increases the antibacterial rate of the Zn-based alloys, reaching values comparable to that of a Ce-bearing alloy (i.e., Zn-2Ce), and the highest efficacy is obtained when using Ag as the primary antibacterial metallic element despite its lower content in comparison to Cu and Ce.

Figure 19 displays the range of mechanical properties reported for the antibacterial Zn-based alloys analyzed. It can be seen that the amount of antibacterial metallic element added to enhance the antibacterial response of Zn-based alloys is comparable to that of previously discussed metal-based alloy systems. Generally, the mere addition of an antibacterial metallic element increases the strength and hardness and reduces the elongation.

Metal-based alloy systems where the antibacterial metallic element is simultaneously added to other alloying elements have higher mechanical strength (Figure 19a–b) but not necessarily lower ductility (Figure 19c) or higher hardness (Figure 19d). This reinforces the influence of the manufacturing process on the overall behavior, including antibacterial efficacy and mechanical performance, of the Zn-based alloys. On the one side, the simultaneous addition of Mg and Sr, whose content is significantly lower in comparison to that of other elements used, stands out as a valid option to achieve high strength and hardness. On the other side, the employment of Dy or Cu with a small extra addition of Ti results in the best compromise between high elongation and relatively high strength.

4.3.6. Other metal-based alloys

Apart from the alloy systems analyzed so far, few reports are available in literature about other metal-based alloys that were tested to address their antibacterial capability. Among them, Cu-based alloys, which are meant to be intrinsically antibacterial due to the presence of Cu, received a bit of attention. Because of

that, investigations focused on modifying Cu with different alloying elements to either understand their effect on the antibacterial efficiency or to produce specific desired mechanical responses such as shape memory effect were investigated. For instance, Jiang et al.^[213] clarified the effect brought about by the modification of Cu by means of Zn and Ni by studying the antibacterial behavior of the Cu-20Zn and Cu-20Ni (wt.%) alloys. Using the plate-count method, both alloys appeared to have a small number of *E. coli* bacterial colonies. The antibacterial rate of the Cu-20Zn alloy was 99.0%, and that of the Cu-20Ni alloy was 76.0%. This was justified by the amount of Cu ions released and changes in electrochemical corrosion on the metal surface induced by the element added. No mechanical properties were mentioned. Villapún et al.^[214] considered the creation of ternary Cu-based metallic glasses (i.e., $\text{Cu}_{50+x}(\text{Zr}_{44}\text{Al}_6)_{50-x}$ alloy where $x=0, 3, \text{ and } 6$ at. %) prepared *via* casting and assessed their antibacterial and mechanical properties. The $\text{Cu}_{56}\text{Zr}_{38.7}\text{Al}_{5.3}$ sample had an antibacterial rate of $\geq 90.0\%$ for *E. coli* and *B. subtilis*, attributed to the fact that bacteria cannot tolerate the toxicity of Cu ions and thus the intracellular components were disrupted. The samples that had a Cu content of 50, 53, and 56 at.% were found to be brittle as they fractured in the elastic area and failed before reaching YS. Finally, Shivasiddaramaiah et al.^[215] studied the antibacterial properties of the quaternary cast Cu-(10-13)Al-(0.4-0.6)Be-(0.2-0.3)Mn (wt.%) alloy developed because of its shape memory effect. Using the agar well diffusion method and CFU with *S. aureus*, it was observed that there was no colony formation in the samples. The mechanical properties were not mentioned.

Apart from Cu, Nb-based alloys and Zr-based metallic glasses have also been investigated. In that respect, Wan et al.^[216] studied the antibacterial behavior and mechanical properties induced by the addition of 1–5 Ag (at. %) to Nb, where the alloys were fabricated using MA and SPS. It was observed using the agar media with *S. aureus* and *E. coli* colonies that the alloys had small CFU and antibacterial rates as high as 99.3% against *E. coli* and 98.9% against *S. aureus*. The incremental addition of Ag enhanced the mechanical performance, reaching YS of 1486 MPa, fracture strain of $\sim 35\%$, and hardness of 410 ± 10 HV. Han et al.^[217] examined the antibacterial properties of cast $\text{Zr}_{58.6}\text{Al}_{15.4}(\text{Co}_{1-x}\text{Cu}_x)_{26}$, where x ranged from 0.2 to 0.8 at. %, metallic glasses developed with the purpose of being used in surgical device applications. Using the plate-count method on *E. coli*, it was observed that almost no bacterial colonies

appeared on the surface of the samples, resulting in an antibacterial rate of 99.9%. It was found that the $\text{Zr}_{58.6}\text{Al}_{15.4}\text{Co}_{18.2}\text{Cu}_{7.8}$ metallic glass had the highest strength, with UCS of 1950 MPa, and similar plasticity in comparison to the other glasses tested.

Zr-based alloys are also emerging as potential materials for implant-associated infection, such as in the work of Yang et al.^[218] who analyzed the antibacterial activity of the Zr-30Ta and Zr-25Ta-5Ti alloys.

4.4. Potential applications

It is clear from literature that both academia and industry are interested in the antibacterial properties of metal-based alloys, as this could significantly shift how infection control and hygiene might be approached. For instance, strict sterilization standards are necessary in medicine. Introducing metal-based alloys with inherent antimicrobial properties will provide additional protection for medical instruments and implants. Surgical tools made from these metal-based alloys will significantly reduce the chances of infection-related post-operative complications.^[219] Orthopedic implants such as hip and knee replacements and dental prostheses made with antibacterial metal-based alloys will also reduce the risk of implant-associated infections,^[220] a significant concern in post-operative care. Public spaces, especially healthcare facilities, are breeding grounds for pathogens. Integrating antibacterial metal-based alloys into frequently contacted surfaces such as door handles, push plates, handrails, and seatings could be considered for limiting or eliminating the potential for bacterial transmission. These modifications will reduce the burden on cleaning staff and act as an active line of defense against outbreaks.^[221] Biofilm formation in pipelines and storage tanks is a perennial issue affecting distributed water purity. Adopting antibacterial metal-based alloys into these systems will combat bacterial colonies, ensuring that the water remains uncontaminated throughout its journey. Such an application will guarantee cleaner water and extends the infrastructure's lifespan by reducing microbial-induced corrosion and biofouling. The latter is also a persistent problem for the marine industry, where antibacterial metal-based alloys could be used to manufacture modified vessels, ensuring smoother sea voyages and decreased maintenance.^[222] Employing antibacterial metal-based alloys in processing equipment will be a game-changer for food safety. By reducing microbial contamination during food handling and production, these antibacterial metal-based alloys could ensure that food products are safer for consumption. Using

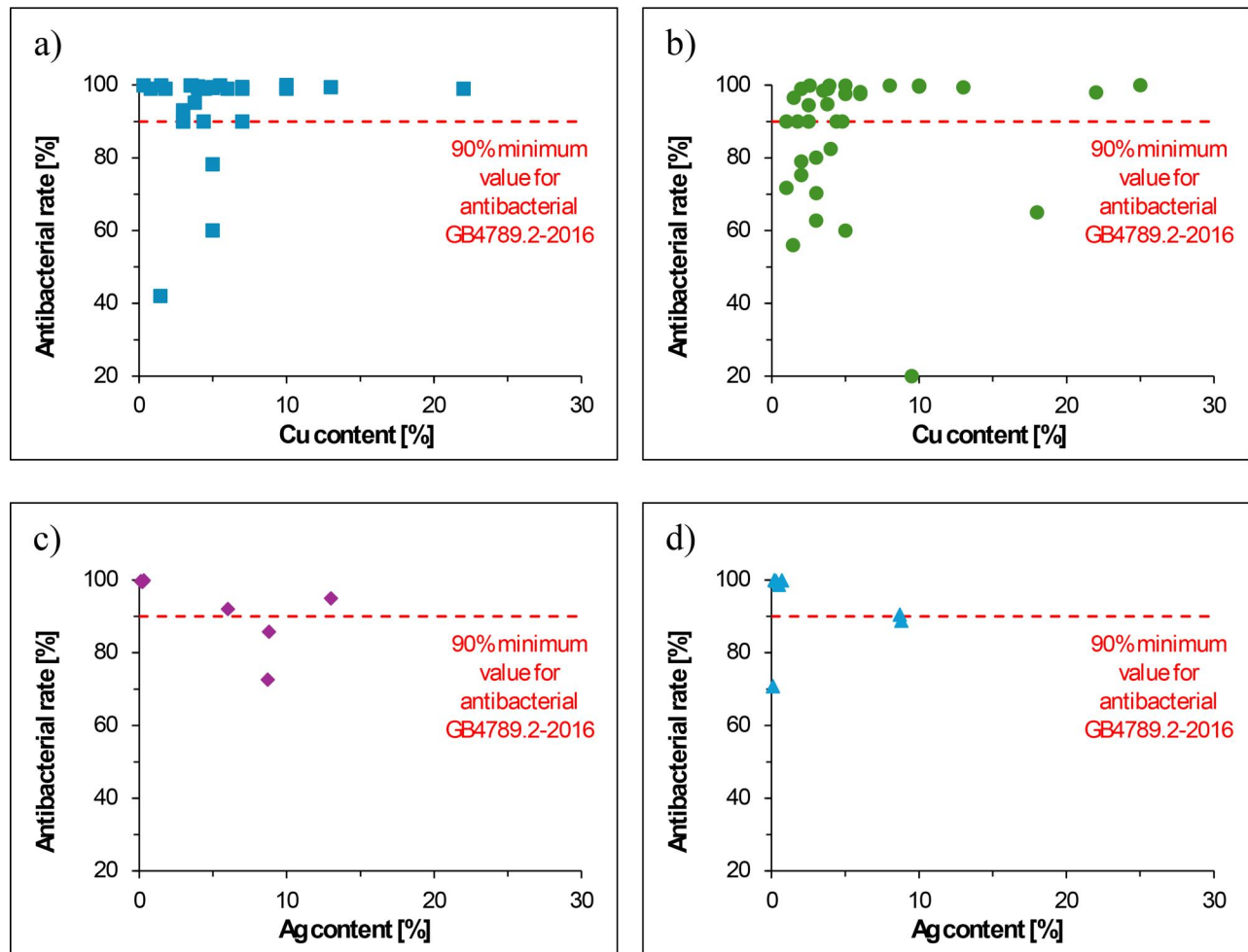


Figure 20. Antibacterial rate achieved in different materials as a function of the amount of Cu or Ag added: (a) efficacy of Cu against gram-positive bacteria, (b) efficacy of Cu against gram-negative bacteria, (c) efficacy of Ag against gram-positive bacteria elongation, and (d) efficacy of Ag against gram-negative bacteria.

containers and food production equipment made of antimicrobial metal-based alloys could also become a protective measure food producers use to help produce contamination-free products.^[223] Finally, components of heating, ventilation, and air conditioning systems made with antibacterial metal-based alloys will be able to deter microbial growth, ensuring healthier air circulation and reducing maintenance costs.

5. Concluding remarks

This work systematically analyzed the efforts made in literature to develop metal-based alloys characterized by antibacterial capability. The mechanisms of bacterial growth and their resistance to ion release have been explained. Additionally, the standard testing methods used for evaluating the antibacterial properties were described, highlighting the factors that may affect the results of these testing methods.

Furthermore, the effects that alloying elements in metal-based alloys have on their antibacterial properties has been analyzed. Due to their ion-release ability, Cu and Ag are the most effective agents for resisting bacteria, as visible from the analysis of the compiled data shown in Figure 20. Firstly, it can be seen that a significantly higher amount of studies have been carried out using Cu rather than Ag, and the overall amount of Ag added to achieve an antibacterial response is generally lower. However, a minimum of 90% antibacterial rate can easily be achieved using a small addition of either Cu or Ag in most instances, regardless of the hosting material (i.e., stainless steel, titanium, etc.). However, the combination of base alloy, amount of antibacterial metallic element added, and manufacturing process used can lead to materials that do not reach the minimum threshold required. In particular, the manufacturing process plays a crucial role in enhancing the metal ion releasing by forming

intermetallic compounds rich in alloying elements, such as Ti_2Cu and Ti_2Ag , and can be leveraged to enhance the antibacterial response.

The most recent work available on antibacterial metallic-based alloys has been reviewed. The comprehensive analysis across various alloy systems reveals a profound potential for these materials in antimicrobial applications, particularly when alloyed with Cu, which consistently enhances the antibacterial efficacy. Alloys bearing Cu as an antibacterial metallic element have shown remarkable effectiveness against both Gram-positive and Gram-negative bacteria, although it is generally higher against the former, suggesting universal applicability in medical and public health settings. The introduction of other elements such as Ag, Ca, Ce, and rare earth elements further influences the antibacterial activity, often enhancing the efficacy. These findings highlight the critical role of elemental composition in the design of alloys for inhibiting bacterial growth. Consequently, such alloys show promise for developing medical implants and devices, potentially significantly reducing infection rates and improving patient outcomes. The responses to different types of bacteria also underscore the necessity for targeted research in alloy development to tailor materials to specific antimicrobial challenges. This positions metal-based alloys as key components in the advancement of healthcare technologies.

6. Challenges and opportunities

It is well known that bacterial infection is a highly dangerous threat to human beings, and, therefore, there is an urge for cutting-edge research worldwide to address novel approaches in the antibacterial research sector. This systematic review discussed the role and importance of using metal-based alloys for antibacterial purposes. The future roadmap for metal-based alloys in antibacterial applications involves several key directions and advancements entailing the modification and/or improvement of the alloys' composition, their structure, and their attributes. This may be part of using high-throughput screening, computational modeling, and advanced manufacturing techniques to determine the best alloy combinations. Moreover, further research into nanotechnology will be essential, as incorporating nanoparticles or nanostructures into metal alloys is a promising route to enhance the antibacterial properties. This includes optimizing nanoparticle size, shape, and distribution to achieve maximum effectiveness against bacterial growth. Future alloys may be designed to possess multiple functionalities beyond antibacterial properties.

They might incorporate attributes like biocompatibility, corrosion resistance, and mechanical strength, making them suitable for various applications, particularly in the medical field. Moreover, the need for biodegradable materials is becoming clearer due to their potential health and environmental benefits. Thus, developing biodegradable metal-based alloys with inherent antibacterial properties is a significant area of interest for further future research. These materials could find applications in temporary implants or devices, gradually degrading while preventing infections. Regardless of the type of metal-based alloy and its foreseen application, efforts should also be focused on improving the sustainability of the manufacturing methods used to process the antibacterial metal-based alloys. Ecologically friendly ways to make these materials to reduce the negative effects of the manufacturing of the antibacterial metal-based alloys on the environment will thus be key. As with any emerging and evolving technology, endeavors should be made to optimize the production processes with the aim of reducing costs and enhancing scalability, which is essential for widespread adoption across various industries. As the great majority of antibacterial metal-based alloys found in literature are envisaged to be used in biomedical applications, extensive clinical studies and real-world evaluations will be necessary to validate efficacy, safety, and long-term performance in practical settings of these metal-based alloys with autogenous antibacterial capability. This will involve collaboration between scientists, medical professionals, and regulatory bodies to ensure compliance with safety standards. The successful development and validation will drive the commercialization and widespread adoption of these antibacterial metal-based alloys across healthcare, food processing, and consumer products.

Disclosure statement

No potential conflict of interest was reported by the author(s).

Data availability statement

All metadata pertaining to this work will be made available on request.

References

1. Klettke, T.; Kappler, O.; Haerberlein, I. R. Anti-Microbial Dental Impression Material. Google Patents **2015**.
2. Hu, S.; Chang, J.; Liu, M.; Ning, C. Study on Antibacterial Effect of 45S5 Bioglass[®]. *J. Mater. Sci.*

- Mater. Med.* **2009**, *20*, 281–286. doi:10.1007/s10856-008-3564-5
3. Simon, V.; Spinu, M.; Stefan, R. Structure and Dissolution Investigation of Calcium-Bismuth-Borate Glasses and Vitroceramics Containing Silver. *J. Mater. Sci. Mater. Med.* **2007**, *18*, 507–512. doi:10.1007/s10856-007-2011-3
 4. Yoshida, K.; Tanagawa, M.; Atsuta, M. Characterization and Inhibitory Effect of Antibacterial Dental Resin Composites Incorporating Silver-Supported Materials. *J. Biomed. Mater. Res.* **1999**, *47*, 516–522. doi:10.1002/(SICI)1097-4636(19991215)47:4<516::AID-JBM7>3.0.CO;2-E
 5. Top, A.; Ülkü, S. Silver, Zinc, and Copper Exchange in a Na-Clinoptilolite and Resulting Effect on Antibacterial Activity. *Appl. Clay Sci.* **2004**, *27*, 13–19. doi:10.1016/j.clay.2003.12.002
 6. Chai, L.-Y.; Wei, S.-W.; Bing, P.; Li, Z.-Y. Effect of Thermal Treating Temperature on Characteristics of Silver-Doped Titania. *Trans. Nonferrous Met. Soc. China* **2008**, *18*, 980–985. doi:10.1016/S1003-6326(08)60169-7
 7. Shiraiishi, K.; Koseki, H.; Tsurumoto, T.; Baba, K.; Naito, M.; Nakayama, K.; Shindo, H. Antibacterial Metal Implant With a TiO₂-Conferred Photocatalytic Bactericidal Effect Against *Staphylococcus aureus*. *Surf. Interface Anal.* **2009**, *41*, 17–22. doi:10.1002/sia.2965
 8. Bolzoni, L.; Alqattan, M.; Yang, F.; Peters, L. Design of β -Eutectoid Bearing Ti Alloys With Antibacterial Functionality. *Mater. Lett.* **2020**, *278*, 128445. doi:10.1016/j.matlet.2020.128445
 9. Bolzoni, L.; Esteban, P. G.; Ruiz-Navas, E. M.; Gordo, E. Mechanical Behaviour of Pressed and Sintered Titanium Alloys Obtained from Prealloyed and Blended Elemental Powders. *J. Mech. Behav. Biomed. Mater.* **2012**, *14*, 29–38. doi:10.1016/j.jmbbm.2012.05.013
 10. B. Balasubramaniam, S. Ranjan, M. Saraf, P. Kar, S.P. Singh, V.K. Thakur, A. Singh, R.K. Gupta, Antibacterial and Antiviral Functional Materials: Chemistry and Biological Activity Toward Tackling COVID-19-Like Pandemics, *ACS Pharmacol. Transl. Sci.* **2021**, *4*(1), 8–54. doi:10.1021/acspsci.0c00174
 11. Zhao, X. Antibacterial Bioactive Materials. *Bioactive Mater. Med.* **2011**, *5*, 97–123.
 12. Sidambe, T. A. Biocompatibility of Advanced Manufactured Titanium Implants-A Review. *Materials* **2014**, *7*, 8168–8188.
 13. Zhao, Q.; Yang, F.; Torrens, R.; Bolzoni, L. *In-Situ* Observation of the Tensile Deformation and Fracture Behaviour of Powder-Consolidated and As-Cast Metastable Beta Titanium Alloys. *Mater. Sci. Eng. A* **2019**, *750*, 45–59. doi:10.1016/j.msea.2019.02.037
 14. Sharma, P. C.; Sharma, D.; Sharma, A.; Saini, N.; Goyal, R.; Ola, M.; Chawla, R.; Thakur, V. K. Hydrazone Comprising Compounds as Promising Anti-Infective Agents: Chemistry and Structure-Property Relationship. *Mater. Today Chem.* **2020**, *18*, 100349. doi:10.1016/j.mtchem.2020.100349
 15. Ates, B.; Koytepe, S.; Ulu, A.; Gurses, C.; Thakur, V. K. Chemistry, Structures, and Advanced Applications of Nanocomposites from Biorenewable Resources. *Chem. Rev.* **2020**, *120*, 9304–9362. doi:10.1021/acs.chemrev.9b00553
 16. Doron, S.; Gorbach, S. L. Bacterial Infections: Overview. In *International Encyclopedia of Public Health*. Amsterdam: Elsevier Science, **2008**, 273–282.
 17. Ribeiro, M.; Monteiro, F. J.; Ferraz, M. P. Infection of Orthopedic Implants With Emphasis on Bacterial Adhesion Process and Techniques Used in Studying Bacterial-Material Interactions. *Biomatter* **2012**, *2*, 176–194. doi:10.4161/biom.22905
 18. Ventola, C. L. The Antibiotic Resistance Crisis: Part 1: Causes and Threats. *P T* **2015**, *40*, 277–283.
 19. Kravanja, K. A.; Finšgar, M. A Review of Techniques for the Application of Bioactive Coatings on Metal-Based Implants to Achieve Controlled Release of Active Ingredients. *Mater. Des.* **2022**, *217*, 110653. doi:10.1016/j.matdes.2022.110653
 20. Silva, R. C. S.; Agrelli, A.; Andrade, A. N.; Mendes-Marques, C. L.; Arruda, I. R. S.; Santos, L. R. L.; Vasconcelos, N. F.; Machado, G. Titanium Dental Implants: An Overview of Applied Nanobiotechnology to Improve Biocompatibility and Prevent Infections. *Materials (Basel)* **2022**, *15*, 3150. doi:10.3390/ma15093150
 21. Pevnick, J. M.; Birkeland, K.; Zimmer, R.; Elad, Y.; Kedan, I. Wearable Technology for Cardiology: An Update and Framework for the Future. *Trends Cardiovasc. Med.* **2018**, *28*, 144–150. doi:10.1016/j.tcm.2017.08.003
 22. Chen, X.; Zhou, J.; Qian, Y.; Zhao, L. Antibacterial Coatings on Orthopedic Implants. *Mater. Today. Bio.* **2023**, *19*, 100586. doi:10.1016/j.mtbio.2023.100586
 23. Hori, K.; Matsumoto, S. Bacterial Adhesion: From Mechanism to Control. *Biochem. Eng. J.* **2010**, *48*, 424–434. doi:10.1016/j.bej.2009.11.014
 24. Seebach, E.; Kubatzky, K. F. Chronic Implant-Related Bone Infections-Can Immune Modulation be a Therapeutic Strategy? *Front. Immunol.* **2019**, *10*, 1724. doi:10.3389/fimmu.2019.01724
 25. Khatoon, Z.; McTiernan, C. D.; Suuronen, E. J.; Mah, T.-F.; Alarcon, E. I. Bacterial Biofilm Formation on Implantable Devices and Approaches to Its Treatment and Prevention. *Heliyon* **2018**, *4*, e01067. doi:10.1016/j.heliyon.2018.e01067
 26. Rao, T. S. Bacterial Biofilms and Implant Infections: A Perspective. *Arch. Orthop.* **2020**, *1*, 98–105.
 27. Li, P.; Yin, R.; Cheng, J.; Lin, J. Bacterial Biofilm Formation on Biomaterials and Approaches to Its Treatment and Prevention. *Int. J. Mol. Sci.* **2023**, *24*, 11680. doi:10.3390/ijms241411680
 28. Serbanescu, M. A.; Apple, C. G.; Fernandez-Moure, J. S. Role of Resident Microbial Communities in Biofilm-Related Implant Infections: Recent Insights and Implications. *Surg. Infect. (Larchmt)* **2023**, *24*, 258–264. doi:10.1089/sur.2023.009
 29. Dadi, N. C. T.; Radochová, B.; Vargová, J.; Bujdáková, H. Impact of Healthcare-Associated Infections Connected to Medical Devices—An

- Update. *Microorganisms* **2021**, *9*, 2332. doi:10.3390/microorganisms9112332
30. Schierholz, J. M.; Beuth, J. Implant Infections: A Haven for Opportunistic Bacteria. *J. Hosp. Infect.* **2001**, *49*, 87–93. doi:10.1053/jhin.2001.1052
 31. Duarte, P. M.; Nogueira Filho, G. R.; Sallum, E. A.; de Toledo, S.; Sallum, A. W.; Nociti Júnior, F. H. The Effect of an Immunosuppressive Therapy and Its Withdrawal on Bone Healing Around Titanium Implants. A Histometric Study in Rabbits. *J. Periodol.* **2001**, *72*, 1391–1397.
 32. Desai, R. J.; Bateman, B. T.; Huybrechts, K. F.; Paterno, E.; Hernandez-Diaz, S.; Park, Y.; Dejene, S. Z.; Cohen, J.; Mogun, H.; Kim, S. C. Risk of Serious Infections Associated With Use of Immunosuppressive Agents in Pregnant Women With Autoimmune Inflammatory Conditions: Cohort Study. *BMJ* **2017**, *356*, j895. doi:10.1136/bmj.j895
 33. Orlicka, K.; Barnes, E.; Culver, E. L. Prevention of Infection Caused by Immunosuppressive Drugs in Gastroenterology. *Ther. Adv. Chronic Dis.* **2013**, *4*, 167–185. doi:10.1177/2040622313485275
 34. Vincent, M.; Duval, R. E.; Hartemann, P.; Engels-Deutsch, M. Contact Killing and Antimicrobial Properties of Copper. *J. Appl. Microbiol.* **2018**, *124*, 1032–1046. doi:10.1111/jam.13681
 35. Fletcher, L. The Influence of Relative Humidity on the UV Susceptibility of Airborne Gram Negative Bacteria. *Univ. Leeds.* **2004**, *1*, 1–7.
 36. Farag, A.; Toghan, A.; Mostafa, M.; Chen, L.; Ge, G. Environmental Remediation Through Catalytic Inhibition of Steel Corrosion by Schiff's Bases: Electrochemical and Biological Aspects. *Catalysts* **2022**, *12*, 838. doi:10.3390/catal12080838
 37. Harrison, S. T. L. Bacterial Cell Disruption: A Key Unit Operation in the Recovery of Intracellular Products. *Biotechnol. Adv.* **1991**, *9*, 217–240. doi:10.1016/0734-9750(91)90005-g
 38. Middelberg, A. P. J. Process-Scale Disruption of Microorganisms. *Biotechnol. Adv.* **1995**, *13*, 491–551. doi:10.1016/0734-9750(95)02007-p
 39. Harrison, S. T. L. 2.47 - Cell Disruption. In *Comprehensive Biotechnology*, 3rd ed.; M. Moo-Young. Pergamon: Oxford, **2011**; pp. 692–712.
 40. Bovenkamp, G. L.; Zanzen, U.; Krishna, K. S.; Hormes, J.; Prange, A. Near-Edge Structure (XANES) Spectroscopy Study of the Interaction of Silver Ions With *Staphylococcus aureus*, *Listeria monocytogenes*, and *Escherichia coli*. *Appl. Environ. Microbiol.* **2013**, *79*, 6385–6390. doi:10.1128/AEM.01688-13
 41. Ahmed, B.; Solanki, B.; Zaidi, A.; Khan, M. S.; Musarrat, J. Bacterial Toxicity of Biomimetic Green Zinc Oxide Nanoantibiotic: Insights Into ZnONP Uptake and Nanocolloid–Bacteria Interface. *Toxicol. Res. (Camb)* **2019**, *8*, 246–261. doi:10.1039/c8tx00267c
 42. Ebrahiminezhad, A.; Bagheri, M.; Taghizadeh, S.-M.; Berenjian, A.; Ghasemi, Y. Biomimetic Synthesis of Silver Nanoparticles Using Microalgal Secretory Carbohydrates as a Novel Anticancer and Antimicrobial. *Adv. Nat. Sci. Nanosci. Nanotechnol.* **2016**, *7*, 015018. doi:10.1088/2043-6262/7/1/015018
 43. van Hengel, I. A. J.; Tierolf, M. W. A. M.; Fratila-Apachitei, L. E.; Apachitei, I.; Zadpoor, A. A. Antibacterial Titanium Implants Biofunctionalized by Plasma Electrolytic Oxidation With Silver, Zinc, and Copper: A Systematic Review. *Int. J. Mol. Sci.* **2021**, *22*, 3800. doi:10.3390/ijms22073800
 44. Riool, M.; de Boer, L.; Jaspers, V.; van der Loos, C. M.; van Wamel, W. J.; Wu, G.; Kwakman, P. H.; Zaat, S. A. *Staphylococcus epidermidis* Originating from Titanium Implants Infects Surrounding Tissue and Immune Cells. *Acta Biomater.* **2014**, *10*, 5202–5212. doi:10.1016/j.actbio.2014.08.012
 45. Joseph, L. A.; Israel, O. K.; Edet, E. J. Comparative Evaluation of Metal Ions Release from Titanium and Ti-6Al-7Nb into Bio-Fluids. *Dent. Res. J. (Isfahan)* **2009**, *6*, 7–11.
 46. Zanzen, U.; Bovenkamp-Langlois, L.; Klysubun, W.; Hormes, J.; Prange, A. The Interaction of Copper Ions With *Staphylococcus aureus*, *Pseudomonas aeruginosa*, and *Escherichia coli*: An X-Ray Absorption Near-Edge Structure (XANES) Spectroscopy Study. *Arch. Microbiol.* **2018**, *200*, 401–412. doi:10.1007/s00203-017-1454-2
 47. Gholami, A.; Mohammadi, F.; Ghasemi, Y.; Omidifar, N.; Ebrahiminezhad, A. Antibacterial Activity of SPIONs Versus Ferrous and Ferric Ions Under Aerobic and Anaerobic Conditions: A Preliminary Mechanism Study. *IET Nanobiotechnol.* **2020**, *14*, 155–160. doi:10.1049/iet-nbt.2019.0266
 48. Ortiz-Benítez, E. A.; Velázquez-Guadarrama, N.; Figueroa, N. V. D.; Quezada, H.; Olivares-Trejo, J. Antibacterial Mechanism of Gold Nanoparticles on *Streptococcus pneumoniae*. *Metallomics* **2019**, *11*, 1265–1276. doi:10.1039/c9mt00084d
 49. Chen, P.; Huang, Z.; Liang, J.; Cui, T.; Zhang, X.; Miao, B.; Yan, L.-T. Diffusion and Directionality of Charged Nanoparticles on Lipid Bilayer Membrane. *ACS Nano* **2016**, *10*, 11541–11547. doi:10.1021/acs-nano.6b07563
 50. Brayner, R.; Ferrari-Iliou, R.; Brivois, N.; Djediat, S.; Benedetti, M. F.; Fiévet, F. Toxicological Impact Studies Based on *Escherichia coli* Bacteria in Ultrafine ZnO Nanoparticles Colloidal Medium. *Nano Lett.* **2006**, *6*, 866–870. doi:10.1021/nl052326h
 51. Bondarenko, O. M.; Sihtmäe, M.; Kuzmičiova, J.; Ragelienė, L.; Kahru, A.; Daugelavičius, R. Plasma Membrane is the Target of Rapid Antibacterial Action of Silver Nanoparticles in *escherichia coli* and *Pseudomonas aeruginosa*. *Int. J. Nanomed.* **2018**, *13*, 6779–6790. doi:10.2147/IJN.S177163
 52. Calvano, C. D.; Picca, R. A.; Bonerba, E.; Tantillo, G.; Cioffi, N.; Palmisano, F. MALDI-TOF Mass Spectrometry Analysis of Proteins and Lipids in *Escherichia coli* Exposed to Copper Ions and Nanoparticles. *J. Mass Spectrom.* **2016**, *51*, 828–840. doi:10.1002/jms.3823
 53. Pelgrift, R. Y.; Friedman, A. J. Nanotechnology as a Therapeutic Tool to Combat Microbial Resistance. *Adv. Drug Deliv. Rev.* **2013**, *65*, 1803–1815. doi:10.1016/j.addr.2013.07.011

54. Zhang, E.; Zhao, X.; Hu, J.; Wang, R.; Fu, S.; Qin, G. Antibacterial Metals and Alloys for Potential Biomedical Implants. *Bioact. Mater.* **2021**, *6*, 2569–2612. doi:10.1016/j.bioactmat.2021.01.030
55. Joe, R. J. T.; Lemire, A. *Mechanisms Underlying the Antimicrobial Capacity of Metals*; New York: Wiley Online Library, **2016**.
56. Lemire, J. A.; Harrison, J. J.; Turner, R. J. Antimicrobial Activity of Metals: Mechanisms, Molecular Targets and Applications. *Nat. Rev. Microbiol.* **2013**, *11*, 371–384. doi:10.1038/nrmicro3028
57. Chitambar, C. R. Gallium and Its Competing Roles With Iron in Biological Systems. *Biochim. Biophys. Acta.* **2016**, *1863*, 2044–2053. doi:10.1016/j.bbamcr.2016.04.027
58. Peter, N. S.; Erskine, T.; Awan, S.; Lambert, R.; Lewis, G.; Tickle, I. J.; Sarwar, M.; Spencer, P.; Thomas, P.; Warren, M. J.; et al. X-Ray Structure of 5-Aminolaevulinatase Dehydratase, a Hybrid Aldolase. *Nat. Struct. Mol. Biol.* **1997**, *4*, 1025–1031.
59. Ogunseitán, O. A.; Yang, S.; Ericson, J. Microbial δ -Aminolevulinatase Dehydratase as a Biosensor of Lead Bioavailability in Contaminated Environments. *Soil Biol. Biochem.* **2000**, *32*, 1899–1906. doi:10.1016/S0038-0717(00)00164-4
60. Lee Macomber, S. P. E.; Hausinger, R. P. Fructose-1,6-Bisphosphate Aldolase (Class II) is the Primary Site of Nickel Toxicity in *Escherichia coli*. *Mol. Microbiol.* **2011**, *82*, 1291–1300.
61. Sies, H.; Belousov, V. V.; Chandel, N. S.; Davies, M. J.; Jones, D. P.; Mann, G. E.; Murphy, M. P.; Yamamoto, M.; Winterbourn, C. Defining Roles of Specific Reactive Oxygen Species (ROS) in Cell Biology and Physiology. *Nat. Rev. Mol. Cell Biol.* **2022**, *23*, 499–515. doi:10.1038/s41580-022-00456-z
62. Godoy-Gallardo, M.; Eckhard, U.; Delgado, L. M.; de Roo Puente, Y. J. D.; Hoyos-Nogués, M.; Gil, F. J.; Perez, R. A. Antibacterial Approaches in Tissue Engineering Using Metal Ions and Nanoparticles: From Mechanisms to Applications. *Bioact. Mater.* **2021**, *6*, 4470–4490. doi:10.1016/j.bioactmat.2021.04.033
63. Phaniendra, A.; Jestadi, D. B.; Periyasamy, L. Free Radicals: Properties, Sources, Targets, and Their Implication in Various Diseases. *Ind. J. Clin. Biochem.* **2015**, *30*, 11–26. doi:10.1007/s12291-014-0446-0
64. Touyz, L. *Reactive Oxygen Species, Textbook of Vascular Medicine*; Berlin: Springer, **2019**.
65. Wang, E.; Huang, Y.; Du, Q.; Sun, Y. Silver Nanoparticle Induced Toxicity to Human Sperm by Increasing ROS (Reactive Oxygen Species) Production and DNA Damage. *Environ. Toxicol. Pharmacol.* **2017**, *52*, 193–199. doi:10.1016/j.etap.2017.04.010
66. Mustila, Y. A. H.; Isojärvi, J.; Aro, E. M.; Eisenhut, M. The Bacterial-Type [4Fe–4S] Ferredoxin 7 Has a Regulatory Function under Photooxidative Stress Conditions in the Cyanobacterium *Synechocystis* sp. PCC 6803. *Biochim. Biophys. Acta (BBA) – Mol. Cell Res.* **2014**, *1837*, 1293–1304.
67. Cloete, T. E. Resistance Mechanisms of Bacteria to Antimicrobial Compounds. *Int. Biodeteriorat. Biodegrad.* **2003**, *51*, 277–282. doi:10.1016/S0964-8305(03)00042-8
68. Zhou, G.; Shi, Q.-S.; Huang, X.-M.; Xie, X.-B. The Three Bacterial Lines of Defense against Antimicrobial Agents. *Int. J. Mol. Sci.* **2015**, *16*, 21711–21733. doi:10.3390/ijms160921711
69. Bruins, M. R.; Kapil, S.; Oehme, F. W. Microbial Resistance to Metals in the Environment. *Ecotoxicol. Environ. Saf.* **2000**, *45*, 198–207. doi:10.1006/eesa.1999.1860
70. Niño-Martínez, N.; Salas Orozco, M. F.; Martínez-Castañón, G.-A.; Torres Méndez, F.; Ruiz, F. Molecular Mechanisms of Bacterial Resistance to Metal and Metal Oxide Nanoparticles. *Int. J. Mol. Sci.* **2019**, *20*, 2808. doi:10.3390/ijms20112808
71. Rouch, D. A.; Lee, B. T.; Morby, A. P. Understanding Cellular Responses to Toxic Agents: A Model for Mechanism-Choice in Bacterial Metal Resistance. *J. Ind. Microbiol.* **1995**, *14*, 132–141. doi:10.1007/BF01569895
72. Scott, J. A.; Palmer, S. J. Sites of Cadmium Uptake in Bacteria Used for Biosorption. *Appl. Microbiol. Biotechnol.* **1990**, *33*, 221–225. doi:10.1007/BF00176529
73. Bryers, J. D. Bacterial Biofilms. *Curr. Opin. Biotechnol.* **1993**, *4*, 197–204. doi:10.1016/0958-1669(93)90125-g
74. Ma, J. F.; Hager, P. W.; Howell, M. L.; Phibbs, P. V.; Hassett, D. J. Cloning and Characterization of the *Pseudomonas aeruginosa* Zwf Gene Encoding Glucose-6-Phosphate Dehydrogenase, an Enzyme Important in Resistance to Methyl Viologen (Paraquat). *J. Bacteriol.* **1998**, *180*, 1741–1749. doi:10.1128/JB.180.7.1741-1749.1998
75. Roca, A.; Rodríguez-Herva, J.-J.; Duque, E.; Ramos, J. L. Physiological Responses of *Pseudomonas putida* to Formaldehyde During Detoxification. *Microb. Biotechnol.* **2008**, *1*, 158–169. doi:10.1111/j.1751-7915.2007.00014.x
76. Kümmerle, N.; Feucht, H. H.; Kaulfers, P. M. Plasmid-Mediated Formaldehyde Resistance in *Escherichia coli*: Characterization of Resistance Gene. *Antimicrob. Agents Chemother.* **1996**, *40*, 2276–2279. doi:10.1128/AAC.40.10.2276
77. Guerrero Correa, M.; Martínez, F. B.; Vidal, C. P.; Streitt, C.; Escrig, J.; de Dicastillo, C. L. Antimicrobial Metal-Based Nanoparticles: A Review on Their Synthesis, Types and Antimicrobial Action. *Beilstein J. Nanotechnol.* **2020**, *11*, 1450–1469. doi:10.3762/bjnano.11.129
78. Parker, N.; Schneegurt, M.; Tu, A.-H. T.; Lister, P.; Forster, B. M. *Microbiology, Openstax*; Rice University, Houston, TX, **2016**.
79. JIS Z 2801 Test for Antimicrobial Activity of Plastics, 2021. Tokyo: Japan Industrial Standard, **2023**.
80. Victor, L. G. D.; Villapún, M.; Cross, A.; González, S. Antibacterial Metallic Touch Surfaces. *Materials* **2016**, *9*, 736.

81. Nishitani, T.; Masuda, K.; Mimura, S.; Hirokawa, T.; Ishiguro, H.; Kumagai, M.; Ito, T. Antibacterial Effect on Microscale Rough Surface Formed by Fine Particle Bombarding. *AMB Exp.* **2022**, *12*, 9. doi:10.1186/s13568-022-01351-8
82. Bolzoni, L.; Raynova, S.; Yang, F. Work Hardening of Microwave Sintered Blended Elemental Ti Alloys. *J. Alloys Compd.* **2020**, *838*, 155559. doi:10.1016/j.jallcom.2020.155559
83. Bolzoni, L.; Esteban, P. G.; Ruiz-Navas, E. M.; Gordo, E. Influence of Powder Characteristics on Sintering Behaviour and Properties of PM Ti Alloys Produced from Prealloyed Powder and Master Alloy. *Powder Metall.* **2011**, *54*, 543–550. doi:10.1179/003258910X12827272082623
84. Fan, X.; Yahia, L.; Sacher, E. Antimicrobial Properties of the Ag, Cu Nanoparticle System. *Biology. (Basel)* **2021**, *10*, 137. doi:10.3390/biology10020137
85. Günen, A.; Ergin, Ö. A Comparative Study on Characterization and High-Temperature Wear Behaviors of Thermochemical Coatings Applied to Cobalt-Based Haynes 25 Superalloys. *Coatings* **2023**, *13*, 1272. doi:10.3390/coatings13071272
86. Gialanella, S.; Malandrucolo, A. Superalloys. In *Aerospace Alloys*; S. Gialanella, A. Malandrucolo, Eds. Springer International Publishing: Cham, **2020**; pp. 267–386.
87. Wang, L.; Zhu, Z.; Wang, F.; Qi, Y.; Zhang, W.; Wang, C. State-of-the-Art and Prospects of Zn-Containing Layered Double Hydroxides (Zn-LDH)-Based Materials for Photocatalytic Water Remediation. *Chemosphere* **2021**, *278*, 130367. doi:10.1016/j.chemosphere.2021.130367
88. Dong, Y.-D.; Shi, Y.; He, Y.-L.; Yang, S.-R.; Yu, S.-Y.; Xiong, Z.; Zhang, H.; Yao, G.; He, C.-S.; Lai, B. Synthesis of Fe-Mn-Based Materials and Their Applications in Advanced Oxidation Processes for Wastewater Decontamination: A Review. *Ind. Eng. Chem. Res.* **2023**, *62*, 10828–10848.
89. Kaseem, M.; Zehra, T.; Hussain, T.; Ko, Y. G.; Fattah-Alhosseini, A. Electrochemical Response of MgO/Co₃O₄ Oxide Layers Produced by Plasma Electrolytic Oxidation and Post Treatment Using Cobalt Nitrate. *J. Magnesium Alloys* **2023**, *11*, 1057–1073. doi:10.1016/j.jma.2022.08.008
90. Fattah-Alhosseini, A.; Chaharmahali, R.; Alizad, S.; Kaseem, M. Corrosion Behavior of Composite Coatings Containing Hydroxyapatite Particles on Mg Alloys by Plasma Electrolytic Oxidation: A Review. *J. Magnesium Alloys* **2023**, *11*, 2999–3011. doi:10.1016/j.jma.2023.09.003
91. Mishchenko, O.; Ovchynnykov, O.; Kapustian, O.; Pogorielov, M. New Zr-Ti-Nb Alloy for Medical Application: Development, Chemical and Mechanical Properties, and Biocompatibility. *Materials* **2020**, *13*, 1306. doi:10.3390/ma13061306
92. Alshammari, Y.; Mendoza, S.; Yang, F.; Bolzoni, L. Effect of Mn on the Properties of Powder Metallurgy Ti-2.5Al-xMn Alloys. *Materials* **2023**, *16*, 4917. doi:10.3390/ma16144917
93. Qi, P.; Li, B.; Wang, T.; Zhou, L.; Nie, Z. Microstructure and Properties of a Novel Ternary Ti-6Zr-xFe Alloy for Biomedical Applications. *J. Alloys Compd.* **2021**, *854*, 157119. doi:10.1016/j.jallcom.2020.157119
94. Alshammari, Y.; Jia, M.; Yang, F.; Bolzoni, L. The Effect of $\alpha + \beta$ Forging on the Mechanical Properties and Microstructure of Binary Titanium Alloys Produced Via a Cost-Effective Powder Metallurgy Route. *Mater. Sci. Eng. A* **2020**, *769*, 138496. doi:10.1016/j.msea.2019.138496
95. Bolzoni, L.; Paul, M.; Yang, F. Effect of Combined Lean Additions of Isomorphous and Eutectoid Beta Stabilisers on the Properties of Titanium. *J. Mater. Res. Technol.* **2022**, *21*, 3828–3843. doi:10.1016/j.jmrt.2022.11.023
96. Campoccia, D.; Montanaro, L.; Arciola, C. R. A Review of the Clinical Implications of anti-Infective Biomaterials and Infection-Resistant Surfaces. *Biomaterials* **2013**, *34*, 8018–8029. doi:10.1016/j.biomaterials.2013.07.048
97. Sreekumari, K. R.; Sato, Y.; Kikuchi, Y. Antibacterial Metals - A Viable Solution for Bacterial Attachment and Microbiologically Influenced Corrosion. *Mater. Trans.* **2005**, *46*, 1636–1645. doi:10.2320/matertrans.46.1636
98. Kawakami, H.; Yoshida, K.; Nishida, Y.; Kikuchi, Y.; Sato, Y. Antibacterial Properties of Metallic Elements for Alloying Evaluated With Application of JIS Z 2801:2000. *ISIJ Int.* **2008**, *48*, 1299–1304.
99. Heidenau, F.; Mittelmeier, W.; Detsch, R.; Haenle, M.; Stenzel, F.; Ziegler, G.; Gollwitzer, H. A Novel Antibacterial Titania Coating: Metal Ion Toxicity and *In Vitro* Surface Colonization. *J. Mater. Sci. Mater. Med.* **2005**, *16*, 883–888. doi:10.1007/s10856-005-4422-3
100. Romero, C.; Yang, F.; Raynova, S.; Bolzoni, L. Thermomechanically Processed Powder Metallurgy Ti-5Fe Alloy: Effect of Microstructure, Texture, Fe Partitioning and Residual Porosity on Tensile and Fatigue Behaviour. *Materialia* **2021**, *20*, 101254. doi:10.1016/j.mtla.2021.101254
101. Zhang, H.; Wang, C.; Pyczak, F.; Ebel, T.; Liu, X. A New Kind of Biomedical Ti-Mn-Nb Alloy. *Phys. Status Solidi (A)* **2023**, *220*, 2200348. doi:10.1002/pssa.202200348
102. Romero, C.; Yang, F.; Zhang, S.; Bolzoni, L. Effect of Thermomechanical Microstructural Modification and Resulting Crystallographic Texture on the Crack Initiation Mechanism and Fatigue Behaviour of PM Ti-6Al-4V. *Mater. Sci. Eng. A* **2020**, *792*, 139836. doi:10.1016/j.msea.2020.139836
103. Sun, S.; Zhang, D.; Palanisamy, S.; Liu, Q.; Dargusch, M. S. Mechanical Properties and Deformation Mechanisms of Martensitic Ti6Al4V Alloy Processed by Laser Powder Bed Fusion and Water Quenching. *Mater. Sci. Eng. A* **2022**, *839*, 142817. doi:10.1016/j.msea.2022.142817
104. Ahmadabadi, H. Y.; Yu, K.; Kizhakkedathu, J. N. Surface Modification Approaches for Prevention of Implant Associated Infections. *Colloids Surf. B*

- Biointerfaces* **2020**, *193*, 111116. doi:10.1016/j.col-surf.2020.111116
105. Priyadarshini, B., Rama, M., Vijayalakshmi, U., Bioactive Coating as a Surface Modification Technique for Biocompatible Metallic Implants: A Review, *J. Asian Ceram. Soc.* **2019**, *7*(4), 397–406. doi:10.1080/21870764.2019.1669861
 106. Bolzoni, L.; Hari Babu, N. Engineering the Heterogeneous Nuclei in Al-Si Alloys for Solidification Control. *Appl. Mater. Today* **2016**, *5*, 255–259. doi:10.1016/j.apmt.2016.11.001
 107. Bolzoni, L.; Nowak, M.; Hari Babu, N. Grain Refining Potency of Nb-B -Nucleation on Al-12Si-0.6Fe-0.5Mn Alloy. *J. Alloys Compd.* **2015**, *623*, 79–82. doi:10.1016/j.jallcom.2014.10.069
 108. Bolzoni, L.; Babu, N. H. Refinement of the Grain Size of the LM25 Alloy (A356) by 96Al-2Nb-2B Master Alloy. *J. Mater. Process. Technol.* **2015**, *222*, 219–223. doi:10.1016/j.jmatprotec.2015.03.011
 109. Bolzoni, L.; Xia, M.; Babu, N. H. Formation of Equiaxed Crystal Structures in Directionally Solidified Al-Si Alloys Using Nb-Based Heterogeneous Nuclei. *Sci. Rep.* **2016**, *6*, 39554. doi:10.1038/srep39554
 110. Jia, M.; Alshammari, Y.; Yang, F.; Bolzoni, L. Effect of Heat Treatment on the Microstructure and Mechanical Properties of Blended Elemental Ti-6Al-4V Produced by Powder Forging. *Mater. Sci. Eng.: A* **2020**, *791*, 139724. doi:10.1016/j.msea.2020.139724
 111. Lei, Z.; Zhang, H.; Zhang, E.; You, J.; Ma, X.; Bai, X. Antibacterial Activities and Biocompatibilities of Ti-Ag Alloys Prepared by Spark Plasma Sintering and Acid Etching. *Mater. Sci. Eng. C Mater. Biol. Appl.* **2018**, *92*, 121–131. doi:10.1016/j.msec.2018.06.024
 112. Romero, C.; Raynova, S.; Yang, F.; Bolzoni, L. Ultrafine Microstructures in Eutectoid Element Bearing Low-Cost Ti-Fe Alloys Enabled by Slow Bainite Formation. *J. Alloys Compd.* **2018**, *769*, 226–232. doi:10.1016/j.jallcom.2018.07.347
 113. Wang, S.; Yang, C.; Shen, M.; Yang, K. Effect of Aging on Antibacterial Performance of Cu-Bearing Martensitic Stainless Steel. *Mater. Technol.* **2014**, *29*, 257–261. doi:10.1179/1753555714Y.0000000156
 114. Xie, Y.; Cui, S.; Hu, J.; Yu, H.; Xuan, A.; Wei, Y.; Lian, Y.; Wu, J.; Du, W.; Zhang, E. Design and Preparation of Ti-xFe Antibacterial Titanium Alloys Based on Micro-Area Potential Difference. *Biometals* **2024**, *37*, 337–355. doi:10.1007/s10534-023-00551-4
 115. Zhang, E.; Wang, X.; Chen, M.; Hou, B. Effect of the Existing Form of Cu Element on the Mechanical Properties, Bio-Corrosion and Antibacterial Properties of Ti-Cu Alloys for Biomedical Application. *Mater. Sci. Eng. C Mater. Biol. Appl.* **2016**, *69*, 1210–1221. doi:10.1016/j.msec.2016.08.033
 116. Chen, M.; Yang, L.; Zhang, L.; Han, Y.; Lu, Z.; Qin, G.; Zhang, E. Effect of Nano/micro-Ag Compound Particles on the Bio-Corrosion, Antibacterial Properties and Cell Biocompatibility of Ti-Ag Alloys. *Mater. Sci. Eng. C Mater. Biol. Appl.* **2017**, *75*, 906–917. doi:10.1016/j.msec.2017.02.142
 117. Romero, C.; Yang, F.; Wei, S.; Bolzoni, L. Thermomechanical Processing of Cost-Affordable Powder Metallurgy Ti-5Fe Alloys from the Blended Elemental Approach: Microstructure, Tensile Deformation Behavior, and Failure. *Metals* **2020**, *10*, 1405. doi:10.3390/met10111405
 118. Li, W.; Wang, X.; Liu, C.; Qin, G.; Zhang, E. Effect of Heat Treatment on the Bio-Corrosion Properties and Wear Resistance of Antibacterial Co-29Cr-6Mo-xCu Alloys. *J. Mater. Sci. Mater. Med.* **2019**, *30*, 112. doi:10.1007/s10856-019-6313-z
 119. Zhang, E.; Li, S.; Ren, J.; Zhang, L.; Han, Y. Effect of Extrusion Processing on the Microstructure, Mechanical Properties, Biocorrosion Properties and Antibacterial Properties of Ti-Cu Sintered Alloys. *Mater. Sci. Eng. C Mater. Biol. Appl.* **2016**, *69*, 760–768. doi:10.1016/j.msec.2016.07.051
 120. Raynova, S.; Collas, Y.; Yang, F.; Bolzoni, L. Advancement in the Pressureless Sintering of CP Titanium Using High-Frequency Induction Heating. *Metall. Mater. Trans. A* **2019**, *50*, 4732–4742. doi:10.1007/s11661-019-05381-z
 121. Fang, Z. Z.; Paramore, J. D.; Sun, P.; Chandran, K. S. R.; Zhang, Y.; Xia, Y.; Cao, F.; Koopman, M.; Free, M. Powder Metallurgy of Titanium - Past, Present, and Future. *Int. Mater. Rev.* **2018**, *63*, 407–459. doi:10.1080/09506608.2017.1366003
 122. Raynova, S.; Yang, F.; Bolzoni, L. Mechanical Behaviour of Induction Sintered Blended Elemental Powder Metallurgy Ti Alloys. *Mater. Sci. Eng. A* **2021**, *799*, 140157. doi:10.1016/j.msea.2020.140157
 123. Ma, Z.; Ren, L.; Liu, R.; Yang, K.; Zhang, Y.; Liao, Z.; Liu, W.; Qi, M.; Misra, R. D. K. Effect of Heat Treatment on Cu Distribution, Antibacterial Performance and Cytotoxicity of Ti-6Al-4V-5Cu Alloy. *J. Mater. Sci. Technol.* **2015**, *31*, 723–732. doi:10.1016/j.jmst.2015.04.002
 124. Peng, C.; Zhang, S.; Sun, Z.; Ren, L.; Yang, K. Effect of Annealing Temperature on Mechanical and Antibacterial Properties of Cu-Bearing Titanium Alloy and Its Preliminary Study of Antibacterial Mechanism. *Mater. Sci. Eng. C Mater. Biol. Appl.* **2018**, *93*, 495–504. doi:10.1016/j.msec.2018.08.018
 125. Yang, S.; Leong, K. F.; Du, Z.; Chua, C. K. The Design of Scaffolds for Use in Tissue Engineering. Part I. Traditional Factors. *Tissue Eng.* **2001**, *7*, 679–689. doi:10.1089/107632701753337645
 126. Rajendran, A.; Pattanayak, D. K. Bioactive and Antimicrobial Macro-/Micro-Nanoporous Selective Laser Melted Ti-6Al-4V Alloy for Biomedical Applications. *Heliyon* **2022**, *8*, e09122. doi:10.1016/j.heliyon.2022.e09122
 127. Guo, S.; Lu, Y.; Wu, S.; Liu, L.; He, M.; Zhao, C.; Gan, Y.; Lin, J.; Luo, J.; Xu, X.; Lin, J. Preliminary Study on the Corrosion Resistance, Antibacterial Activity and Cytotoxicity of Selective-Laser-Melted Ti6Al4V-xCu Alloys. *Mater. Sci. Eng. C Mater. Biol. Appl.* **2017**, *72*, 631–640. doi:10.1016/j.msec.2016.11.126
 128. Frazier, W. E. Metal Additive Manufacturing: A Review. *J. Mater. Eng. Perform.* **2014**, *23*, 1917–1928. doi:10.1007/s11665-014-0958-z
 129. Behjat, A.; Shamanian, M.; Sadeghi, F.; Iuliano, L.; Saboori, A. Additive Manufacturing of a Novel in-

- Situ Alloyed AISI316L-Cu Stainless Steel: Microstructure and Antibacterial Properties. *Mater. Lett.* **2024**, 355, 135363. doi:10.1016/j.matlet.2023.135363
130. Zhang, E.; Liu, C. A New Antibacterial Co-Cr-Mo-Cu Alloy: Preparation, Biocorrosion, Mechanical and Antibacterial Property. *Mater. Sci. Eng. C Mater. Biol. Appl.* **2016**, 69, 134–143. doi:10.1016/j.msec.2016.05.028
131. Duan, J-z.; Yang, Y.; Wang, H. Effects of Antibacterial Co-Cr-Mo-Cu Alloys on Osteoblast Proliferation, Differentiation, and the Inhibition of Apoptosis. *Orthop. Surg.* **2022**, 14, 758–768. doi:10.1111/os.13253
132. Zhang, E.; Ge, Y.; Qin, G. Hot Deformation Behavior of an Antibacterial Co-29Cr-6Mo-1.8Cu Alloy and Its Effect on Mechanical Property and Corrosion Resistance. *J. Mater. Sci. Technol.* **2018**, 34, 523–533. doi:10.1016/j.jmst.2016.09.025
133. Lu, Y.; Ren, L.; Xu, X.; Yang, Y.; Wu, S.; Luo, J.; Yang, M.; Liu, L.; Zhuang, D.; Yang, K.; Lin, J. Effect of Cu on Microstructure, Mechanical Properties, Corrosion Resistance and Cytotoxicity of CoCrW Alloy Fabricated by Selective Laser Melting. *J. Mech. Behav. Biomed. Mater.* **2018**, 81, 130–141. doi:10.1016/j.jmbbm.2018.02.026
134. Wang, S.; Yang, C.; Ren, L.; Shen, M.; Yang, K. Study on Antibacterial Performance of Cu-Bearing Cobalt-Based Alloy. *Mater. Lett.* **2014**, 129, 88–90. doi:10.1016/j.matlet.2014.05.020
135. Gao, J.; Jin, Y.; Fan, Y.; Xu, D.; Meng, L.; Wang, C.; Yu, Y.; Zhang, D.; Wang, F. Fabricating Antibacterial CoCrCuFeNi High-Entropy Alloy Via Selective Laser Melting and *In-Situ* Alloying. *J. Mater. Sci. Technol.* **2022**, 102, 159–165. doi:10.1016/j.jmst.2021.07.002
136. Jiang, F.; Zhu, W.; Zhao, C.; Li, Y.; Wei, P.; Wan, T.; Ye, H.; Pan, S.; Ren, F. A Strong, Wear- and Corrosion-Resistant, and Antibacterial Co-30 at.% Cr-5 at.% Ag Ternary Alloy for Medical Implants. *Mater. Des.* **2019**, 184, 108190. doi:10.1016/j.matdes.2019.108190
137. Esteban, P. G.; Ruiz-Navas, E. M.; Bolzoni, L.; Gordo, E. Low-Cost Titanium Alloys? Iron May Hold the Answers. *Met. Powder Rep.* **2008**, 63, 24–27. doi:10.1016/S0026-0657(09)70040-2
138. Guo, Y.; Zhao, M.-C.; Xie, B.; Zhao, Y.-C.; Yin, D.; Gao, C.; Shuai, C.; Atrens, A. *In Vitro* Corrosion Resistance and Antibacterial Performance of Novel Fe-xCu Biomedical Alloys Prepared by Selective Laser Melting. *Adv. Eng. Mater.* **2021**, 23, 2001000.
139. Deng, B.; Guo, Y.; Zhao, M.-C.; Li, Q.-F.; Ma, B.; Duan, B.; Yin, D.; Atrens, A. Study on a Novel Biodegradable and Antibacterial Fe-Based Alloy Prepared by Microwave Sintering. *Materials* **2021**, 14, 3784.
140. Ma, Z.; Gao, M.; Na, D.; Li, Y.; Tan, L.; Yang, K. Study on a Biodegradable Antibacterial Fe-Mn-C-Cu Alloy as Urinary Implant Material. *Mater. Sci. Eng. C Mater. Biol. Appl.* **2019**, 103, 109718. doi:10.1016/j.msec.2019.05.003
141. Hong, I. T.; Koo, C. H. Antibacterial Properties, Corrosion Resistance and Mechanical Properties of Cu-Modified SUS 304 Stainless Steel. *Mater. Sci. Eng. A* **2005**, 393, 213–222. doi:10.1016/j.msea.2004.10.032
142. Xi, T.; Shahzad, M. B.; Xu, D.; Sun, Z.; Zhao, J.; Yang, C.; Qi, M.; Yang, K. Effect of Copper Addition on Mechanical Properties, Corrosion Resistance and Antibacterial Property of 316L Stainless Steel. *Mater. Sci. Eng. C Mater. Biol. Appl.* **2017**, 71, 1079–1085. doi:10.1016/j.msec.2016.11.022
143. Lou, Y.; Lin, L.; Xu, D.; Zhao, S.; Yang, C.; Liu, J.; Zhao, Y.; Gu, T.; Yang, K. Antibacterial Ability of a Novel Cu-Bearing 2205 Duplex Stainless Steel against *Pseudomonas aeruginosa* Biofilm in Artificial Seawater. *Int. Biodeteriorat. Biodegrad.* **2016**, 110, 199–205. doi:10.1016/j.ibiod.2016.03.026
144. Nan, L.; Yang, K. Effect of Cu Addition on Antibacterial Property of Type 200 Stainless Steel. *Mater. Technol.* **2016**, 31, 44–47. doi:10.1179/1753555715Y.0000000025
145. Zhuang, Y.; Zhang, S.; Yang, K.; Ren, L.; Dai, K. Antibacterial Activity of Copper-Bearing 316L Stainless Steel for the Prevention of Implant-Related Infection. *J. Biomed. Mater. Res. B Appl. Biomater.* **2020**, 108, 484–495. doi:10.1002/jbm.b.34405
146. Nan, L.; Yang, K. Cu Ions Dissolution from Cu-Bearing Antibacterial Stainless Steel. *J. Mater. Sci. Technol.* **2010**, 26, 941–944. doi:10.1016/S1005-0302(10)60152-1
147. Zhang, D.; Ren, L.; Zhang, Y.; Xue, N.; Yang, K.; Zhong, M. Antibacterial Activity against *Porphyromonas gingivalis* and Biological Characteristics of Antibacterial Stainless Steel. *Colloids Surf. B Biointerf.* **2013**, 105, 51–57. doi:10.1016/j.colsurfb.2012.12.025
148. Sun, D.; Xu, D.; Yang, C.; Chen, J.; Shahzad, M. B.; Sun, Z.; Zhao, J.; Gu, T.; Yang, K.; Wang, G. Inhibition of *Staphylococcus aureus* Biofilm by a Copper-Bearing 317L-Cu Stainless Steel and Its Corrosion Resistance. *Mater. Sci. Eng. C Mater. Biol. Appl.* **2016**, 69, 744–750. doi:10.1016/j.msec.2016.07.050
149. Chai, H.; Guo, L.; Wang, X.; Fu, Y.; Guan, J.; Tan, L.; Ren, L.; Yang, K. Antibacterial Effect of 317L Stainless Steel Contained Copper in Prevention of Implant-Related Infection *In Vitro* and *In Vivo*. *J. Mater. Sci. Mater. Med.* **2011**, 22, 2525–2535. doi:10.1007/s10856-011-4427-z
150. Guan, B.; Hong, S.-H.; Schulz, C.; Stanford, N. The Microstructure, Antimicrobial Properties, and Corrosion Resistance of Cu-Bearing Strip Cast Steel. *Adv. Eng. Mater.* **2020**, 22, 1901265. doi:10.1002/adem.201901265
151. Xiang, H.; Liu, D.; Chen, X.; Cao, H.; Dong, X. On the Microstructure and Mechanical Properties of Silver-Bearing Antibacterial CD4MCu Duplex Stainless Steels: Solid Solution Temperature. *Mat. Exp.* **2019**, 9, 1067–1075. doi:10.1166/mex.2019.1600
152. Liao, K.-H.; Ou, K.-L.; Cheng, H.-C.; Lin, C.-T.; Peng, P.-W. Effect of Silver on Antibacterial

- Properties of Stainless Steel. *Appl. Surf. Sci.* **2010**, 256, 3642–3646. doi:10.1016/j.apsusc.2010.01.001
153. Yang, S.-M.; Chen, Y.-C.; Pan, Y.-T.; Lin, D.-Y. Effect of Silver on Microstructure and Antibacterial Property of 2205 Duplex Stainless Steel. *Mater. Sci. Eng. C Mater. Biol. Appl.* **2016**, 63, 376–383. doi:10.1016/j.msec.2016.03.014
154. Yuan, J. P.; Li, W.; Wang, C. Effect of the La Alloying Addition on the Antibacterial Capability of 316L Stainless Steel. *Mater. Sci. Eng. C* **2013**, 33, 446–452. doi:10.1016/j.msec.2012.09.012
155. Li, Y.; Liu, L.; Wan, P.; Zhai, Z.; Mao, Z.; Ouyang, Z.; Yu, D.; Sun, Q.; Tan, L.; Ren, L.; et al. Biodegradable Mg-Cu Alloy Implants With Antibacterial Activity for the Treatment of Osteomyelitis: *In Vitro* and *In Vivo* Evaluations. *Biomaterials* **2016**, 106, 250–263. doi:10.1016/j.biomaterials.2016.08.031
156. Chen, J.; Peng, W.; Zhu, L.; Tan, L.; Etim, I. P.; Wang, X.; Yang, K. Effect of Copper Content on the Corrosion Behaviors and Antibacterial Properties of Binary Mg-Cu Alloys. *Mater. Technol.* **2018**, 33, 145–152. doi:10.1080/10667857.2018.1432170
157. Zhao, X.; Wan, P.; Wang, H.; Zhang, S.; Liu, J.; Chang, C.; Yang, K.; Pan, Y. An Antibacterial Strategy of Mg-Cu Bone Grafting in Infection-Mediated Periodontics. *Biomed Res. Int.* **2020**, 2020, 7289208. doi:10.1155/2020/7289208
158. Liu, C.; Fu, X.; Pan, H.; Wan, P.; Wang, L.; Tan, L.; Wang, K.; Zhao, Y.; Yang, K.; Chu, P. K. Biodegradable Mg-Cu Alloys With Enhanced Osteogenesis, Angiogenesis, and Long-Lasting Antibacterial Effects. *Sci. Rep.* **2016**, 6, 27374. doi:10.1038/srep27374
159. Feng, Y.; Zhu, S.; Wang, L.; Chang, L.; Hou, Y.; Guan, S. Fabrication and Characterization of Biodegradable Mg-Zn-Y-Nd-Ag Alloy: Microstructure, Mechanical Properties, Corrosion Behavior and Antibacterial Activities. *Bioact. Mater.* **2018**, 3, 225–235. doi:10.1016/j.bioactmat.2018.02.002
160. Tie, D.; Feyerabend, F.; Müller, W. D.; Schade, R.; Liefelth, K.; Kainer, K. U.; Willumeit, R. Antibacterial Biodegradable Mg-Ag Alloys. *Eur. Cell. Mater.* **2013**, 25, 284–298; discussion 298. doi:10.22203/ecm.v025a20
161. Qin, H.; Zhao, Y.; An, Z.; Cheng, M.; Wang, Q.; Cheng, T.; Wang, Q.; Wang, J.; Jiang, Y.; Zhang, X.; Yuan, G. Enhanced Antibacterial Properties, Biocompatibility, and Corrosion Resistance of Degradable Mg-Nd-Zn-Zr Alloy. *Biomaterials* **2015**, 53, 211–220. doi:10.1016/j.biomaterials.2015.02.096
162. Xie, K.; Wang, N.; Guo, Y.; Zhao, S.; Tan, J.; Wang, L.; Li, G.; Wu, J.; Yang, Y.; Xu, W.; et al. Additively Manufactured Biodegradable Porous Magnesium Implants for Elimination of Implant-Related Infections: An *In Vitro* and *In Vivo* Study. *Bioact. Mater.* **2022**, 8, 140–152. doi:10.1016/j.bioactmat.2021.06.032
163. Liu, Z.; Schade, R.; Luthringer, B.; Hort, N.; Rothe, H.; Müller, S.; Liefelth, K.; Willumeit-Römer, R.; Feyerabend, F. Influence of the Microstructure and Silver Content on Degradation, Cytocompatibility, and Antibacterial Properties of Magnesium-Silver Alloys *In Vitro*. *Oxid. Med. Cell. Longev.* **2017**, 2017, 8091265. doi:10.1155/2017/8091265
164. Brooks, E. K.; Ahn, R.; Tobias, M. E.; Hansen, L. A.; Luke-Marshall, N. R.; Wild, L.; Campagnari, A. A.; Ehrensberger, M. T. Magnesium Alloy AZ91 Exhibits Antimicrobial Properties *In Vitro* But Not *In Vivo*. *J. Biomed. Mater. Res. B Appl. Biomater.* **2018**, 106, 221–227. doi:10.1002/jbm.b.33839
165. Zhang, C.; Lin, J.; Nguyen, N.-Y. T.; Guo, Y.; Xu, C.; Seo, C.; Villafana, E.; Jimenez, H.; Chai, Y.; Guan, R.; Liu, H. Antimicrobial Bioresorbable Mg-Zn-Ca Alloy for Bone Repair in a Comparison Study With Mg-Zn-Sr Alloy and Pure Mg. *ACS Biomater. Sci. Eng.* **2020**, 6, 517–538. doi:10.1021/acsbomaterials.9b00903
166. He, G.; Wu, Y.; Zhang, Y.; Zhu, Y.; Liu, Y.; Li, N.; Li, M.; Zheng, G.; He, B.; Yin, Q.; et al. Addition of Zn to the Ternary Mg-Ca-Sr Alloys Significantly Improves Their Antibacterial Properties. *J. Mater. Chem. B* **2015**, 3, 6676–6689. doi:10.1039/C5TB01319D
167. Liu, B.-s.; Cao, M.-m.; Zhang, Y.-z.; Hu, Y.; Gong, C.-w.; Hou, L.-f.; Wei, Y.-h. Microstructure, Anticorrosion, Biocompatibility and Antibacterial Activities of Extruded Mg-Zn-Mn Strengthened With Ca. *Trans. Nonferrous Met. Soc. China* **2021**, 31, 358–370. doi:10.1016/S1003-6326(21)65501-2
168. Gao, Z.; Song, M.; Liu, R.-L.; Shen, Y.; Ward, L.; Cole, I.; Chen, X.-B.; Liu, X. Improving *In Vitro* and *In Vivo* Antibacterial Functionality of Mg Alloys Through Micro-Alloying With Sr and Ga. *Mater. Sci. Eng. C Mater. Biol. Appl.* **2019**, 104, 109926. doi:10.1016/j.msec.2019.109926
169. Sahoo, S. N.; Mandal, S.; Khan, R.; Dutta, S.; Pal, S.; Ghosh, D.; Nandi, S. K.; Roy, M. Synergistic Effects of Cerium and Hot Forging on Biodegradation, Antibacterial Properties, and *In Vivo* Biocompatibility of Microalloyed Mg-Zr-Sr Alloys. *ACS Biomater. Sci. Eng.* **2023**, 9, 2495–2513. doi:10.1021/acsbomaterials.3c00097
170. Aboutalebianaraki, N.; Zeblysky, P.; Sarker, M. D.; Jeyaranjan, A.; Sakthivel, T. S.; Fu, Y.; Lucchi, J.; Baudelet, M.; Seal, S.; Kean, T. J.; Razavi, M. An Osteogenic Magnesium Alloy With Improved Corrosion Resistance, Antibacterial, and Mechanical Properties for Orthopedic Applications. *J. Biomed. Mater. Res. A* **2023**, 111, 556–574. doi:10.1002/jbm.a.37476
171. Zhou, X.; Fang, H.; Yuan, T.; Li, R. Effect of Slight Sn Modification on Mechanical Properties and Corrosion Behavior of Ti- (2-4 wt%) Mn Alloys Fabricated via Powder Metallurgy. *Mater. Charact.* **2023**, 203, 113068. doi:10.1016/j.matchar.2023.113068
172. Jia, M. T.; Gabbitas, B.; Bolzoni, L. Evaluation of Reactive Induction Sintering as a Manufacturing Route for Blended Elemental Ti-5Al-2.5Fe Alloy. *J. Mater. Process. Technol.* **2018**, 255, 611–620. doi:10.1016/j.jmatprotec.2018.01.013

173. Alshammari, Y.; Yang, F.; Bolzoni, L. Fabrication and Characterisation of Low-Cost Powder Metallurgy Ti-xCu-2.5Al Alloys Produced for Biomedical Applications. *J. Mech. Behav. Biomed. Mater.* **2022**, *126*, 105022. doi:10.1016/j.jmbbm.2021.105022
174. Yang, H.-L.; Zhu, M.-Z.; Wang, J.-Y.; Ma, C.-X.; Zhou, X.-W.; Xing, H.-X.; Zhang, E.-L.; Ji, S.-X. Optimization of Mechanical and Antibacterial Properties of Ti-3wt%Cu Alloy Through Cold Rolling and Annealing. *Rare Met.* **2022**, *41*, 610–620. doi:10.1007/s12598-021-01841-x
175. Yang, H.-L.; Zou, L.; Juaim, A. N.; Ma, C.-X.; Zhu, M.-Z.; Xu, F.; Chen, X.-N.; Wang, Y.-Z.; Zhou, X.-W. Copper Release and ROS in Antibacterial Activity of Ti-Cu Alloys Against Implant-Associated Infection. *Rare Met.* **2023**, *42*, 2007–2019. doi:10.1007/s12598-022-02242-4
176. Bao, M.; Liu, Y.; Wang, X.; Yang, L.; Li, S.; Ren, J.; Qin, G.; Zhang, E. Optimization of Mechanical Properties, Biocorrosion Properties and Antibacterial Properties of Wrought Ti-3Cu Alloy by Heat Treatment. *Bioact. Mater.* **2018**, *3*, 28–38. doi:10.1016/j.bioactmat.2018.01.004
177. Wu, J.-H.; Chen, K.-K.; Chao, C.-Y.; Chang, Y.-H.; Du, J.-K. Effect of Ti₂Cu Precipitation on Antibacterial Property of Ti-5Cu Alloy. *Mater. Sci. Eng. C Mater. Biol. Appl.* **2020**, *108*, 110433. doi:10.1016/j.msec.2019.110433
178. Yi, C.; Ke, Z.; Zhang, L.; Tan, J.; Jiang, Y.; He, Z. Antibacterial Ti-Cu Alloy With Enhanced Mechanical Properties as Implant Applications. *Mater. Res. Exp.* **2020**, *7*, 105404. doi:10.1088/2053-1591/abc371
179. Zhang, W.; Zhang, S.; Liu, H.; Ren, L.; Wang, Q.; Zhang, Y. Effects of Surface Roughening on Antibacterial and Osteogenic Properties of Ti-Cu Alloys With Different Cu Contents. *J. Mater. Sci. Technol.* **2021**, *88*, 158–167. doi:10.1016/j.jmst.2021.01.067
180. Liu, J.; Li, F.; Liu, C.; Wang, H.; Ren, B.; Yang, K.; Zhang, E. Effect of Cu Content on the Antibacterial Activity of Titanium-Copper Sintered Alloys. *Mater. Sci. Eng. C Mater. Biol. Appl.* **2014**, *35*, 392–400. doi:10.1016/j.msec.2013.11.028
181. Zhang, E.; Li, F.; Wang, H.; Liu, J.; Wang, C.; Li, M.; Yang, K. A New Antibacterial Titanium-Copper Sintered Alloy: Preparation and Antibacterial Property. *Mater. Sci. Eng. C Mater. Biol. Appl.* **2013**, *33*, 4280–4287. doi:10.1016/j.msec.2013.06.016
182. Alqattan, M.; Peters, L.; Yang, F.; Bolzoni, L. Microstructure, Mechanical Behaviour and Antibacterial Activity of Biomedical Ti-xMn-yCu Alloys. *J. Alloys Compd.* **2021**, *856*, 158165. doi:10.1016/j.jallcom.2020.158165
183. Alqattan, M.; Peters, L.; Alshammari, Y.; Yang, F.; Bolzoni, L. Antibacterial Ti-Mn-Cu Alloys for Biomedical Applications. *Regen. Biomater.* **2021**, *8*, rbaa050. doi:10.1093/rb/rbaa050
184. Bolzoni, L.; Alqattan, M.; Peters, L.; Alshammari, Y.; Yang, F. Ternary Ti Alloys Functionalised With Antibacterial Activity. *Sci. Rep.* **2020**, *10*, 22201. doi:10.1038/s41598-020-79192-3
185. Alqattan, M.; Alshammari, Y.; Yang, F.; Peters, L.; Bolzoni, L. Biomedical Ti-Cu-Mn Alloys With Antibacterial Capability. *J. Mater. Res. Technol.* **2021**, *10*, 1020–1028. doi:10.1016/j.jmrt.2020.12.044
186. Xu, W.; Hou, C.; Mao, Y.; Yang, L.; Tamaddon, M.; Zhang, J.; Qu, X.; Liu, C.; Su, B.; Lu, X. Characteristics of Novel Ti-10Mo-xCu Alloy by Powder Metallurgy for Potential Biomedical Implant Applications. *Bioact. Mater.* **2020**, *5*, 659–666. doi:10.1016/j.bioactmat.2020.04.012
187. Hussein, M. A.; Kumar, A. M.; Azeem, M. A.; Sorour, A. A.; Saravanan, S. Ti-30Nb-3Ag Alloy With Improved Corrosion Resistance and Antibacterial Properties for Orthopedic and Dental Applications Produced by Mechanical Alloying. *J. Mech. Behav. Biomed. Mater.* **2023**, *142*, 105851. doi:10.1016/j.jmbbm.2023.105851
188. Fu, S.; Zhao, X.; Yang, L.; Qin, G.; Zhang, E. A Novel Ti-Au Alloy With Strong Antibacterial Properties and Excellent Biocompatibility for Biomedical Application. *Biomater. Adv.* **2022**, *133*, 112653. doi:10.1016/j.msec.2022.112653
189. Ren, L.; Ma, Z.; Li, M.; Zhang, Y.; Liu, W.; Liao, Z.; Yang, K. Antibacterial Properties of Ti-6Al-4V-xCu Alloys. *J. Mater. Sci. Technol.* **2014**, *30*, 699–705. doi:10.1016/j.jmst.2013.12.014
190. Xu, J.; Lu, Y.; Pan, X.; Zhan, D.; Wang, Q.; Zhang, N. Antibacterial Performance of a Porous Cu-Bearing Titanium Alloy by Laser Additive Manufacturing. *Front. Bioeng. Biotechnol.* **2023**, *11*, 1226745. doi:10.3389/fbioe.2023.1226745
191. Mao, X.; Shi, A.; Wang, R.; Nie, J.; Qin, G.; Chen, D.; Zhang, E. The Influence of Copper Content on the Elastic Modulus and Antibacterial Properties of Ti-13Nb-13Zr-xCu Alloy. *Metals* **2022**, *12*, 1132. doi:10.3390/met12071132
192. Yuan, Y.; Ke, Z.; Zhang, L.; Jiang, Y.; He, Z. Mechanical, Corrosion and Antibacterial Properties of Ti-13Nb-13Zr-Based Alloys With Various Cu Contents. *Mater. Res. Exp.* **2021**, *8*, 115403. doi:10.1088/2053-1591/ac2f74
193. Cai, D.; Zhao, X.; Yang, L.; Wang, R.; Qin, G.; Chen, D.-f.; Zhang, E. A Novel Biomedical Titanium Alloy With High Antibacterial Property and Low Elastic Modulus. *J. Mater. Sci. Technol.* **2021**, *81*, 13–25. doi:10.1016/j.jmst.2021.01.015
194. Geetha, M.; Singh, A. K.; Asokamani, R.; Gogia, A. K. Ti Based Biomaterials, the Ultimate Choice for Orthopaedic Implants - A Review. *Prog. Mater. Sci.* **2009**, *54*, 397–425. doi:10.1016/j.pmatsci.2008.06.004
195. Venezuela, J.; Johnston, S.; Dargusch, M. S.; Atrens, A. 14 - Corrosion of Metallic Biomaterials. In *Metallic Biomaterials Processing and Medical Device Manufacturing*, C. Wen, Eds. UK: Woodhead Publishing, **2020**; pp. 469–515.
196. Qu, X.; Yang, H.; Jia, B.; Yu, Z.; Zheng, Y.; Dai, K. Biodegradable Zn-Cu Alloys Show Antibacterial Activity against MRSA Bone Infection by Inhibiting Pathogen Adhesion and Biofilm Formation. *Acta*

- Biomater.* **2020**, *117*, 400–417. doi:10.1016/j.actbio.2020.09.041
197. Shuai, C.; Dong, Z.; He, C.; Yang, W.; Peng, S.; Yang, Y.; Qi, F. A Peritectic Phase Refines the Microstructure and Enhances Zn Implants. *J. Mater. Res. Technol.* **2020**, *9*, 2623–2634. doi:10.1016/j.jmrt.2020.04.037
 198. Li, P.; Zhang, W.; Dai, J.; Xepapadeas, A. B.; Schweizer, E.; Alexander, D.; Scheideler, L.; Zhou, C.; Zhang, H.; Wan, G.; Geis-Gerstorf, J. Investigation of Zincopper Alloys as Potential Materials for Craniomaxillofacial Osteosynthesis Implants. *Mater. Sci. Eng. C Mater. Biol. Appl.* **2019**, *103*, 109826. doi:10.1016/j.msec.2019.109826
 199. Qu, X.; Yang, H.; Jia, B.; Wang, M.; Yue, B.; Zheng, Y.; Dai, K. Zinc Alloy-Based Bone Internal Fixation Screw With Antibacterial and anti-Osteolytic Properties. *Bioact. Mater.* **2021**, *6*, 4607–4624. doi:10.1016/j.bioactmat.2021.05.023
 200. Yang, Y.; Yang, M.; He, C.; Qi, F.; Wang, D.; Peng, S.; Shuai, C. Rare Earth Improves Strength and Creep Resistance of Additively Manufactured Zn Implants. *Compos. B: Eng.* **2021**, *216*, 108882. doi:10.1016/j.compositesb.2021.108882
 201. Sun, J.; Zhang, X.; Shi, Z.-Z.; Gao, X.-X.; Liu, X.-F.; Wang, J.-Q.; Wang, L.-N. Adjusting Comprehensive Properties of Biodegradable Zn-Mn Alloy Through Solution Heat-Treatment. *Mater. Today Commun.* **2020**, *23*, 101150. doi:10.1016/j.mtcomm.2020.101150
 202. Tong, X.; Han, Y.; Zhou, R.; Jiang, W.; Zhu, L.; Li, Y.; Huang, S.; Ma, J.; Wen, C.; Lin, J. Biodegradable Zn-Dy Binary Alloys With High Strength, Ductility, Cytocompatibility, and Antibacterial Ability for Bone-Implant Applications. *Acta Biomater.* **2023**, *155*, 684–702. doi:10.1016/j.actbio.2022.10.053
 203. Zhang, W.; Li, P.; Shen, G.; Mo, X.; Zhou, C.; Alexander, D.; Rupp, F.; Geis-Gerstorf, J.; Zhang, H.; Wan, G. Appropriately Adapted Properties of Hot-Extruded Zn-0.5Cu-xFe Alloys Aimed for Biodegradable Guided Bone Regeneration Membrane Application. *Bioact. Mater.* **2021**, *6*, 975–989. doi:10.1016/j.bioactmat.2020.09.019
 204. Lin, J.; Tong, X.; Shi, Z.; Zhang, D.; Zhang, L.; Wang, K.; Wei, A.; Jin, L.; Lin, J.; Li, Y.; Wen, C. A Biodegradable Zn-1Cu-0.1Ti Alloy With Antibacterial Properties for Orthopedic Applications. *Acta Biomater.* **2020**, *106*, 410–427. doi:10.1016/j.actbio.2020.02.017
 205. Zhan, J.; Huang, X.; Yang, Y.; Kolawole, S. K.; Siddiqui, M. A.; Wang, J.; Su, X.; Chen, J. Effects of Cu Content on the Mechanical, Degradable, and Antibacterial Properties of the As-Cast Zn-3Al-xCu Alloys. *J. Materi. Eng. Perform.* **2023**, *32*, 10039–10056. doi:10.1007/s11665-023-07870-0
 206. Xiao, C.; Zhao, D. W.; Sun, Q.; Su, Y.; Cui, D. P.; Zhang, X. Z.; Dong, X. L.; Wang, H. X.; Wang, F.; Ren, Y. P.; Qin, G. W. Morphology and Mechanical, Corrosive, and Antibacterial Behaviors of Indirectly Extruded Zn-0.05wt.%Mg-(0.5, 1 wt.%)Ag Alloys. *J. Materi. Eng. Perform.* **2019**, *28*, 6864–6872. doi:10.1007/s11665-019-04297-4
 207. Wątroba, M.; Bednarczyk, W.; Kawalko, J.; Mech, K.; Marciszko, M.; Boelter, G.; Banzhaf, M.; Bała, P. Design of Novel Zn-Ag-Zr Alloy With Enhanced Strength as a Potential Biodegradable Implant Material. *Mater. Des.* **2019**, *183*, 108154. doi:10.1016/j.matdes.2019.108154
 208. Wu, H.; Xie, X.; Wang, J.; Ke, G.; Huang, H.; Liao, Y.; Kong, Q. Biological Properties of Zn-0.04Mg-2Ag: A New Degradable Zinc Alloy Scaffold for Repairing Large-Scale Bone Defects. *J. Mater. Res. Technol.* **2021**, *13*, 1779–1789. doi:10.1016/j.jmrt.2021.05.096
 209. Čapek, J.; Kubásek, J.; Pinc, J.; Fojt, J.; Krajewski, S.; Rupp, F.; Li, P. Microstructural, Mechanical, *In Vitro* Corrosion and Biological Characterization of an Extruded Zn-0.8Mg-0.2Sr (wt%) as an Absorbable Material. *Mater. Sci. Eng. C Mater. Biol. Appl.* **2021**, *122*, 111924. doi:10.1016/j.msec.2021.111924
 210. Li, W.-Y.; Dai, Y.-L.; Cai, W.-H.; Lin, S.-H.; Guo, L.; Zhang, D.-C.; Li, Y.; Wen, C. Ultrahigh Strength and Uniform Corrosion in Zn-Li Alloys Through Ultrahigh Pressure Supersaturated Solid Solution Treatment for Biodegradable Orthopedic Applications. *Rare Met.* **2024**, *43*, 5284–5304. doi:10.1007/s12598-024-02753-2
 211. Tong, X.; Shen, T.; Zhou, X.; Zeng, J.; Tao, J.; Munir, K.; Li, Y.; Huang, S.; Wu, X.; Ma, J.; et al. Biodegradable Zn-Cu-Li Alloys With Ultrahigh Strength, Ductility, Antibacterial Ability, Cytocompatibility, and Suitable Degradation Rate for Potential Bone-Implant Applications. *Smart Mater. Manuf.* **2023**, *1*, 100012. doi:10.1016/j.smmf.2022.100012
 212. Niu, K.-n.; Zhang, D.-c.; Qi, F.-g.; Lin, J.-g.; Dai, Y.-l. Achieving High Strength and Antibacterial Zn-4Ag-Mn Alloy With Homogenous Corrosion Behavior via High-Pressure Solid Solution. *Trans. Nonferrous Met. Soc. China* **2024**, *34*, 2231–2244. doi:10.1016/S1003-6326(24)66537-4
 213. Jiang, Y.; Zhang, W.-J.; Mi, X.-J.; Huang, G.-J.; Xie, H.-F.; Feng, X.; Peng, L.-J.; Yang, Z. Antibacterial Property, Corrosion and Discoloration Resistance of Pure Copper Containing Zn or Ni. *Rare Metals.* **2022**, *41*, 4041–4046. doi:10.1007/s12598-022-02098-8
 214. Villapún, V. M.; Zhang, H.; Howden, C.; Chow, L. C.; Esat, F.; Pérez, P.; Sort, J.; Bull, S.; Stach, J.; González, S. Antimicrobial and Wear Performance of Cu-Zr-Al Metallic Glass Composites. *Mater. Des.* **2017**, *115*, 93–102. doi:10.1016/j.matdes.2016.11.029
 215. Shivasiddaramaiah, A. G.; Mallik, U. S.; Mahato, R.; Shashishekar, C.; Shivaramu, L.; Prashantha, S. Evaluation of Biocompatibility of Cu-Al-Be-Mn Quaternary Shape Memory Alloys Using Antibacterial Test by AGARWELL Diffusion Method. *Mater. Today: Proc.* **2019**, *17*, 61–69. doi:10.1016/j.matpr.2019.06.401
 216. Wan, T.; Chu, K.; Fang, J.; Zhong, C.; Zhang, Y.; Ge, X.; Ding, Y.; Ren, F. A High Strength, Wear and Corrosion-Resistant, Antibacterial and Biocompatible Nb-5 at.% Ag Alloy for Dental and Orthopedic

- Implants. *J. Mater. Sci. Technol.* **2021**, *80*, 266–278. doi:10.1016/j.jmst.2020.11.049
217. Han, K.; Jiang, H.; Wang, Y.; Qiang, J.; Yu, C. Antimicrobial Zr-Based Bulk Metallic Glasses for Surgical Devices Applications. *J. Non-Cryst. Solids* **2021**, *564*, 120827. doi:10.1016/j.jnoncrysol.2021.120827
218. Yang, H.-L.; Juaim, A. N.; Zou, L.; Zhu, M.-Z.; Chen, X.-N.; Ma, C.-X.; Zhou, X.-W. Antibacterial Activity and Mechanism of Newly Developed Zr-30Ta and Zr-25Ta-5Ti Alloys Against Implant-Associated Infection. *Rare Met.* **2022**, *41*, 4176–4187. doi:10.1007/s12598-022-02144-5
219. Perrault, D. P.; Sharma, A.; Kim, J. F.; Gurtner, G. C.; Wan, D. C. Surgical Applications of Materials Engineered With Antimicrobial Properties. *Bioengineering (Basel)* **2022**, *9*, 138. doi:10.3390/bioengineering9040138
220. Romanò, C. L.; Tsuchiya, H.; Morelli, I.; Battaglia, A. G.; Drago, L. Antibacterial Coating of Implants: Are we Missing Something? *Bone Joint Res.* **2019**, *8*, 199–206. doi:10.1302/2046-3758.85.BJR-2018-0316
221. Dauvergne, E.; Mullié, C. Brass Alloys: Copper-Bottomed Solutions against Hospital-Acquired Infections? *Antibiotics (Basel)* **2021**, *10*, 286. doi:10.3390/antibiotics10030286
222. Donnelly, B.; Sammut, K.; Tang, Y. Materials Selection for Antifouling Systems in Marine Structures. *Molecules* **2022**, *27*, 3408. doi:10.3390/molecules27113408
223. DeFlorio, W.; Liu, S.; White, A. R.; Taylor, T. M.; Cisneros-Zevallos, L.; Min, Y.; Scholar, E. M. A. Recent Developments in Antimicrobial and Antifouling Coatings to Reduce or Prevent Contamination and Cross-Contamination of Food Contact Surfaces by Bacteria. *Compr. Rev. Food Sci. Food Saf.* **2021**, *20*, 3093–3134. doi:10.1111/1541-4337.12750